Expression and localization of ephrin-B1, EphB2 and EphB4 in the mouse testis and epididymis in the adult and during the postnatal development

大阪府立大学博士（獣医学）学位論文

Expression and localization of ephrin-B1, EphB2 and EphB4 in the mouse testis and epididymis in the adult and during the postnatal development
(成体と生後発達期のマウスの精巣と精巣上体における ephrin-B1, EphB2, EphB4 の発現と局在について)

MD. ROYHAN GOFUR

2019 年

Contents

General introduction

In the male genital system, spermatogenesis and steroidogenesis occur in the testis and the maturation and storage of spermatozoa occur in the epididymis. The testis is composed of a highly convoluted and organized tubular system covered and surrounded by connective tissues termed the tunica albuginea, septa, and mediastinum testis. The tubular system consists of seminiferous tubules, straight tubules, and the rete testis. Seminiferous tubules, the spermatogenic region in the tubular system, are lined by a complex stratified epithelium composed of two basic cell populations: Sertoli cells and spermatogenic cells. The Sertoli cells confer structural organization to the tubules as they extend through the full thickness of the epithelium and form apical and lateral processes that surround adjacent spermatogenic cells and occupy the spaces between them. Spermatogenic cells are organized in poorly defined layers of progressive development between adjacent Sertoli cells in the seminiferous epithelium: the most immature cells, termed spermatogonia, reside on the basal lamina, spermatocytes are located in the basal and middle layers, and the most mature cells, termed spermatids, form one or two layers in the apical side and are attached to the Sertoli cells to form the luminal border of the tubules (Ross and Pawlina, 2015). Leydig cells reside in a group in the connective tissue stroma of seminiferous tubules. These large polygonal cells are the primary source of androgens, particularly testosterone, which is essential for the maintenance of spermatogenesis, genital excurrent ducts, and accessory sex glands in adults (Shima et al., 2013; Ross and Pawlina, 2015). Smooth muscle cells termed peritubular myoid cells, another major component of the testicular interstitium, surround the seminiferous tubules with interposition of the basal lamina; they are responsible for the rhythmic peristaltic waves of tubular contractions leading to the movement of spermatozoa and testicular fluid through the seminiferous tubules via intratesticular ducts to the extratesticular excurrent duct system (Ross and Pawlina, 2015). The intratesticular excurrent duct system consists of the straight tubules and the rete testis. Seminiferous tubules generally form loops and both ends are connected to straight tubules, with a short terminal region of seminiferous tubules (50 μm in length in mice), which are lined only by Sertoli cells and form an abrupt constriction at the junction. The straight tubules empty into the rete testis, a complex series of interconnecting channels lined by a simple cuboidal epithelium. The rete testis, generally located in the mediastinum testis in larger mammals but just beneath the tunica albuginea in rodents, is

converged at one pole of the testis facing the epididymis side (Foley, 2001; Silvan and Arechaga, 2012; Ross and Pawlina, 2015).

The efferent ductules, the initial part of the extratesticular excurrent duct system, connect the rete testis with the ductus epididymis. The efferent ductules, which are lined with a ciliated simple/pseudostratified columnar epithelium and surrounded by a circular layer of smooth muscle cells, run in the connective tissues between the testis and epididymis and also in the proximal part of the epididymis (Hess, 2015). The epididymis is grossly divided into three parts: the caput, corpus, and cauda epididymis. The duct of the epididymis (ductus epididymis) is a highly coiled tube lined with a nonciliated pseudostratified columnar epithelium and surrounded by a circular layer of smooth muscle cells; the thickness of the epithelium progressively decreases along the duct and the lumen becomes wider in the cauda epididymis (Sullivan and Mieusset, 2016; Ross and Pawlina, 2015). Spermatozoa mature during their passage through the duct in the caput and corpus epididymis to obtain motility and fertilization capacity, and are stored in the cauda epididymis (Cornwall, 2009; Dacheux and Dacheux, 2014). The duct of the epididymis can be histologically and histochemically divided into more segments. The caput epididymis is subdivided into three segments by lectin histochemistry based on specific expression of glycoconjugates or sugar chains in the epithelium (Burkett et al., 1987). These segments are almost identical to a histological subdivision by connective tissue septa of the epididymis and a segment-specific gene expression pattern has been identified in mice (Johnston et al., 2005; Sipila and Bjorkgren, 2016).

As described above, the testis and epididymis are composed of a series of a tubule/ductule/duct system lined with tissue-specific epithelia. The seminiferous/straight tubules and rete testis originate from the testicular cords (seminiferous cords), whereas the ductus epididymis originates from the mesonephric duct and the efferent ductules from mesonephric tubules (Lupien et al., 2006; Ross and Pawlina, 2015). Therefore, two developmental boundaries are assigned to the junction at the proximal and distal end of the efferent ductules in the genital tubule/duct system, and these boundaries are also histologically maintained in the epithelia of these tissues. However, to the best of the author’s knowledge, the mechanisms underlying the maintenance of these boundaries accompanied by the morphological transition of the epithelia are not completely clear.

During the development, the testis is developed from the primitive sex cords in which primordial germ cells/gonocytes migrate from the yolk sac. At birth, seminiferous tubules are lined by Sertoli cells and contain gonocytes. Gonocytes differentiate into spermatogonial stem

cells/spermatogonia during days 3–6 after birth in the mouse: according to this transformation, cell position changes from the luminal to basal side (gonocytes in the luminal side and spermatogonia in the basal side) (Bellve et al., 1977). Then spermatogonia differentiate into spermatocytes that undergo meiosis and give rise to haploid round spermatids, which finally differentiate into spermatozoa. Spermatogenesis starts shortly after birth (postnatal days 3 to 6) and the first wave of spermatogenesis completes at postnatal day 35 (Abe et al., 1991; Montoto et al., 2012; Tiptanavattana et al., 2015). Therefore, all types of germ cells appear in the seminiferous epithelium at 5 weeks of age in mouse, i.e., the seminiferous epithelium is completed at 5 weeks. In contrast, in the intratesticular duct system, the rete testis connects to efferent ductules at embryonic day 13.5 (E13.5), and the efferent ductules also connect to the ductus epididymis around this time (Murashima et al., 2015). The intratesticular duct system is histologically completed around postnatal day 18 when seminiferous tubules, straight tubules and the rete testis clearly appear with morphological characteristics of adult types peculiar to respective epithelia (Malolina and Kulibin, 2017). In the postnatal development of the epididymis, the ductus epididymis is poorly developed and the most epididymal tissues are occupied with mesenchymal tissues/stromata at birth (Mendive et al., 2006). Until 2-3 weeks, the ductus epididymis is lined by immature/undifferentiated columnar cells undergoing cell division. Thereafter, the epididymal epithelium begins to mature/differentiate and appears with morphological and histochemical characteristics of adult types at 5weeks of age in mice or during puberty when spermatozoa appeared in the lumen of the ductus epididymis (Abou-Haila and Fain-Maurel, 1985; Bjorkgren et al., 2012; Jun et al., 2014; Robaire et al., 2006).

The Eph receptors constitute the largest family of receptor tyrosine kinases. Eph receptors and their ligands, ephrins, are expressed in many tissues and organs and serve as a cell–cell communication system with a variety of roles (Pasquale, 2005; Pasquale, 2010). These membrane proteins regulate cell adhesion and migration as well as cell–cell repulsion by regulating the organization of the actin cytoskeleton mainly via the Rho-family GTPases. In mammals, Eph receptors are divided into EphA (A1–A8 and A10) and EphB (B1–B4 and B6) classes based on the amino acid sequence homology of their extracellular domains (Pasquale, 2005; Pasquale, 2008). Members of these two receptor classes promiscuously bind to ligands of the ephrin-A (A1–A5) and -B (B1–B3) classes, respectively. This interaction of the Eph receptors with ephrins results in bidirectional signal propagation in both receptor- and ligand-expressing cells. Forward signaling by Eph receptors mainly depends on their autophosphorylation and phosphorylation by other tyrosine kinases, as well as on the

association of the receptors with various effector proteins, whereas reverse signaling by ephrins largely depends on the Src kinase family proteins (Pasquale, 2005; Pasquale, 2008).

The roles of Eph receptors and ephrins have been extensively characterized in developing tissues, especially the central nervous system and vascular system, where they regulate axon guidance, tissue-border formation, cell migration, and blood vessel maturation (Kullander and Klein, 2002; Pasquale, 2005). Recently, Eph receptors and ephrins have also been implicated in the physiology and homeostasis of normal adult tissues and organs (Miao and Wang, 2009; Pasquale, 2008). In adult epithelial tissues, Eph/ephrin signaling is implicated in maintaining epithelial integrity and homeostasis in variety of epithelia such as the small and large intestine, epidermis, and mammary glands (Miao and Wang, 2009; Perez White and Getsios, 2014). Previous studies examined the expression levels and functions of EphB and ephrin-B in the rodent gastric glandular and nonglandular epithelia and suggested that EphB and ephrin-B are involved in (1) maintenance of the gastric epithelial unit composed of gastric pits (apical compartment), the isthmus (middle compartment), and gastric glands (basal compartment) (Ishii et al., 2011b; Ogawa et al., 2011b; Uchiyama et al., 2015) and (2) formation of an epithelial boundary at the squamocolumnar junction along the proximal-to-distal axis of the gastric epithelia (Ogawa et al., 2013). A study on the expression levels and functions of EphB and ephrin-B in the rodent kidney suggested that EphB receptor signaling through Rho family GTPases regulates the cytoarchitecture and spatial organization of the tubule cells in the adult kidney medulla (Ogawa et al., 2006). These findings indicate that Eph/ephrin cell–cell communication system operates extensively in the epithelia of adult tissues and organs to maintain their integrity and homeostasis. Therefore, it would not be surprising if Eph receptors and ephrin ligands are also expressed in the male genital system. Certain EphB receptors and ephrin-B ligands have been implicated in prostate development (Ashley et al., 2010) and in the invasion and metastasis of prostate cancers (Xia et al., 2005); however, to the best of the author's knowledge, the expression patterns of Eph receptors and ephrins have not been reported in the testis and epididymis. Therefore, the author investigated the expression and localization of EphB receptors and ephrin-B ligands in the adult testis and epididymis especially to determine whether their expression boundaries exist in the series of the excurrent tubule/ductule/duct system in mice. The author also investigated the expression and localization of EphB/ephrin-B in those organs of the postnatal development to determine when their expression boundaries are formed/completed during the postnatal development if existed. The present findings may contribute insight toward regeneration of the male genital duct system, which is formed by the binding of developmentally different tissues.

Chapter 1

Expression and localization of ephrin-B1, EphB2 and EphB4 in the adult mouse testis and epididymis

Introduction

The testis and epididymis are composed of a series of a tubule/ductule/duct system lined with tissue-specific epithelia. The testis is composed of seminiferous tubules, the intratesticular excurrent duct system consisting of straight tubules and the rete testis as the tubule/ductule/duct system, and the connective tissue stroma. Seminiferous tubules generally form loops and both ends are connected to straight tubules, with a short terminal region of seminiferous tubules (50 μm in length in mice), which are lined only by Sertoli cells and form an abrupt constriction at the junction. The straight tubules empty into the rete testis, a complex series of interconnecting channels lined by a simple cuboidal epithelium (Foley, 2001; Silvan and Arechaga, 2012; Ross and Pawlina, 2015). In the connective tissue stroma among seminiferous tubules Leydig cells reside in a group: they are large polygonal cells responsible for the primary source of androgens, particularly testosterone essential for the mentainance of spermatogenesis, genital excurrent ducts, and accessory sex glands in the adult (Li et al., 2013; Shima et al., 2013). As another major cell component of the testicular interstitium, smooth muscle cells termed peritubular myoid cells surround seminiferous tubules with interposition of the basal lamina: they are responsible for rhythmic peristaltic waves of tubular contractions leading to the movement of spermatozoa and testicular fluid through the seminiferous tubules via intratesticular ducts to the extratesticular excurrent duct system (Ross and Pawlina, 2015). The efferent ductules are lined with a ciliated simple/pseudostratified columnar epithelium and surrounded by a circular layer of smooth muscle cells, run in the connective tissues between the testis and epididymis and also in the proximal part of the epididymis (Hess, 2015). The ductus epididymis, a highly coiled tube which is lined with a non-ciliated pseudostratified columnar epithelium and surrounded by a layer of circularly arranged smooth muscle cells: the thickness of the epithelium progressively decreases along the duct and the lumen become generally wider in the cauda epididymis (Sullivan and Mieusset, 2016; Ross and Pawlina, 2015). Spermatozoa mature during their

passage through the duct in the caput and corpus epididymis to obtain the ability forward, and fertilization capacity and are stored in the cauda epididymis (Cornwall, 2009; Dacheux and Dacheux, 2014). The seminiferous/straight tubules and rete testis originate from the testicular cords (seminiferous cords), whereas the ductus epididymis originates from the mesonephric duct and the efferent ductules from mesonephric tubules (Lupien et al., 2006; Ross and Pawlina, 2015). Therefore, two developmental boundaries are assigned to the junction at the proximal and distal end of the efferent ductules in the genital tubule/duct system, and these boundaries are histologically maintained in the epithelia of adult tissues. However, the mechanisms underlying the maintenance of these boundaries accompanied by the morphological transition of the epithelia are not completely clear.

Eph/ephrin system is a cell-cell communication system that regulates spatial organizations in various tissues and organs by repulsive or adhesive signals arising from contact between Eph- and ephrin-bearing cells. The roles of Eph receptors and ephrins have been extensively characterized in developing tissues. Many different biological functions have been attributed to these proteins (Noren and Pasquale, 2004; Palmer and Klein, 2003; Pasquale, 2005; Poliakov et al., 2004). Recently, Eph receptors and ephrins have also been implicated in the physiology and homeostasis of normal adult tissues and organs (Miao and Wang, 2009; Pasquale, 2008). Among them EphB2, EphB4 and ephrin-B1 are likely implicated in epithelial boundary formation along the luminal-to-basal axis of gastric units as well as along the proximal-to-distal axis of the squamocolumnar epithelial junction in the rodent stomach (Ishii et al., 2011b; Ogawa et al., 2013; Uchiyama et al., 2015). Therefore, the author hypothesized that EphB2, EphB4 and ephrin-B1 might play a role in the boundary formation of the tubule/ductule/duct system in the male genital system; however, the expression of EphB receptors and ephrin-B ligands in the testis and epididymis has not yet been examined. Therefore, the author investigated the expression and localization of EphB receptors and ephrin-B ligands in the adult mouse testis and epididymis, especially to determine whether their expression boundaries exist in the series of tubule/ductule/duct system.

In this chapter, the author investigated the expression and/or localization of EphB receptors and ephrin-B ligands, especially of EphB2, EphB4 and ephrin-B1, in the adult mouse testis and epididymis by reverse transcription-polymerase chain reaction (RT-PCR), immunoblotting and immunohistochemistry.

Chapter 1-1

Ephrin-B and EphB expression in the adult mouse testis and epididymis

Materials and methods

Animals

ICR male mice (8-9 week-old) kept under standard housing and feeding conditions were used for RT-PCR, and immunoblotting. Mice were anesthetized with pentobarbital, and the testis and epididymis were removed. Animal experimentation protocols were approved by the Animal Research Committee of Osaka Prefecture University.

RT-PCR analysis

Total RNA was isolated from the adult testis (without tunica albuginea) and epididymis using TRIzol reagent (Invitrogen, Carlsbad, CA, USA). RT-PCR analysis was performed according to the method of Ogawa et al. (Ogawa et al., 2011b) with some modifications. Briefly, 1 μg total RNA was transcribed into first-strand cDNA using M-MLV reverse transcriptase, RNase H^- (Promega, Madison, WI, USA), and oligo $(dT)_{18}$ primer, according to the manufacturer's instructions. For the detection of endogenous ephrin-B ligands, EphB receptors, and GAPDH, 0.5 μL of the 25 μL reaction mixture was amplified with Taq DNA polymerase (ExTaq; Takara Bio Inc., Otsu, Japan) using the reverse-transcribed cDNA as template. The primer pairs and cycle numbers used for PCR amplification in this study are shown in Table 1-1. The RT reaction was omitted for the negative controls. PCR products were separated on 1.5% agarose gels and visualized by ethidium bromide staining.

Immunoprecipitation and immunoblotting

The testis without tunica albuginea, and the caput and cauda epididymis were homogenized in modified RIPA buffer (50 mM Tris-HCl pH 7.5, 150 mM NaCl, 1.5 mM $MgCl_2$, 1 mM EDTA, 10 mM sodium pyrophosphate, 100 mM sodium fluoride, 10% glycerol, 1% sodium deoxycholate, 1% Triton X-100, and 0.1% SDS) containing a phosphatase inhibitor (1 mM sodium orthovanadate) and protease inhibitors (0.5 mM

phenylmethylsulfonyl fluoride, 10 μg/mL aprotinin, 10 μg/mL leupeptin, and 2 μg/mL pepstatin-A). Supernatants were collected after high-speed centrifugation (for 10 min at 13,000 × *g* and 4°C), and protein concentrations were measured using a Protein Assay kit (Bio-Rad Laboratories, Hercules, CA, USA).

Immunoprecipitation and immunoblotting were performed according to the method of Ogawa et al. (Ogawa et al., 2006) with some modifications. In brief, for immunoprecipitation, 1000 μg of tissue extracts was incubated overnight at 4℃ with 1.5 μg anti-EphB2 (AF467; R&D Systems, Minneapolis, MN, USA), anti-EphB4 (AF446, R&D Systems), or 0.5 μL normal goat serum (as a control; Vector Laboratories, Burlingame, CA, USA), followed by treatment with 15 μL protein G magnetic beads (Thermo Scientific, Waltham, MA, USA) for 60 min at 4°C. The immunoprecipitates were separated on 10% polyacrylamide gels and transferred onto polyvinylidene fluoride membranes, which were incubated overnight at 4 °C in Tris-buffered saline with 0.1% Triton X-100 (TBS-T) containing 3% bovine serum albumin (BSA) and 1:5,000 HRP-conjugated PY20 (BD Transduction Laboratories, San Jose, CA, USA). Immunoblots were developed using ECL Prime chemiluminescence reagents (Amersham Biosciences, Uppsala, Sweden). The membrane was reprobed with 0.15 μg/mL anti-EphB2 or anti-EphB4 antibody in TBS-T containing 3% BSA and 0.2% non-fat dry milk. After incubation with 1:20,000 HRP-conjugated mouse anti-goat IgG (Jackson ImmunoResearch Laboratories, West Grove, PA, USA) the immunoblots were developed again in a same manner.

Results

mRNA expression of ephrin-B ligands and EphB receptors in the adult testis and epididymis

To identify the ephrin-B ligands and EphB receptors present in the adult testis and epididymis, the author screened the testis (without the tunica albuginea) and epididymis of adult mice by RT-PCR. Transcripts for all mammalian ephrin-B and EphB molecules (EphB5 has only been detected in the chicken) were detected in both the testis and epididymis, although EphB1 was faintly detected in the epididymis with 35 cycles of PCR amplification (Fig. 1-1).

Protein expression and tyrosine-phosphorylation of EphB2 and EphB4 in the adult testis

and epididymis

EphB2 and EphB4 proteins were detected by immunoprecipitation in both the testis and epididymis. Bands showing EphB2 protein expression in the caput were more intense than those in the cauda epididymis (Fig. 1-2). In order to determine whether EphB2 and EphB4 receptors are endogenously phosphorylated on tyrosine in the adult testis and epididymis, the PVDF membranes were reprobed by an anti-phosphotyrosine antibody: EphB2 in the testis and EphB4 in the testis and epididymis were tyrosine-phosphorylated (Fig. 1-2).

Discussion

EphB receptor tyrosine kinases and their interacting ephrin-B ligands are transmembrane proteins, and together, they function as cell–cell communication molecules to play crucial roles in the establishment of spatial organization of cells in various tissues and organs by repulsive or adhesive signals arising from contact between EphB- and ephrin-B-bearing cells via the tyrosine-phosphorylation of these molecules. This communication system involves in the development (Kullander and Klein, 2002; Pasquale, 2005). Recently, much attention to EphB and ephrin-B molecules has been focused on the physiology and homeostasis of normal adult tissues and organs (Kania and Klein, 2016; Miao and Wang, 2009; Pasquale, 2008). Certain EphB receptors and ephrin-B ligands have been implicated in prostate development (Ashley et al., 2010) and in the invasion and metastasis of prostate cancers (Xia et al., 2005); however, their expression in the testis and epididymis has not yet been examined. Therefore, the author investigated the expression of EphB receptors and ephrin-B ligands in the adult mouse testis and epididymis. The author found that all mammalian ephrin-B and EphB molecules were expressed in both the testis and epididymis. Moreover, EphB2 in the testis and EphB4 in the testis and epididymis were tyrosine-phosphorylated, suggesting that EphB2-bearing cells in the testis and EphB4-bearing cells in the testis and epididymis are in contact with ephrin-B-bearing cells and that these receptors are activated in the adult testis and/or epididymis *in vivo*. This indicates that EphB2, EphB4 and ephrin-B molecules may involve in maintaining the integrity and homeostasis of adult testis and epididymis.

Chapter 1-2

Ephrin-B1, EphB2 and EphB4 localization in adult mouse testis and epididymis

Materials and methods

Animals

The testis and epididymis of 8–9 week-old ICR male mice were used for immunofluorescence and lectin fluorescence staining.

Antibodies and lectins

A goat polyclonal antibody against the mouse ephrin-B1 extracellular domain (AF473; less than 1% cross-reactivity with mouse ephrin-B2 and human ephrin-B3, based on direct ELISA) was obtained from R&D Systems, Inc. (Minneapolis, MN, USA). A rabbit polyclonal antibody against the ephrin-B carboxy terminus (anti-ephrin-B1/2/3, C-18) was purchased from Santa Cruz Biotechnology (Dallas, TX, USA). This antibody recognizes all three ephrin-B ligands, which share the antigen peptide. The author used this antibody to detect the combined overall expression of the ephrin-B ligands. Goat polyclonal antibodies against the mouse EphB2 extracellular domain (AF467; approximately 5% cross-reactivity with rat EphB1, mouse EphB3, and mouse EphB6, based on western blot), and the mouse EphB4 extracellular domain (AF446; approximately 5% cross-reactivity with mouse EphB6 and less than 1% cross-reactivity with mouse EphB2 and mouse EphB3, based on direct ELISA) were also obtained from R&D Systems. The author selected these EphB/ephrin-B antibodies owing to their high reliability and specificity based on the previous application for immunohistochemistry, immunoprecipitation, and immunoblotting (Ishii et al., 2011a; Ishii et al., 2011b; Ogawa et al., 2013; Ogawa et al., 2011b; Ogawa et al., 2006). Anti-vimentin rabbit monoclonal antibody (ab92547) and anti-alpha smooth muscle actin (α-SMA) rabbit polyclonal antibody (ab5694) were purchased from Abcam (Cambridge, UK), and rabbit polyclonal CYP17A1 antibody was purchased from Proteintech (Rosemont, Illinois, USA). Rat monoclonal antibody against mouse epithelial cellular adhesion molecule (EpCAM, also known as CD326) was purchased from eBioscience Inc. (San Diego, CA, USA), rat anti-mouse thymic stromal cell antigen (ER-TR7) monoclonal antibody was obtained from Novus

Biologicals (Littleton, CO, USA), and rat anti-mouse CD31 monoclonal antibody was obtained from BD Biosciences (Franklin Lakes, NJ, USA). Alexa Fluor 488-conjugated donkey anti-goat IgG, Alexa Fluor 488-conjugated donkey anti-rabbit IgG, Alexa Fluor 568-conjugated donkey anti-rabbit IgG, and Alexa Fluor 594-conjugated donkey anti-rat IgG were obtained from Molecular Probes, Inc. (Eugene, OR, USA). Fluorescein isothiocyanate-conjugated peanut agglutinin lectin (FITC-PNA) and rhodamine-conjugated Ulex Europaeus Agglutinin I lectin (Rh-UEA-I) were obtained from Sigma-Aldrich (St. Louis, MO, USA) and Vector Laboratories (Burlingame, CA, USA), respectively.

Immunofluorescence and lectin fluorescence staining

The testis and epididymis were fixed with 10% formalin in phosphate buffered saline (PBS) for approximately 4 h at 4°C. After washing with PBS, the tissues were immersed in 30% sucrose in PBS overnight and mounted in optimum cutting temperature (OCT) compound (Sakura Finetechnical Co., Ltd., Tokyo, Japan). Then, 5 to 6 μm-thick cryostat sections were used for fluorescence staining.

Single- or double-immunofluorescence staining was performed according to the method of Ogawa et al. (Ogawa et al., 2011b) with some modifications(Ogawa et al., 2011a). Briefly, cryostat sections were incubated in a humid chamber with 1% BSA in PBS (BSA-PBS), followed by incubation with a single or mixture of primary antibodies at a concentration of 4 μg/mL (anti-EphB2 and anti-EphB4), 1 μg/mL (anti-ephrin-B1, anti-ephrin-B1/2/3, anti-EpCAM, anti-ER-TR7), 1:200 (anti-CYP17A1), 1:400 (α-SMA), or 1:2000 (anti-CD31, anti-vimentin) for 1.5 h at 32°C. After washing with PBS, the sections were incubated with (1) Alexa Fluor 488-conjugated donkey anti-goat IgG (5 μg/mL) in BSA-PBS, (2) Alexa Fluor 488-conjugated donkey anti-rabbit IgG (5 μg/mL), (3) a mixture of Alexa Fluor 488-conjugated donkey anti-goat IgG (5 μg/mL) and Alexa Fluor 568-conjugated donkey anti-rabbit IgG (5 μg/mL), or (4) a mixture of Alexa Fluor 488-conjugated donkey anti-goat IgG (5 μg/mL) and Alexa Fluor 594-conjugated donkey anti-rat IgG (5 μg/mL) for 30 min at 32°C. The sections were then washed with PBS, mounted with PermaFluor (Thermo Scientific), and photographed under an inverted fluorescence microscope (IX71; Olympus, Tokyo, Japan) using a digital camera (DP72; Olympus) controlled by the manufacturer's software (DP2-BSW; Olympus). Some of the sections were stained with 4′, 6-diamidino-2-phenylindole dihydrochloride (DAPI, 2 μg/mL; Wako Pure Chemical Industries, Ltd., Osaka Japan), which was included in the mixture of secondary antibodies. Green, red/orange, and/or blue fluorescence images of the same field were

captured using 4×, 10×, 20×, and 40× objective lenses (IX71; Olympus), and some fluorescence micrographs were merged using Adobe Photoshop (San Jose, CA, USA). The specificity of the staining was verified by incubation without the primary or secondary antibodies.

Lectin fluorescence staining was performed according to the method of Ogawa et al. (Ogawa et al., 2011b). In brief, cryostat sections were incubated for 30 min at 25°C in a humid chamber with BSA-PBS, followed by incubation with FITC-PNA (5 μg/mL) and/or Rh-UEA-I (1 μg/mL) for 30 min at 32°C. The sections were then washed with PBS, mounted with PermaFluor, and photographed under a fluorescence microscope.

Results

Localization of ephrin-B ligands, EphB2, and EphB4 in the adult mouse testis

To determine the localization of ephrin-B ligands, EphB2, and EphB4 in the adult mouse testis, the author performed single- and double-immunofluorescence staining of tissue sections. EpCAM (CD326) immunostaining was used to identify the spermatogonia in the seminiferous tubules of testis; CYP17A1 immunostaining was used to identify the Leydig cells; Vimentin immunostaining was used to identify the Sertoli cells; ER-TR7 immunostaining was used to identify the fibroblasts; α-SMA immunostaining was used to identify the peritublar myoid cells/smooth muscle cells and CD31 immunostaining was used to identify the endothelial cells of blood vessels.

Ephrin-B1 immunoreactivity was weakly detected in EpCAM-positive spermatogonia (Fig. 1-3A). Ephrin-B1 immunoreactivity was also found in α-SMA-positive peritubular myoid cells (Fig. 1-3B). These ephrin-B1-positive myoid cells were ER-TR7-positive. Strong ephrin-B1 immunoreactivity was detected in CYP17A1-positive Leydig cells (Fig. 1-3C). Ephrin-B1 immunoreactivity was faint or almost negative in the epithelial cells lining of straight tubules lined by Sertoli cells, which were vimentin-positive, strong in the rete testis, and weak in the efferent ductules (Fig. 1-3D, E). A similar staining pattern was obtained in the testis when an ephrin-B1/2/3 antibody, which recognizes all three ephrin-B ligands, was used, whereas ephrin-B1/2/3 immunoreactivity in myoid cells was faint and much weaker compared to ephrin-B1 immunoreactivity (Fig. 1-3F, G).

Strong EphB2 immunoreactivity was detected in elongated spermatids attached to Sertoli cells and the spermatozoa in the lumen of the intratesticular excurrent duct system (Fig.

1-4). EphB2 immunoreactivity was also detected in epithelial cells lining the rete testis and efferent ductules, but not in those lining the straight tubule; EphB2 expression peaked in epithelial cells of the efferent ductules in the genital duct system (Fig. 1-4). In contrast, EphB4 immunoreactivity was detected in spermatogonia, which were EpCAM-positive and located between vimentin-positive Sertoli cells, as well as in peritubular myoid cells and Leydig cells (Fig. 1-5A, B). The expression pattern of EphB4 was similar to that of EphB2 in epithelia of the intratesticular excurrent duct system, except for the straight tubules. Strong EphB4 immunoreactivity was detected in the epithelial cells lining the straight tubules and efferent ductules (Fig. 1-5C, D). Moreover, EphB4 immunoreactivity was faint in the proximal part of the rete testis but was somewhat stronger, although still weak, in the distal part of the rete testis.

Identification of the efferent ductules and segments of the ductus epididymis by lectin staining

The ductus epididymis is histologically divided into five segments: segments I, II, and III in the caput, and segments IV and V in the corpus and cauda epididymis, respectively (Fig. 1-6A). Staining patterns in the epithelia of the ductus epididymis with various lectins, including PNA and UEA-I, have been used to identify these five segments and the efferent ductules (Burkett et al., 1987). Thus, the author used a combination of PNA and UEA-I lectin fluorescence staining to clearly distinguish the ductules and the segments, especially those in the caput epididymis.

The efferent ductules originate from the rete testis by transition from a simple cuboidal epithelium to a simple columnar epithelium. Epithelial cells of the rete testis were PNA-negative, whereas those of the efferent ductules were strongly labeled by PNA (Fig. 1-6B, C). Moreover, epithelial cells of segment I of the ductus epididymis were PNA-negative, whereas the smooth muscle cells surrounding the efferent ductules and all segments of the ductus epididymis were PNA-positive. Thus, the efferent ductules could be easily identified in the caput epididymis by PNA lectin staining. By contrast, UEA-1 staining was faint or negative for epithelial cells of the rete testis, the efferent ductules, and segments I and V; weak for those of segment IV; and strong for those of segments II and III (Fig. 1-6C, D). Both PNA and UEA-I strongly labeled spermatozoa in the lumen of the efferent ductules and ductus epididymis. Thus, the author demonstrated that the combination of PNA and UEA-I lectin staining is a simple method to identify the segments of the mouse genital duct system. The PNA and UEA-I staining patterns are summarized in Table 1-2.

Localization of ephrin-B molecules in the epididymis

Ephrin-B1 immunoreactivity was detected in epithelial cells of the efferent ductules and in all segments of the ductus epididymis (Fig. 1-7A). In particular, ephrin-B1 was strongly expressed in the epithelial cells of segments I, IV, and V of the ductus epididymis. A similar staining pattern was obtained with an ephrin-B1/2/3 antibody in the epithelium of epididymis (Fig. 1-7B). Ephrin-B1 immunoreactivity was localized in the basolateral membrane of principal cells and basal cells of the efferent ductules and the ductus epididymis (Fig. 1-7C).

Ephrin-B1 was also expressed in the smooth muscle cells surrounding the efferent ductules and ductus epididymis; these cells were also α-SMA- and ER-TR7-positive (Fig. 1-8A). ER-TR7-positive and α-SMA-negative cells; i.e., fibroblasts, also expressed ephrin-B1 in the interstitial tissue of the epididymis (Fig. 1-8B).

Localization of EphB2 and EphB4 in the epididymis

EphB2 and EphB4 immunoreactivity were detected in epithelial cells of the efferent ductules. EphB2 immunoreactivity was faint or almost negative in those of the epididymis while EphB4 immunoreactivity was almost negative in principle cells but still faint in basal cells in epithelium of the epididymis (Fig. 1-9).

EphB2 was also expressed in ER-TR7-positive fibroblasts in the interstitial tissue of the epididymis, especially those located at the boundaries between the segments; i.e., the connective tissue septa of the epididymis (Fig. 1-10A). Moreover, EphB2 immunoreactivity was detected in spermatozoa present in the lumen of the proximal parts of the excurrent ductule/duct system. Spermatozoa were strongly EphB2-positive in the lumen extending from the rete testis to segment II of the ductus epididymis, whereas spermatozoa were rarely observed in the lumen of the efferent ductules and segment I in the epididymis (Fig. 1-10B, C). EphB2 immunoreactivity in spermatozoa gradually decreased from segment II to segment V, in which spermatozoa were almost EphB2-negative.

EphB4 immunoreactivity was detected in the α-SMA-positive and ER-TR7-positive smooth muscle cells surrounding the efferent ductules and ductus epididymis (Fig. 1-11A). ER-TR7-positive and α-SMA-negative cells, i.e., fibroblasts, also expressed EphB4 in the interstitial tissue of the epididymis (Fig. 1-11B). EphB4 was also expressed in CD31-positive vascular endothelial cells and, notably, blood vessels were more densely located in segment I

compared to the other segments of the epididymis (Fig. 1-11C).

The author verified the specificity of the staining by incubation the tissue sections without the primary or secondary antibodies. There was no specific immunoreactivity in the control sections without the primary or secondary antibodies. The overall expression patterns of ephrin-B1, EphB2, and EphB4 in the adult mouse testis and epididymis are illustrated in Fig. 1-12.

Discussion

EphB receptors and ephrin-B ligands have been implicated in the physiology and homeostasis of normal adult tissues and organs (Miao and Wang, 2009; Pasquale, 2008). Recent studies have revealed essential roles of EphB receptors and ephrin-B ligands for the maintenance of epithelial integrity, homeostasis and boundary formation in variety of epithelia such as the intestine, stomach, epidermis, and mammary glands (Miao and Wang, 2009; Perez White and Getsios, 2014). The diverse functions assigned to EphB/ephrin-B in the epithelial tissues are mainly related to the complementary expression pattern of the receptors and ligands in adjacent epithelial compartments, although overlapping expression pattern also exists in the epithelial tissues (Miao and Wang, 2009). Such a complementary expression pattern of EphB and ephrin-B has been detected along the crypt-villus axis in the adult intestinal epithelium, and interaction between the EphB-bearing and ephrin-B-bearing cells was shown to induce a cell–cell repulsive signal that prevented EphB-bearing cells from migrating upward into compartments with ephrin-B1-bearing cells; thus, separate ephrin-B- and EphB-expressing compartments are formed in the intestinal epithelium (Batlle and Wilkinson, 2012; Cortina et al., 2007). A similar expression pattern of EphB and ephrin-B was detected along the pit-gland axis of the gastric unit in adult gastric glandular epithelium, and EphB activation by ephrin-B1 was shown to induce a cell–cell repulsive signal in the gastric glandular cells (Ishii et al., 2011b; Ogawa et al., 2011b). Complementary expression patterns of EphB2 and ephrin-B1 were also detected along the proximal-to-distal axis of the adult rodent gastric epithelia across the squamocolumnar epithelial junction (Ogawa et al., 2013), which is located at the boundary between the stomach and esophagus in humans. Moreover, EphB and ephrin-B activation by ephrin-B1 and EphB2, respectively, were shown to induce cell repulsion/lateral migration in primary cultured gastric keratinocytes, suggesting the involvement of EphB2 and ephrin-B1 in epithelial boundary formation at the

squamocolumnar junction (Ogawa et al., 2013). On the basis of these findings, the author hypothesized that the EphB/ephrin-B cell–cell communication system plays a key role in the establishment of tissue organization in the seminiferous tubule, intratesticular tubule/ductule, and the excurrent duct system in the epididymis, which are lined with the tubule/ductule/duct-specific epithelia, respectively. Therefore, the author investigated the EphB/ephrin-B expression in these tubule/ductule/ducts in normal adult mice.

Among the epithelia in the testis and epididymis, the author found that (i) ephrin-B1 was expressed extensively in the excurrent tubule/ductule/duct system, except for the straight tubule, and was highly upregulated in the rete testis and segment I of the ductus epididymis, thus showing two prominent ephrin-B1 expression compartments; (ii) EphB2 was expressed in the rete testis and more strongly in the efferent ductule, thus showing one prominent EphB2 expression compartment; and (iii) EphB4 was expressed in the excurrent system from the straight tubule to the efferent ductule and was highly upregulated in the straight tubule and the efferent ductule, thus showing two prominent EphB4 expression compartments. These expression patterns indicate that the ephrin-B- and EphB-predominant expression compartments appear alternately along the excurrent system, which is lined with the tubule/ductule/duct-specific epithelia. Thus, the compartmentalization based on the ephrin-B and EphB expression patterns corresponds to the histological compartments in the excurrent tubule/ductule/duct system of the testis and caput epididymis as well as the developmental compartments composed of testicular cords (which differentiate into the seminiferous/straight tubules and rete testis), mesonephric tubules (which differentiate into the efferent ductules), and mesonephric duct (which differentiates into the ductus epididymis) (Lupien et al., 2006; Ross and Pawlina, 2015). These expression patterns suggest that strong EphB/ephrin-B signaling likely arises at every epithelial junction along the excurrent tubule/ductule/duct system of the testis and epididymis, specifically at the epithelial junctions between the straight tubules and the rete testis (EphB4/ephrin-B1 signaling), between the rete testis and the efferent ductule (EphB2/ephrin-B1 and EphB4/ephrin-B1 signaling), and between the efferent ductule and segment I of the ductus epididymis (EphB2/ephrin-B1 and EphB4/ephrin-B1 signaling), because EphB receptors promiscuously bind ephrin-B ligands within the same B-subclass (Pasquale, 2005). This speculation is partly supported by the immunoblots showing that EphB2 and EphB4 were tyrosine-phosphorylated in the testis and/or epididymis. It is well accepted that the EphB/ephrin-B cell–cell communication system is involved in tissue-border formation by initiating cell–cell repulsive signals between ephrin-B-bearing and EphB-bearing cells (Batlle and Wilkinson, 2012; Kullander and Klein, 2002; Pasquale, 2005).

Therefore, the author proposes that the interplay between EphB and ephrin-B may regulate/maintain epithelial boundaries along the excurrent tubule/ductule/duct system of the testis and epididymis.

In the testis, the author found that spermatogonia, peritubular myoid cells, and Leydig cells express ephrin-B1 and EphB4. Leydig cells and myoid cells are considered to be cellular components of the niche for spermatogonial stem cells, a subtype of undifferentiated spermatogonia (Potter and DeFalco, 2017); however, it is difficult to clearly distinguish spermatogonial stem cells from spermatogonia in the adult testis, and therefore the niche itself, because it was shown that spermatogonia committed to differentiation and undergoing spermatogenesis recover stem cell potential (Nakagawa et al., 2010). In the bone marrow, EphB/ephrin-B has been implicated in modulating the niche for hematopoietic stem cells (Nguyen et al., 2016). Stromal cells and hematopoietic stem cells express EphB4 and ephrin-B2, respectively, and EphB4/ephrin-B2 signaling arising from cell–cell contact regulates the expression of diverse cytokines to mediate hematopoiesis (Nguyen et al., 2015) as well as the migration and colonization of the hematopoietic cells (Okubo et al., 2006). It is intriguing whether EphB4/ephrin-B1 signaling mediated by cell–cell contacts among spermatogonia, myoid cells, and Leydig cells is involved in spermatogonial niche formation, similar to that observed in the niche for hematopoietic stem cells. A laminin-immunostaining study showed that basement membranes surrounding seminiferous tubules are discontinuous in certain regions (Hager et al., 2005). This indicates that spermatogonia possibly contact the stromal cells, and thus EphB4/ephrin-B1 signaling arises from cell–cell contacts not only within spermatogonia but also between the spermatogonia and stromal cells. The author found relatively strong tyrosine phosphorylation of EphB4 in the testis, suggesting the contact of EphB4-bearing cells with ephrin-B-bearing cells. Further investigations will be required to reveal the EphB4/ephrin-B1 interaction implicated in spermatogonial niche formation.

Furthermore, elongated spermatids adhering to the Sertoli cells expressed EphB2 as well as immature spermatozoa, located in the lumen of the excurrent tubule/ductule system in the testis and the ductus epididymis in the caput and corpus, also expressed EphB2 but not the mature spermatozoa located in the cauda epididymis. Moreover, EphB2 was tyrosine-phosphorylated in the testis although the author did not immunohistochemically detect the ephrin-B-expressing cells that likely come in contact with the EphB2-positive spermatids (i.e., the Sertoli cells) possibly because of the difference in the detection ability between the blotting and immunohistochemistry techniques. It is reported that EphB2 signaling induced by ephrin-B1 activates the membrane-bound metalloproteinase ADAM10 (Solanas et al., 2011),

which is involved in the ectodomain cleavage of transmembrane proteins, including cell adhesion molecules of the junctional adhesion molecule (JAM) family and nectin family (Buchanan et al., 2017; Koenen et al., 2009; Saftig and Lichtenthaler, 2015), both of which are expressed in spermatids and are located in the apical compartment at the Sertoli–spermatid interface (*i.e.*, the apical ES, or F-actin-rich endoplasmic specialization) to connect spermatids with the Sertoli cells (Qian et al., 2014). Moreover, ADAM10 is expressed in spermatids and spermatozoa (Urriola-Munoz et al., 2014). Thus, it is possible that EphB2 signaling via ADAM10 activation in spermatids is involved in the shedding of junctional adhesion molecules and nectin molecules, thus leading to spermiation, during which destabilization of adhesion proteins occurs in the apical ES (Qian et al., 2014). Further investigations will be required to reveal the role of EphB2 signaling in spermiation. However, the author cannot speculate the biological significance of the EphB2 expression in spermatozoa located in the lumen of the excurrent tubule/ductule/duct system at present, because the EphB2 expression disappeared in the spermatozoa located in the ductus epididymis of the cauda epididymis, where mature spermatozoa with fertilizing capacity are temporarily stored (Cornwall, 2009). This indicates that EphB2 is not required by mature spermatozoa and that EphB2 expression can be a new negative indicator for the maturation of spermatozoa. In contrast, EphB2 expression in immature spermatozoa in the ductus epididymis in the caput and corpus suggests the potential involvement of EphB2 in sperm communication with the somatic cells during post-testicular sperm maturation. In particular, ephrin-B1 was expressed strongly in the epithelial cells but was localized in the basolateral membrane. Thus, EphB2 interaction with ephrin-B1 is unlikely to occur when immature spermatozoa contact with the epithelial cells. This may be partly supported by the immunoblotting finding that EphB2 was not tyrosine-phosphorylated in the caput epididymis.

The author also found that (i) ephrin-B1 was extensively expressed in the basolateral membrane of epithelial cells in the ductus epididymis system of all segments and (ii) EphB4 and ephrin-B1 were expressed in the smooth muscle cells surrounding the ductus epididymis, and EphB4 was extensively tyrosine-phosphorylated in the epididymis. A similar expression pattern was reported in the rodent mammary gland: EphB4 and ephrin-B2 were primarily expressed in myoepithelial cells surrounding the ducts/alveoli and the luminal epithelial cells of mouse mammary glands, respectively, in an estrogen-dependent manner in ovariectomized mice. Moreover, these expression patterns were disrupted during experimental mammary carcinogenesis (Nikolova et al., 1998). The development and homeostasis of the epididymis are largely regulated by androgen (Cornwall, 2009; Robaire and Hamzeh, 2011). Thus,

androgen may control the expression of EphB/ephrin-B, thereby regulating homeostasis of the ductus epididymis. The ductus epididymis consists of a pseudostratified epithelium of several cell types, including principal cells and basal cells, and is surrounded by a few layers of smooth muscle cells. The cell–cell interactions within the epithelium can directly affect the luminal environment, and ultimately sperm maturation. The principal cells form tight junctions with one another, thus forming the blood–epididymis barrier, which creates an immunoprotective site essential for sperm maturation, within the epididymal lumen (Cornwall, 2009). Several androgen-dependent transmembrane proteins, including occludin and claudins, contribute to the formation of these tight junctions (Cyr et al., 2007). It is reported that ephrin-B1 directly interacts with claudins, and this interaction affects tight junction integration in normal epithelial cells (Tanaka et al., 2005). Thus, it is intriguing whether ephrin-B1, without interaction with EphB receptors, directly regulates tight junction integration between epithelial cells in the ductus epididymis. Further investigation will be required to reveal the role of ephrin-B1 in formation of the blood–epididymis barrier.

Summary

The present study represents the first expression analysis of EphB receptors and ephrin-B ligands in the normal adult testis and epididymis. All mammalian EphB receptors and ephrin-B ligands were expressed in the testis and epididymis of the adult mouse. The author found the characteristic ephrin-B1, EphB2 and EphB4 expression patterns in the epithelia of the excurrent tubule/ductule/duct system in the testis and epididymis: ephrin-B1 was strongly expressed in epithelia of the rete testis and the segment I in the ductus epididymis while EphB2 and/or EphB4 were strongly expressed in those of the straight tubules and the efferent ductules, *i.e.*, the ephrin-B1- and EphB-predominant expression compartments appear alternately along the excurrent system, which is lined with the tubule/ductule/duct-specific epithelia. This compartmentalization corresponds to the histological compartments in the excurrent tubule/ductule/duct system as well as the developmental compartments composed of the testicular cords, mesonephric tubules, and mesonephric duct. The author also found that EphB4 and ephrin-B1 was expressed in spermatogonia, peritubular myoid cells and Leydig cells, and EphB2 was expressed in elongated spermatids and immature spermatozoa (in the proximal part (caput and corpus) of epididymis), and that these receptors were tyrosine-phosphorylated and activated in the testis

and/or epididymis, suggesting that EphB/ephrin-B signaling might occur in seminiferous tubules as well as epithelial junctions among the straight tubules, the rete testis, the efferent ductules and the epididymal duct. Based on these findings, the author proposes that the EphB receptors and the ephrin-B ligand represent candidate molecules for regulating epithelial boundary formation in the excurrent tubule/ductule/duct system as well as for modulating spermatogenesis and spermiation. Moreover, EphB2 expression can be a new negative indicator for the maturation of spermatozoa. The present findings may bring a new insight toward regeneration of the male genital duct system, which is formed by the binding of developmentally different tissues.

Table 1-1 Primers and cycle numbers for PCR amplification

Primer			Product size (bp)	Annealing temp. (°C)	Cycle number
ephrin-B1	Forward	5´-TGCTTGATCCCAATGTACTG-3´	520	55.0	35
	Reverse	5´-CGGAGCTTGAGTAGTAGGAC-3´			
ephrin-B2	Forward	5´-ACCCACAGATAGGAGACAAA-3´	371	53.5	35
	Reverse	5´-GGTTGATCCAGCAGAACTTG-3´			
ephrin-B3	Forward	5´-CCGCTTCACCATCAAGTTCC-3´	618	55.1	35
	Forward	5´-TCACCGCTCACCTTCTCGTA-3´			
EphB1	Forward	5´-AATGGCATCATCCTGGACTA-3´	464	53.4	35
	Reverse	5´-TCAATCTCCTTGGCAAACTC-3´			
EphB2	Forward	5´-CGACGAGAACATGAACACTA-3´	583	53.0	35
	Reverse	5´-CCCGTTACAGTAGAGTTTGA-3´			
EphB3	Forward	5´- TGAGACCTCGCTAATCCTCG-3´	555	59.0	35
	Reverse	5´-TGTCCGTAACCCGCTACTGT-3´			
EphB4	Forward	5´-AGCCCCAAATAGGAGACGAG-3´	540	57.9	35
	Reverse	5´-GGATAGCCCATGACAGGATC-3´			
EphB6	Forward	5´-CCGAGAGACCTTCACCCTTT-3´	484	58.5	35
	Reverse	5´-CCTGCCTTCGCCATTACAGT-3´			
GAPDH	Forward	5´-GACTCCACTCACGGCAAATT-3´	689	57.5	23
	Reverse	5´-TCCTCAGTGTAGCCCAAGAT-3´			

Table 1-2 PNA and UEA-I lectin staining pattern in the epithelium of the excurrent duct system of adult mouse

Epithelium	PNA	UEA-I
Rete testis (RT)	−	−
Efferent ductule (ED)	++	−
Segment I, epididymis (Seg I)	−	±
Segment II, epididymis (Seg II)	+	++
Segment III, epididymis (Seg III)	++	++
Segment IV, epididymis (Seg IV)	++	+
Segment V, epididymis (Seg V)	++	±

–, negative; ±, faint stain; +, weak stain; ++, strong stain

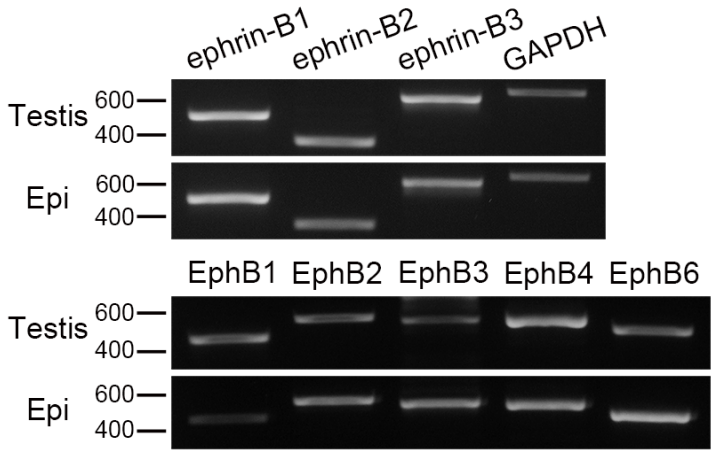
ephrin-B1
ephrin-B2
ephrin-B3
GAPDH
Testis
600
400
Epi
600
400
EphB1
EphB2
EphB3
EphB4
EphB6
Testis
600
400
Epi
600
400

Fig. 1-1

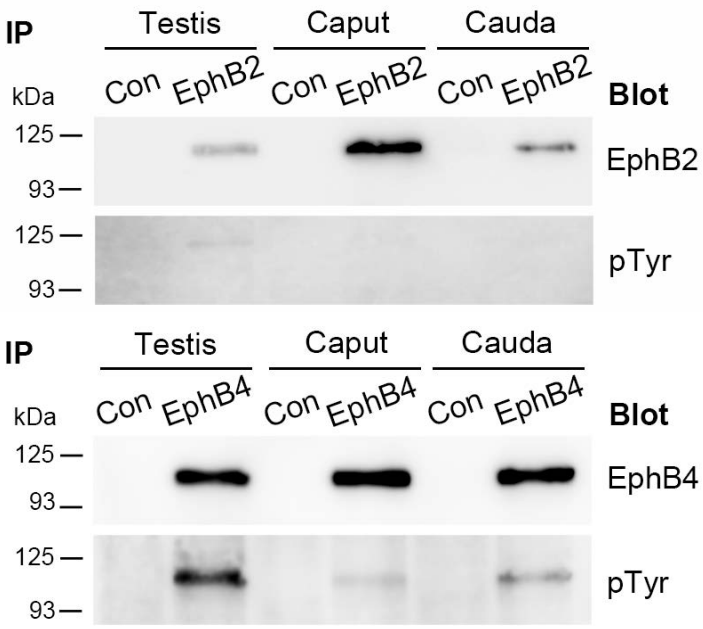
IP
Testis
Caput
Cauda
kDa
Con
EphB2
Con
EphB2
Con
EphB2
Blot
125
93
EphB2
125
93
pTyr
IP
Testis
Caput
Cauda
kDa
Con
EphB4
Con
EphB4
Con
EphB4
Blot
125
93
EphB4
125
93
pTyr

Fig. 1-2

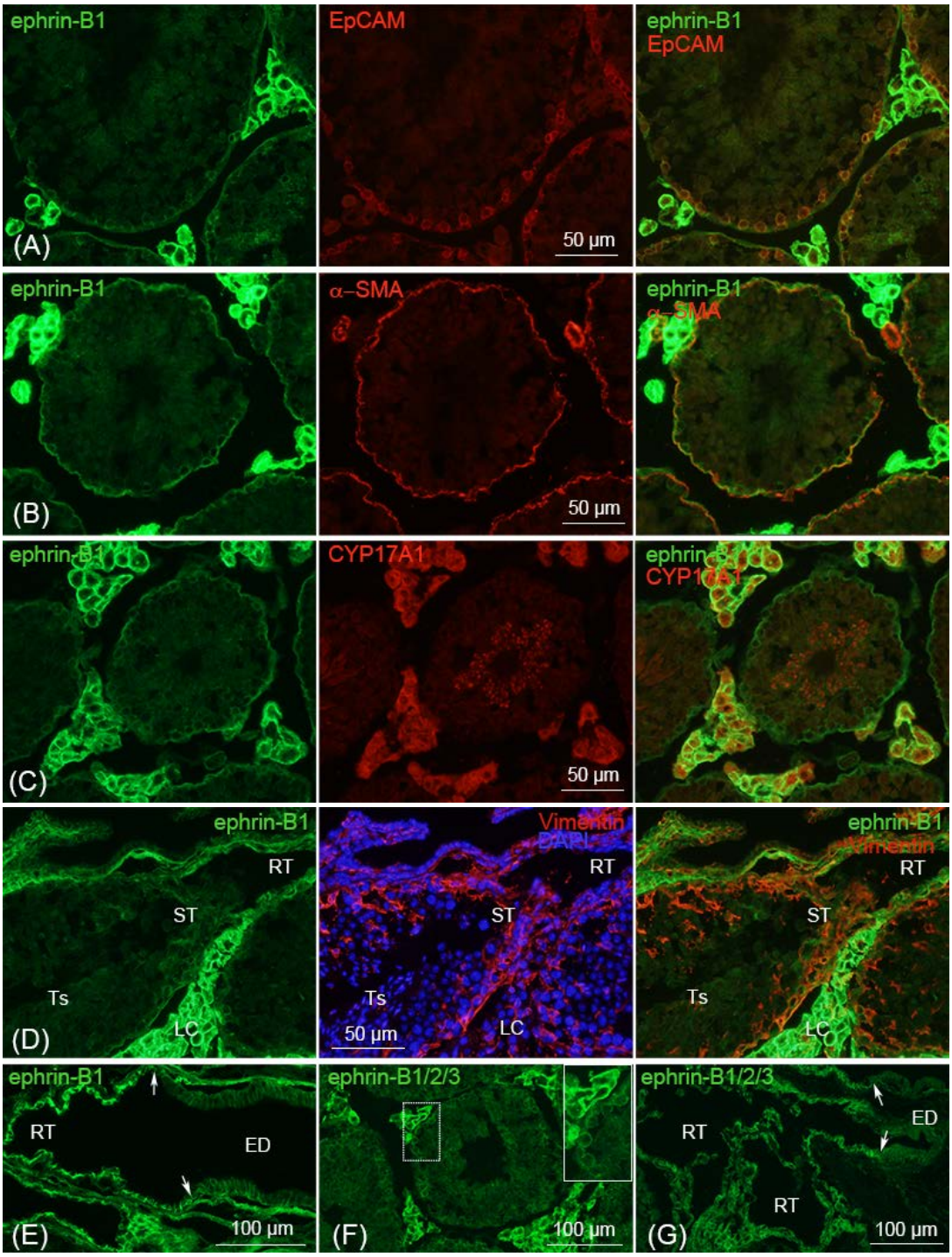
ephrin-B1
EpCAM
ephrin-B1
EpCAM
(A)
50 μm
ephrin-B1
α–SMA
ephrin-B1
α–SMA
(B)
50 μm
ephrin-B1
CYP17A1
ephrin-B1
CYP17A1
(C)
50 μm
ephrin-B1
RT
ST
Ts
LC
(D)
Vimentin
DAPI
RT
ST
Ts
LC
50 μm
ephrin-B1
Vimentin
RT
ST
Ts
LC
ephrin-B1
RT
ED
(E)
100 μm
ephrin-B1/2/3
(F)
100 μm
ephrin-B1/2/3
RT
ED
RT
(G)
100 μm

Fig. 1-3

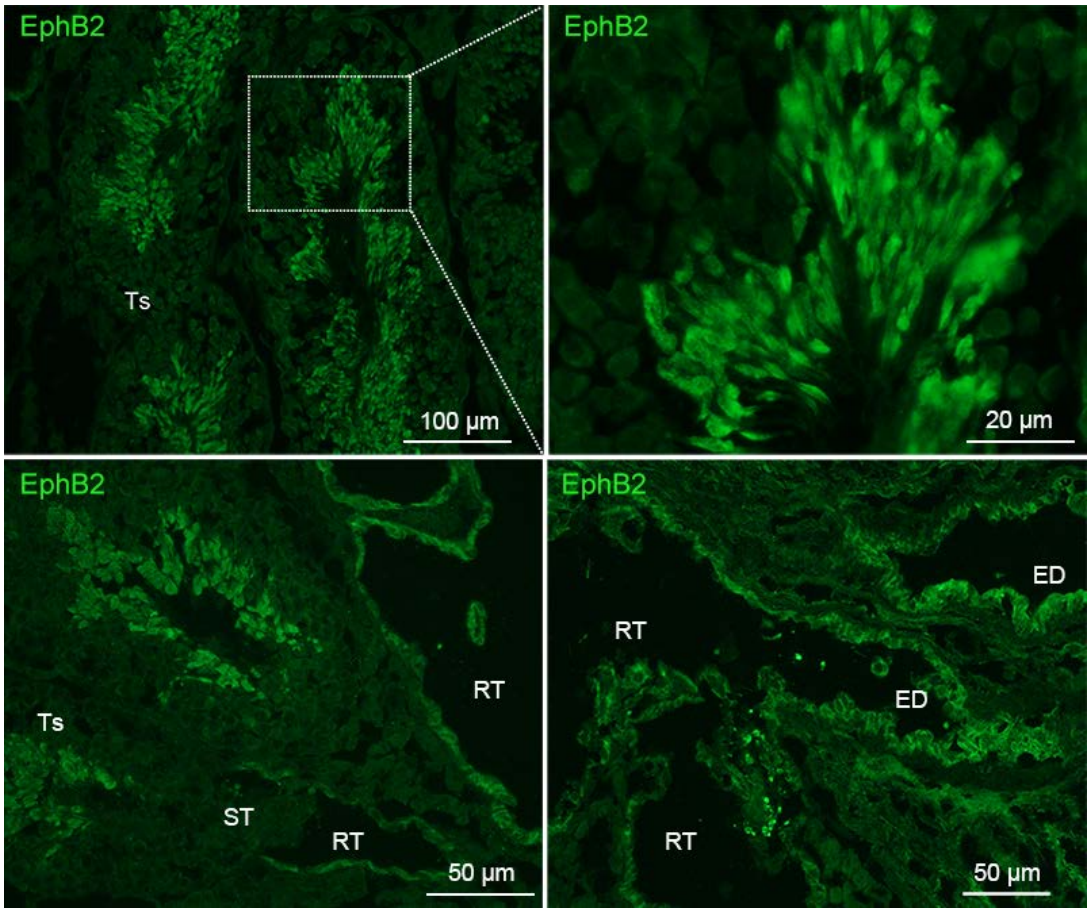
EphB2
Ts
100 μm
EphB2
20 μm
EphB2
Ts
RT
ST
RT
50 μm
EphB2
ED
RT
ED
RT
50 μm

Fig. 1-4

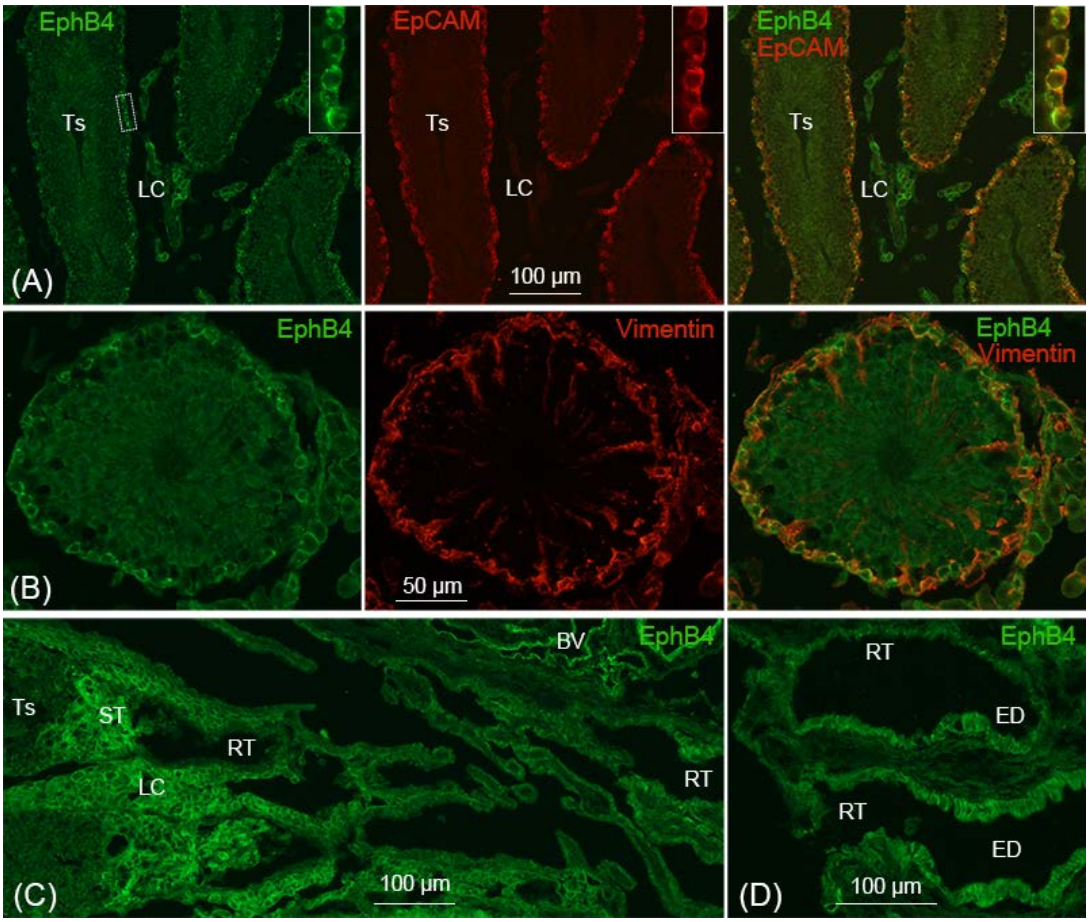
EphB4
Ts
LC
(A)
EpCAM
Ts
LC
100 μm
EphB4
EpCAM
Ts
LC
EphB4
(B)
Vimentin
50 μm
EphB4
Vimentin
BV
EphB4
Ts
ST
RT
LC
RT
100 μm
(C)
RT
EphB4
ED
RT
ED
100 μm
(D)

Fig. 1-5

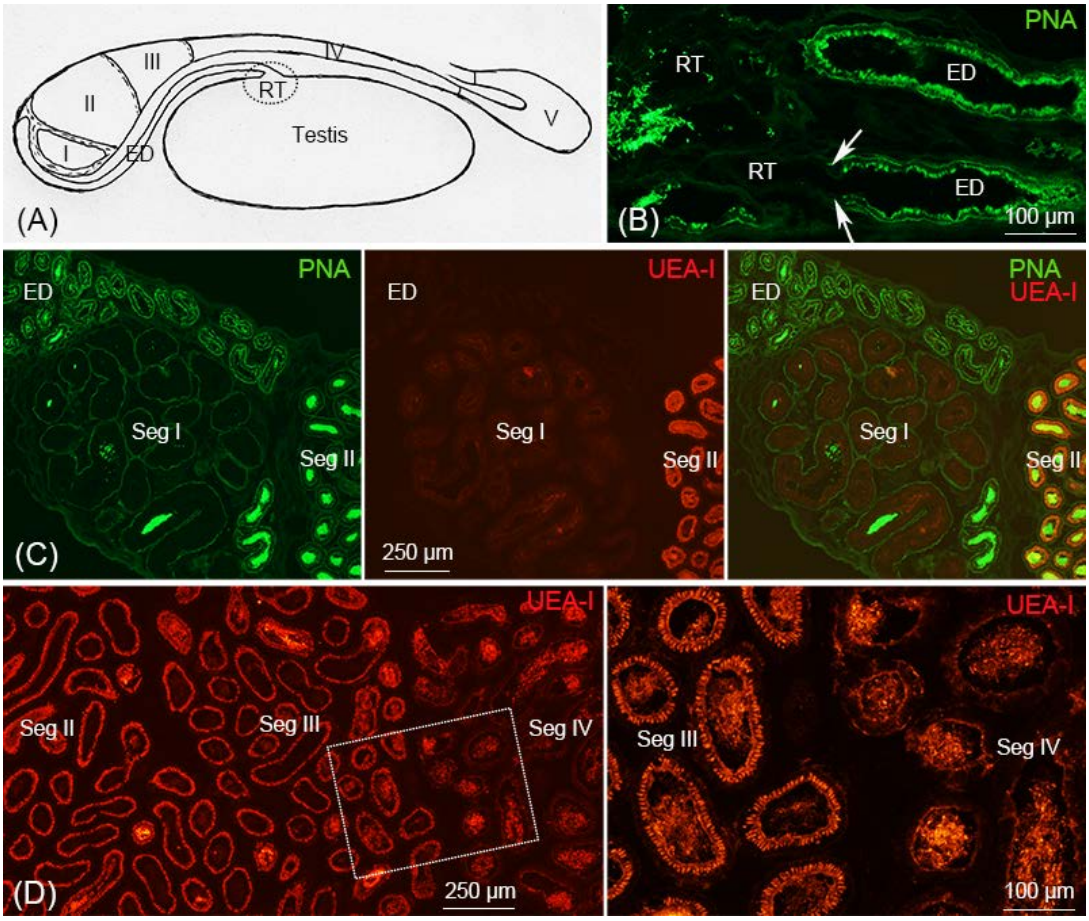
(A)
I
II
III
IV
V
RT
ED
Testis
(B)
PNA
RT
ED
RT
ED
100 µm
(C)
PNA
ED
Seg I
Seg II
UEA-I
ED
Seg I
Seg II
250 µm
PNA
UEA-I
ED
Seg I
Seg II
(D)
UEA-I
Seg II
Seg III
Seg IV
250 µm
UEA-I
Seg III
Seg IV
100 µm

Fig. 1-6

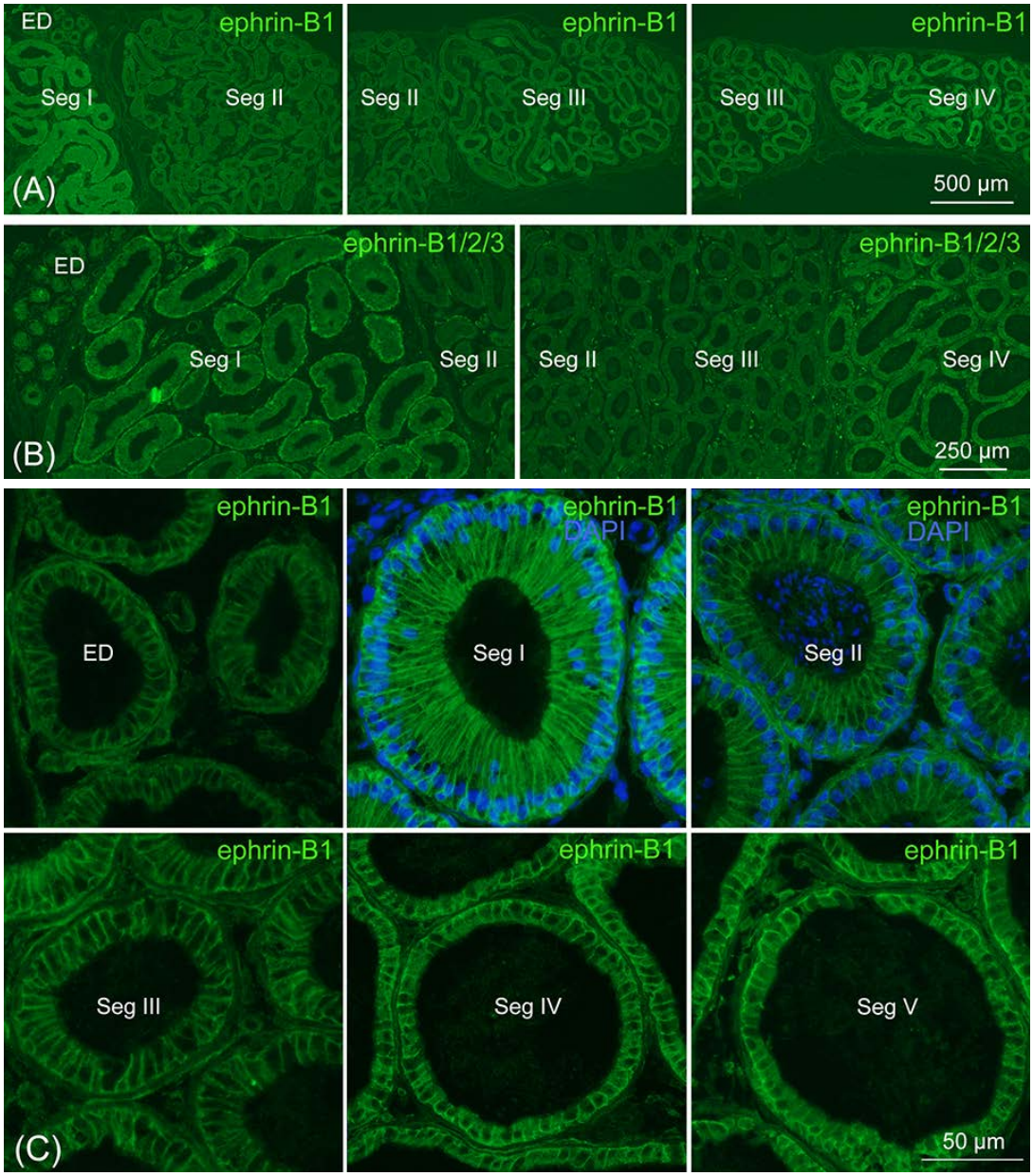
ED
ephrin-B1
Seg I
Seg II
(A)
ephrin-B1
Seg II
Seg III
ephrin-B1
Seg III
Seg IV
500 μm
ephrin-B1/2/3
ED
Seg I
Seg II
(B)
ephrin-B1/2/3
Seg II
Seg III
Seg IV
250 μm
ephrin-B1
ED
ephrin-B1
DAPI
Seg I
ephrin-B1
DAPI
Seg II
ephrin-B1
Seg III
(C)
ephrin-B1
Seg IV
ephrin-B1
Seg V
50 μm

Fig. 1-7

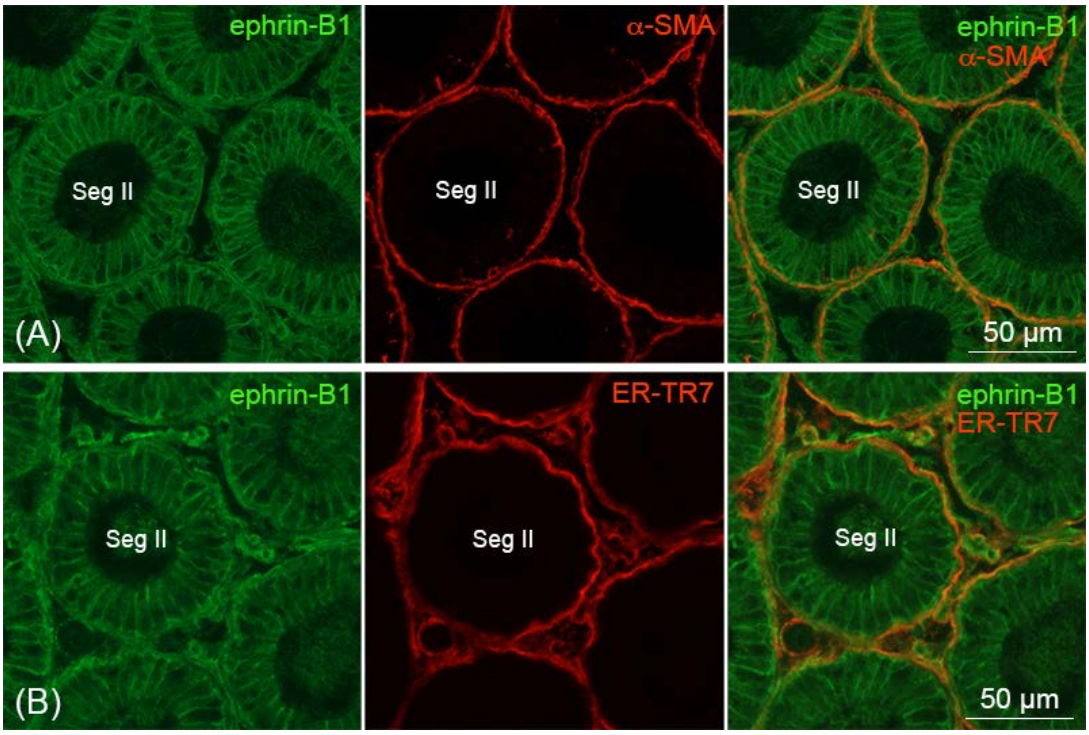
ephrin-B1
Seg II
α-SMA
Seg II
ephrin-B1
α-SMA
Seg II
(A)
50 μm
ephrin-B1
Seg II
ER-TR7
Seg II
ephrin-B1
ER-TR7
Seg II
(B)
50 μm

Fig. 1-8

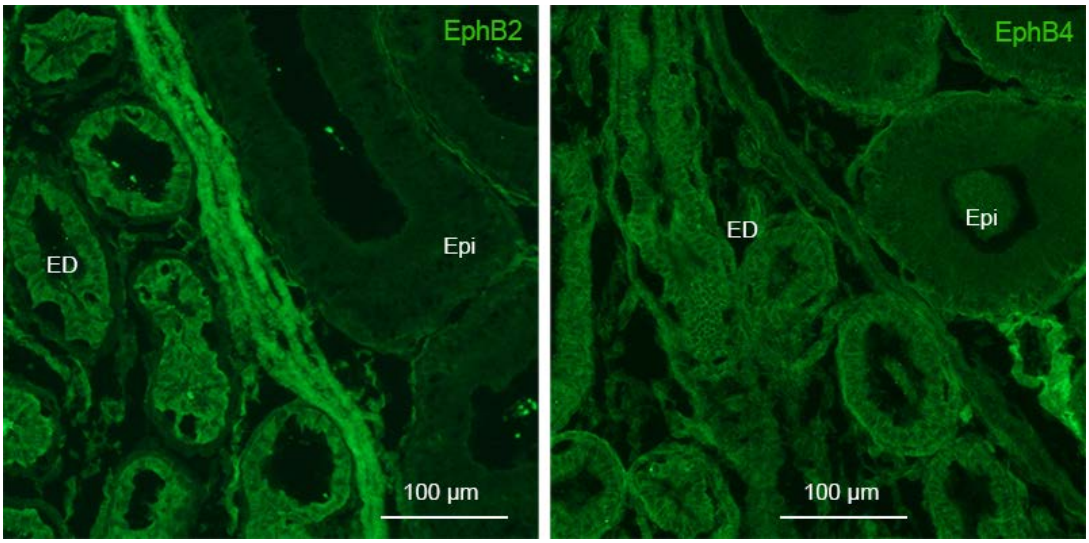

Fig. 1-9

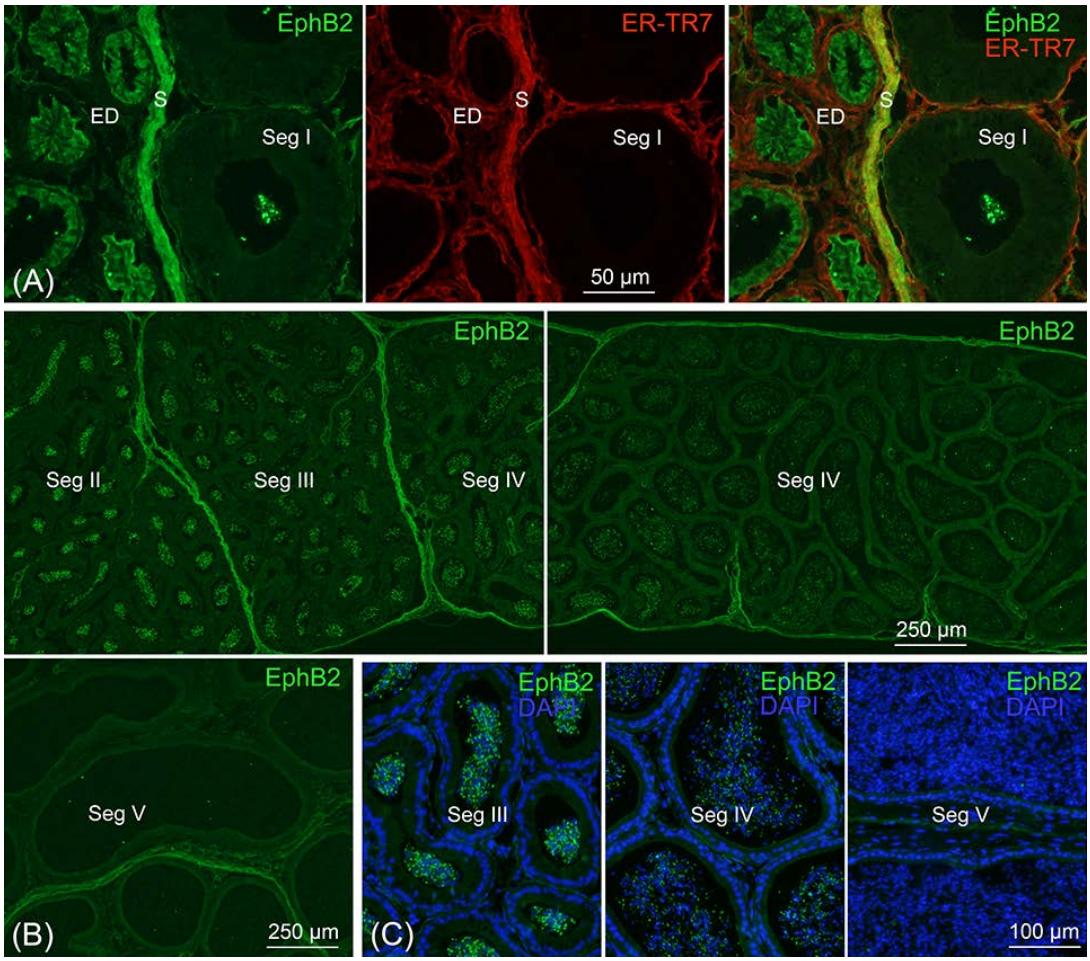
EphB2
ED
S
Seg I
(A)
ER-TR7
50 μm
EphB2
ER-TR7
Seg II
Seg III
Seg IV
250 μm
Seg V
(B)
DAPI
(C)
100 μm

Fig. 1-10

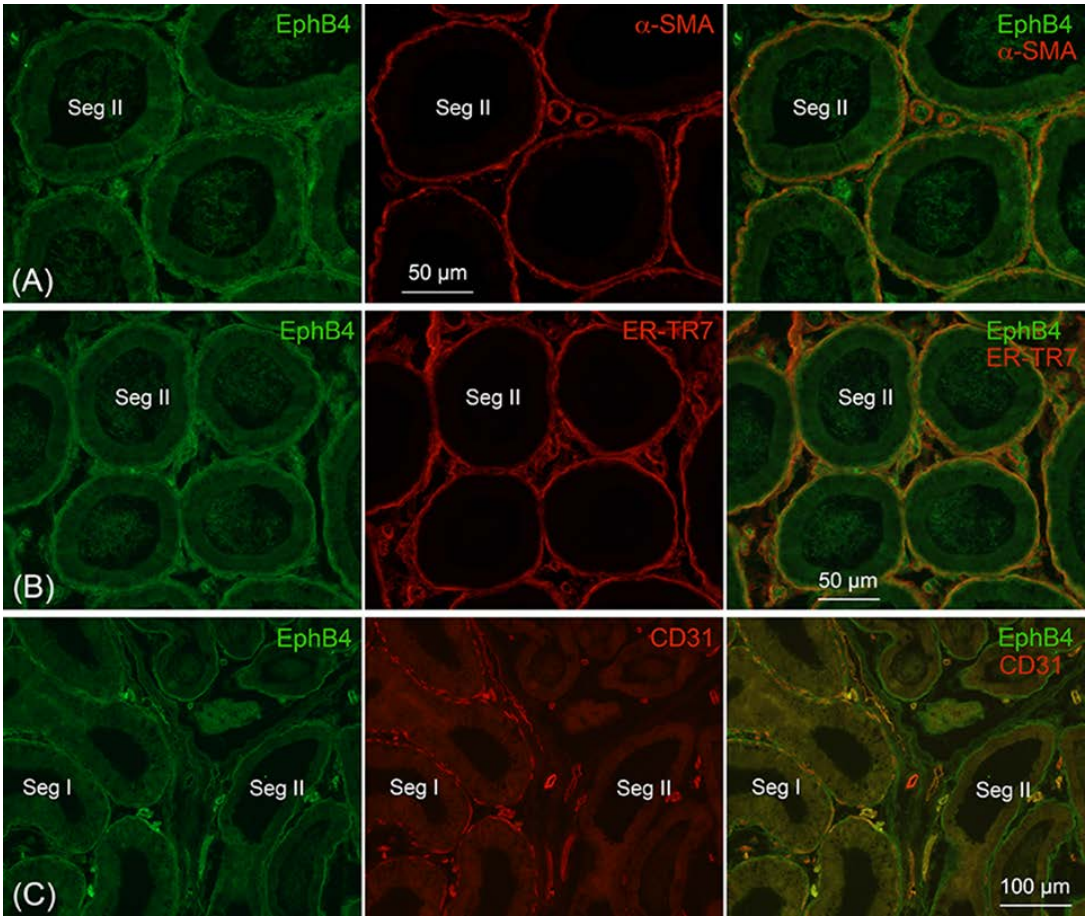
EphB4
Seg II
α-SMA
Seg II
50 μm
EphB4
α-SMA
Seg II
(A)
EphB4
Seg II
ER-TR7
Seg II
EphB4
ER-TR7
Seg II
50 μm
(B)
EphB4
Seg I
Seg II
CD31
Seg I
Seg II
EphB4
CD31
Seg I
Seg II
100 μm
(C)

Fig. 1-11

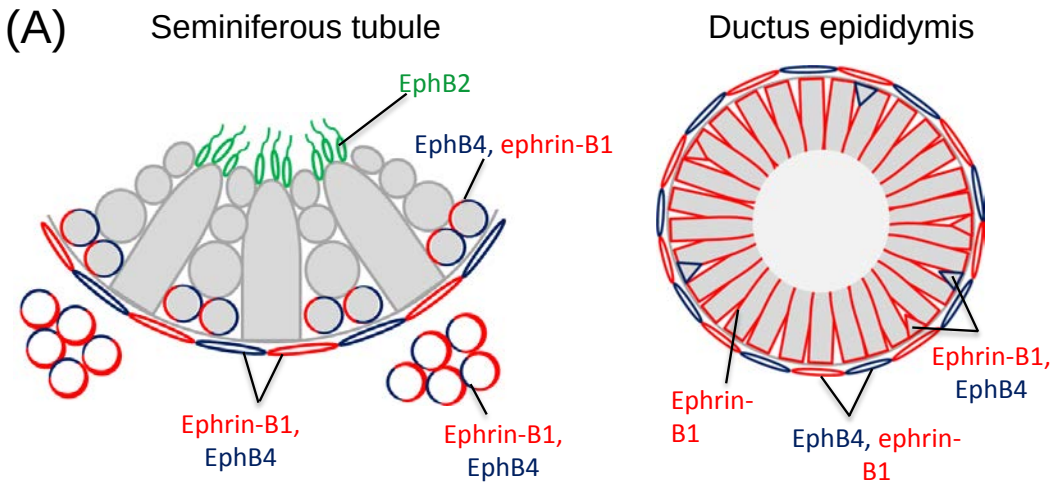
(A)
Seminiferous tubule
Ductus epididymis
EphB2
EphB4, ephrin-B1
Ephrin-B1, EphB4
Ephrin-B1, EphB4
Ephrin-B1
Ephrin-B1, EphB4
EphB4, ephrin-B1
(B) Epithelia of the excurrent duct system
Testis
ED
Epididymis
Ts
ST
RT
I
II
III
IV
V
Expression level
ephrin-B1
EphB2
EphB4

Fig. 1-12

Figure legends

Figure 1-1

Expression of ephrin-B and EphB in the testis and epididymis (Epi) of the adult mouse. Amplification of for ephrin-B and EphB mRNA by RT-PCR. Total RNA was isolated from the testis (without tunica albuginea) and epididymis and transcribed into first-strand cDNA using M-MLV RNase H^- reverse transcriptase and oligo $(dT)_{18}$ primer. The reaction mixture was amplified by PCR with Taq DNA polymerase to detect endogenous ephrin-B ligands and EphB receptors. Substantial levels of endogenous all mammalian EphB receptors (B1, B2, B3, B4, B6) and ephrin-B ligands (B1-B3) are amplified in both testis and epididymis, although EphB1 is faintly detected in epididymis with 35 cycles of PCR amplification.

Figure 1-2

EphB2 and EphB4 protein expression and tyrosine phosphorylation in the testis and epididymis of the adult mouse. Lysates (1000 μg protein) from the testis, the caput and cauda epididymis were immunoprecipitated with the indicated anti-EphB antibodies (IP). Immunoprecipitates were separated on 10% polyacrylamide gels and transferred onto PVDF membranes. The PVDF membranes were incubated with 1:5,000 anti-phosphotyrosine antibody (pTyr). Immunoblots were developed using using ECL Prime chemiluminescence reagents. The membrane was reprobed with the indicated antibodies. EphB2 and EphB4 proteins are detected in the testis and epididymis. EphB2 protein expression in the caput are more intense than that in the cauda epididymis. EphB2 in the testis and EphB4 in the testis and epididymis are tyrosine-phosphorylated. Con, control.

Figure 1-3

Immunofluorescence micrographs showing ephrin-B localization in the adult mouse testis. Sections were stained with the indicated antibodies and/or DAPI. (A) Double immunofluorescence staining showing ephrin-B1 and EpCAM expression in the seminiferous tubules. Ephrin-B1 is expressed in EpCAM-positive spermatogonia. (B) Double immunofluorescence staining showing ephrin-B1 and α-SMA expression in the seminiferous tubules. Ephrin-B1 is expressed in α-SMA-positive peritubular myoid cells. (C) Double immunofluorescence staining showing ephrin-B1 and CYP17A1 expression in the seminiferous tubules. Ephrin-B1 is expressed strongly in CYP17A1-positive Leydig cells. (D) Double immunofluorescence staining showing ephrin-B1 and vimentin expression in the

intratesticular excurrent duct system. Ephrin-B1 is expressed in epithelial cells of the rete testis. (E) Ephrin-B1 expression in epithelial cells in the rete testis is stronger than that in epithelial cells in the efferent ductules. (F, G) Immunofluorescence micrographs using a pan-ephrin-B antibody (ephrin-B1/2/3). The immunoreactivity with the ephrin-B1/2/3 antibody is similar to that detected with the ephrin-B1 antibody. Arrows indicate the epithelial boundary between the rete testis and efferent ductules. ED, efferent ductule; LC, Leydig cell; RT, rete testis; ST, straight tubule; Ts, seminiferous tubule.

Figure 1-4

Immunofluorescence micrographs showing EphB2 localization in the adult mouse testis. EphB2 immunoreactivity is detected in elongated spermatids in the seminiferous tubules, and in the epithelial cells of the rete testis and efferent ductules. ED, efferent ductule; RT, rete testis; ST, straight tubule; Ts, seminiferous tubule.

Figure 1-5

Immunofluorescence micrographs showing EphB4 localization in the adult mouse testis. Sections were stained with the indicated antibodies. (A) Double immunofluorescence staining showing EphB4 and EpCAM expression in the seminiferous tubules. EphB4 is expressed in EpCAM-positive spermatogonia and Leydig cells. (B) Double immunofluorescence staining showing EphB4 and vimentin expression in the seminiferous tubules. EphB4-positive spermatogonia are located between vimentin-positive Sertoli cells. EphB4 is also expressed in peritubular myoid cells and Leydig cells. (C, D) EphB4 immunoreactivity in the intratesticular excurrent system. EphB4 immunoreactivity in epithelial cells is strong in the straight tubules, faint in the proximal part of the rete testis, gradually increases toward the distal part of the rete testis, and again is relatively strong in the efferent ductules. BV, blood vessel; ED, efferent ductule; LC, Leydig cell; RT, rete testis; ST, straight tubule; Ts, seminiferous tubule.

Figure 1-6

Subdivision of the excurrent duct system in the adult mouse epididymis by lectin histochemistry. (A) A schematic drawing of the testis and epididymis showing five segments (I–V). (B-D) PNA and UEA-I lectin staining of the excurrent duct system showing clear divisions into the efferent ductules; segments I, II, and III in the caput, and segment IV corresponding to the corpus epididymis. Arrows in panel (B) indicate the boundary between

the rete testis and efferent ductule. ED, efferent ductule; RT, rete testis; Seg, segment; ST, straight tubule; Ts, seminiferous tubule.

Figure 1-7

Immunofluorescence micrographs showing ephrin-B localization in the epithelium of the adult mouse epididymis. Sections were stained with the indicated antibodies and/or DAPI. (A) Immunofluorescence micrographs showing an overview of ephrin-B1 expression. Ephrin-B1 immunoreactivity is strong in the ductus epididymis of segments I and IV. (B) Immunofluorescence micrographs using a pan-ephrin-B antibody (ephrin-B1/2/3). The immunoreactivity with the ephrin-B1/2/3 antibody is similar to that detected with the ephrin-B1 antibody. (C) Immunofluorescence micrographs showing ephrin-B1 expression in epithelial cells of the ductus epididymis. Ephrin-B1 immunoreactivity is localized in the basolateral membrane of principal cells and basal cells of the epithelium. ED, efferent ductule; Seg, segment.

Figure 1-8

Double immunofluorescence micrographs showing ephrin-B1 localization in the adult mouse epididymis. (A) Double immunofluorescence staining showing ephrin-B1 and α-SMA expression in the ductus epididymis. Ephrin-B1 is expressed in α-SMA-positive periductal smooth muscle cells. (B) Double immunofluorescence staining showing ephrin-B1 and ER-TR7 expression in the ductus epididymis. Ephrin-B1 is expressed in ER-TR7-positive fibroblasts. Seg II, segment II.

Figure 1-9

Immunofluorescence micrographs showing EphB2 and EphB4 localization in the efferent ductules and caput epididymis. Sections were stained with the indicated antibodies. EphB2 and EphB4 immunoreactivity are detected in epithelial cells of the efferent ductules. EphB2 immunoreactivity is almost negative in those of the epididymis while EphB4 immunoreactivity is almost negative in principle cells but faint in basal cells in epithelium of the epididymis. ED, efferent ductule; Epi, ductus epididymis.

Figure 1-10

Immunofluorescence micrographs showing EphB2 localization in the adult mouse epididymis. Sections were stained with the indicated antibodies and/or DAPI. (A) Double

immunofluorescence staining showing EphB2 and ER-TR7 expression in the caput epididymis. EphB2 is expressed in epithelia of the efferent ductules and ER-TR7-positive fibroblasts, and is prominently expressed in the connective tissue septa of the epididymis. (B, C) EphB2 immunoreactivity in spermatozoa in the lumen of the ductus epididymis is strong in the proximal parts and gradually decreases from segment II to segment V, in which almost all spermatozoa are EphB2-negative. ED, efferent ductule; S, Septa; Seg, segment.

Figure 1-11

Immunofluorescence micrographs showing EphB4 localization in the adult mouse epididymis. Sections were stained with the indicated antibodies. (A) Double immunofluorescence staining showing EphB4 and α-SMA expression in the ductus epididymis. EphB4 is expressed in α-SMA-positive periductal smooth muscle cells. (B) Double immunofluorescence staining showing EphB4 and ER-TR7 expression. EphB4 is expressed in ER-TR7-positive fibroblasts in the interstitial tissue. (C) Double immunofluorescence staining showing EphB4 and CD31 expression. EphB4 is expressed in CD31-positive blood vessels, which are dense in the interstitial tissue of the segment I. Seg, segment.

Figure 1-12

Schematic drawings of the testis and epididymis illustrating expression patterns and levels of ephrin-B1, EphB2, and EphB4. (A) Schematic drawing of the seminiferous tubule and ductus epididymis, illustrating the expression patterns of ephrin-B1, EphB2, and EphB4. (B) Schematic drawing illustrating the relative expression levels of ephrin-B1, EphB2, and EphB4 in epithelia in the intratesticular excurrent system and the ductus epididymis. Ephrin-B1- and EphB-predominant expression compartments appear alternately in the epithelia along the excurrent duct system. ED, efferent ductule; RT, rete testis; ST, straight tubule; Ts, seminiferous tubule; I–V, segments I–V.

Chapter 2

Expression and localization of ephrin-B1, EphB2 and EphB4 in the mouse testis during the postnatal development

Introduction

The testis is the primary organ of male reproductive system and is developed from the primary sex cords, in which primordial germ cells/gonocytes migrate from the yolk sac. The primary sex cords differentiate into testicular cords (seminiferous cords) and then seminiferous tubules. Seminiferous tubules at birth are lined by Sertoli cells and contain gonocytes. Gonocytes differentiate into spermatogonial stem cells/spermatogonia during days 3–6 after birth in the mouse: according to this differentiation, cell position changes from the luminal to basal side (gonocytes in the luminal side and spermatogonia in the basal side of seminiferous tubules) (Bellve et al., 1977). Then spermatogonia differentiate into spermatocytes that undergo meiosis and give rise to haploid round spermatids, which finally differentiate into spermatozoa: according to this differentiation, cell position changes from the basal to luminal side (spermatogonia in the basal side and spermatocytes in the luminal side of seminiferous tubules) (Bellve et al., 1977). Spermatogenesis starts shortly after birth (postnatal days 3 to 6) and the first wave of spermatogenesis completes at postnatal day 35 in mice (Abe et al., 1991; Montoto et al., 2012; Tiptanavattana et al., 2015). Therefore, all types of germ cells in the differentiation process appear in the seminiferous tubules at 5 weeks of age in mouse, i.e., the seminiferous tubules are completed in the adult morphology at 5 weeks. In contrast, though the rete testis connects to efferent ductules at embryonic day 13.5 (E13.5) (Murashima et al., 2015), the intratesticular duct system is histologically completed around postnatal day 18 in mice when seminiferous tubules, straight tubules and the rete testis clearly appear with adult morphological characteristics peculiar to respective epithelia (Malolina and Kulibin, 2017). Moreover, the ratio of the stromal/interstitial tissue to the parenchyma (seminiferous tubules) is decreased during postnatal development (Montoto et al., 2012). Leydig cells, which reside in a group in the connective tissue stroma between seminiferous tubules in the adult testis, increase in number during postnatal development until they reach the adult population (Chen et al., 2009). Leydig cells per testis mostly increase between postnatal days 21 to 31 in mice, and decrease slightly thereafter (Vergouwen et al., 1993).

Smooth muscle cells termed peritubular myoid cells are another major component in the testicular interstitium. They are cuboidal or fusiform before birth, become more elongated after birth, and surround the seminiferous tubules with interposition of the basal lamina (Vergouwen et al., 1993; Ross and Pawlina, 2015). Peritubular myoid cells mature during puberty in terms of contractility and ultrastructure (Kormano and Hovatta, 1972). The seminiferous/straight tubules and rete testis originate from the testicular cords, whereas the efferent ductules originate from the mesonephric tubules (Lupien et al., 2006; Ross and Pawlina, 2015). Therefore, a developmental boundary is assigned at the junction between the rete testis and the proximal end of the efferent ductules in the excurrent tubule/ductule/duct system, and this boundary is histologically maintained among the epithelia of these tissues. However, the mechanisms underlying the maintenance of this boundary accompanied by the morphological transition of the epithelia are not completely clear.

Eph receptors and ephrin ligands serve as a cell-cell communication system. The roles of Eph receptors and ephrins have been extensively characterized in developing tissues (Noren and Pasquale, 2004; Palmer and Klein, 2003; Pasquale, 2005; Poliakov et al., 2004). Recently EphB receptors and ephrin-B ligands have been implicated in the physiology and homeostasis of normal adult tissues and organs such as essential roles on the maintenance of epithelial integrity, homeostasis and boundary formation in variety of epithelia in the intestine, stomach, epidermis, and mammary glands (Ishii et al., 2011b; Miao and Wang, 2009; Ogawa et al., 2013; Ogawa et al., 2011b; Pasquale, 2008; Perez White and Getsios, 2014; Uchiyama et al., 2015). However, to the best of the author's knowledge, the expression patterns of EphB and ephrin-B have not been reported in the testis and epididymis in the adult as well as during the postnatal development. Therefore, the author investigated the expression and localization of EphB and ephrin-B in the adult testis, and found the ephrin-B1- and EphB2/B4-predominant expression compartments appear alternately along the intratesticular excurrent duct system in the adult mouse testis, which is lined with the tubule/ductule-specific epithelia (see Chapter 1). This compartmentalization corresponds to the histological compartments in the intratesticular excurrent duct system as well as the developmental compartments composed of the testicular cords and mesonephric tubules. Therefore in this Chapter, the author investigated the expression and localization of ephrin-B1, EphB2 and EphB4 in the mouse testis during the postnatal development to determine when their expression compartments are formed/completed during the postnatal development. In Chapter 1, the author also found that spermatogonia express ephrin-B1 and EphB4, elongated spermatids express EphB2, and peritubular myoid cells and Leydig cells express ephrin-B1 and EphB4.

Therefore the author also investigated these expressions during the postnatal development to determine the expression behaviors in those cells during the postnatal development.

Materials and methods

Animals

The testis of ICR mice of 1 day, 1, 2, 3, 4, 5, 6, and 8 week-old were used for the reverse transcription-polymerase chain reaction (RT-PCR) and immunohistochemical analyses. The animal experimentation protocol was approved by the Animal Research Committee of the Osaka Prefecture University.

Total RNA extraction and semi-quantitative RT-PCR analysis

Total RNA was isolated from the testis without tunica albuginea of 1 day, 1, 2, 3, 4, 5, 6, and 8 week-old mice using TRIzol reagent (Invitrogen, Carlsbad, CA, USA), and RT-PCR analysis was performed according to the method of Ogawa et al. with some modifications (Ogawa et al., 2011b). In brief, 1 μg total RNA was transcribed into first-strand cDNA using M-MLV reverse transcriptase, RNase H^- (Promega, Madison, WI, USA), and oligo $(dT)_{18}$ primer, according to the manufacturer's instructions. For the detecting endogenous ephrin-B1, EphB2, EphB4, and β-actin, 0.5 μL of the 25-μL reaction mixture was amplified with Taq DNA polymerase (TaKaRa Ex Taq HS; Takara Bio Inc., Otsu, Japan) using the reverse-transcribed cDNA as template. The primer pairs and cycle numbers used for PCR amplification in this study are shown in Table 2-1. The RT reaction was omitted for the negative controls. PCR products were separated on 1.5% agarose gels and visualized by ethidium bromide staining. Expression levels of amplified ephrin-B1, EphB2 and EphB4 mRNA were determined from three independent experiments, normalized to the levels of β-actin mRNA as an internal control (amplified over 21 cycles), and compared with those of the testis of 8 week-old mice.

Statistical analysis

Statistical analyses were performed with Microsoft Excel and the statistical software on the web (http://statpages.info/anova1sm.html). The bar graphs represent means ± SD. Differences in mean ephrin-B1/EphB2/EphB4 mRNA expression levels among postnatal developing ages

were evaluated by one-way ANOVA, followed by Turkey HSD post-hoc analysis. *P* values less than 0.05 were considered significant.

Antibodies

Goat polyclonal antibodies against the mouse ephrin-B1 extracellular domain, the mouse EphB2 extracellular domain, and the mouse EphB4 extracellular domain were obtained from R&D Systems, Inc. (Minneapolis, MN, USA). The detailed information of these antibodies is described in the previous section (Chapter 1-2, pages 10). Anti-vimentin rabbit monoclonal antibody (ab92547) and anti-alpha smooth muscle actin (α-SMA) rabbit polyclonal antibody (ab5694) were purchased from Abcam (Cambridge, UK) and rabbit polyclonal CYP17A1 antibody was purchased from Proteintech (Rosemont, Illinois, USA). Rat monoclonal antibody against mouse epithelial cellular adhesion molecule (EpCAM, also known as CD326) was purchased from eBioscience Inc. (San Diego, CA, USA), and rat anti-mouse thymic stromal cell antigen (ER-TR7) monoclonal antibody was obtained from Novus Biologicals (Littleton, CO, USA). Alexa Fluor 488-conjugated donkey anti-goat IgG, Alexa Fluor 568-conjugated donkey anti-rabbit IgG, and Alexa Fluor 594-conjugated donkey anti-rat IgG were obtained from Molecular Probes, Inc. (Eugene, OR, USA).

Immunofluorescence staining

The mice testes of the different postnatal ages were fixed with 10% formalin in phosphate buffered saline (PBS) at 4°C for the different period of time in the different ages shown in Table 2-2. After washing with PBS, the tissues were immersed in 30% sucrose in PBS for 3.5 hr to overnight (Table 2-2) and mounted in optimum cutting temperature (OCT) compound (Sakura Finetechnical Co., Ltd., Tokyo, Japan). Then, 5 μm-thick cryostat sections were used for fluorescence staining. Single- or double-immunofluorescence staining was performed as the same protocol as described in Chapter 1-2 (pages 11-12).

Results

Ephrin-B1, EphB2 and EphB4 mRNA expression in the mouse testis during the postnatal development

To investigate relative expression levels of ephrin-B1, EphB2 and EphB4 in the mouse testis during the postnatal development, semi-quantitative RT-PCR was performed

using the testis of 1 day, 1, 2, 3, 4, 5, 6, and 8 week-old ICR mice. Transcripts of ephrin-B1, EphB2 and EphB4 were detected in testis at all postnatal ages examined (Fig. 2-1). Transition patterns of relative expression levels in the testis during the postnatal development were similar among ephrin-B1, EphB2 and EphB4 (Fig. 2-2). Their expression levels decreased with age until 4 weeks, and thereafter were almost similar until adult (8 weeks). These findings indicate that expression levels of ephrin-B1, EphB2 and EphB4 are close to those in the adult until 4 weeks of age.

Ephrin-B1, EphB2 and EphB4 localization in the intratesticular excurrent duct system during the postnatal development

In Chapter 1 the author found ephrin-B1- and EphB2/EphB4-predominant expression compartments present alternatively in the intratesticular excurrent duct system in the adult mouse testis and therefore tried to determine when these compartments appear during the postnatal development. Vimentin immunostaining was used to identify Sertoli cells in seminiferous and straight tubules of the testis. Ephrin-B1 and EphB2 were faintly or almost negatively expressed in epithelia of seminiferous and straight tubules in all ages of postnatal development examined (Fig. 2-3, 2-4). In contrast in epithelia of the rete testis and efferent ductules, they were faintly or weakly expressed uniformly at 1 day and 1 week. Thereafter compartments of predominant ephrin-B1 and EphB2 expression complementarily appeared in the epithelia from 2 weeks of age: ephrin-B1 immunoreactivity became strong in the rete testis and remained weak in the efferent ductules (Fig. 2-3) while EphB2 immunoreactivity remained weak/faint in the rete testis and became relatively strong in the efferent ductules (Fig. 2-4). By contrast EphB4 expression compartments unclearly and incompletely appeared in epithelia of intratesticular excurrent duct system from the beginning of the postnatal development examined, i.e., at 1 day: EphB4 immunoreactivity was faint in epithelia of straight tubules and the rete testis while it was weak in epithelia of efferent ductules (Fig. 2-5B). At 1 week and thereafter the expression boundary of EphB4 between the rete testis and efferent ductules became clear. Moreover EphB4 immunoreactivity clearly appeared in straight tubules at 2 weeks of age and thereafter (Fig. 2-5A). Thus EphB4 expression compartments appeared alternatively in the regions of intratesticular excurrent duct system from 2 weeks of age and continued thereafter. These findings indicate that ephrin-B1-predominant expression compartment (the rete testis) and EphB2- and/or EphB4-predominant expression compartment (straight tubules and efferent ductules) formed in the intratesticular excurrent duct system from 2 weeks of age during the postnatal development.

Ephrin-B1, EphB2 and EphB4 localization in seminiferous tubules during the postnatal development

In Chapter 1 the author found ephrin-B1 and EphB4 expression in spermatogonia and EphB2 in elongated spermatids and immature spermatozoa in seminiferous tubules and therefore investigated their expression behaviors in the testis during the postnatal development. Based on EpCAM immunostaining as a maker of spermatogonia, spermatogonia were not distributed in seminiferous tubules at 1 day of age. Then, either EpCAM strongly or faintly/weakly positive spermatogonia were densely packed in the seminiferous tubules at 1 week and densely distributed at the margin of seminiferous tubules at 2 weeks. Thereafter EpCAM-positive spermatogonia were localized at the margin of seminiferous tubules less densely close to the adult pattern at 4 weeks, when EpCAM immunoreactivity was homogenous in spermatogonia among seminiferous tubules (Fig. 2-6, 2-8; Fig. 1-3A, 1-5A in Chapter 1). At 1 day, ephrin-B1 and EphB4 immunoreactivity were almost negative in germ cells in seminiferous tubules, where gonocytes exclusively reside as germ cells before the postnatal day 3 in the mouse testis because gonocytes do not begin to differentiate into spermatogonial stem cells/spermatogonia (Abe et al., 1991; Montoto et al., 2012; Tiptanavattana et al., 2015). Ephrin-B1 and EphB4 immunoreactivity were faint or weak but clearly positive in EpCAM-positive spermatogonia at 1 week and thereafter. Moreover, ephrin-B1 immunoreactivity in spermatogonia was prominent at 2 weeks while EphB4 immunoreactivity in spermatogonia unchanged from 1 week to 8 weeks of age. On the other hand, EphB2 immunoreactivity was faint or almost negative in germ cells in seminiferous tubules from 1 day to 3 weeks during the postnatal development. Strong EphB2 immunoreactivity abruptly appeared at 4 weeks in a few round and elongated spermatids sparsely in some seminiferous tubules, and at 5 weeks and thereafter EphB2-positive elongated spermatids attached to Sertoli cells accumulated in the luminal margin of seminiferous tubules (Fig. 2-7).

Ephrin-B1, EphB2 and EphB4 localization in testicular stromal cells during the postnatal development

In Chapter 1, the author found ephrin-B1 and EphB4 expression in Leydig cells, peritubular myoid cells and fibroblasts in the testicular stroma and therefore investigated their expression behaviors in the stromal cells during the postnatal development. ER-TR7 immunostaining was used to identify the fibroblasts; CYP17A1 immunostaining was used to

identify the Leydig cells; α-SMA immunostaining was used to identify the peritublar myoid cells/smooth muscle cells. ER-TR7 as a marker for fibroblasts labels also α-SMA-positive cells like peritubular myoid cells and vascular smooth muscle cells in the testis, and thus ER-TR7 immunostaining is likely useful to determine stromal areas and stromal margin against parenchyma in tissue sections: The relative ratio of the stroma covered by ER-TR7 immunoreactivity to parenchyma (seminiferous tubules) was sharply decreased from 1 day towards 3-4 weeks of age (Fig. 2-9).

Ephrin-B1 was expressed in fibroblasts, peritubular myoid cells and Leydig cells. Ephrin-B1 immunoreactivity remained almost unchanged in ER-TR7-positive fibroblasts and peritubular myoid cells during the postnatal development, while ephrin-B1-positive fibroblasts were prominent at 1 day and became less prominent among testicular stromal cells with the advance of age due to decrease of fibroblasts in the testicular stroma (Fig. 2-9). By contrast ephrin-B1 immunoreactivity in Leydig cells was weak similar to other stromal cells like fibroblasts, became strong gradually until 4 weeks and remained strong thereafter (Fig. 2-10): ephrin-B1-positive Leydig cells were prominent at 4 weeks and thereafter because sizes of Leydig cells also became large until 4 weeks and remained large thereafter. Ephrin-B1 immunoreactivity remained almost unchanged in peritubular myoid cells during the postnatal development (Fig. 2-9, 2-10, 2-11A).

EphB2 was weakly expressed in α-SMA-positive peritubular myoid cells and ER-TR7-positive fibroblasts from 1 day until 2–3 weeks, and almost negative at 4 weeks of age and thereafter (Fig. 2-7, 2-11B). EphB4 was weakly expressed in ER-TR7-positive fibroblasts, CYP17A1-positive Leydig cells and α-SMA-positive peritubular myoid cells, and EphB4 immunoreactivity was largely unchanged in these cells during the postnatal development (Fig. 2-8, 2-11C, 2-12). The overall expression patterns of ephrin-B1, EphB2 and EphB4 in the mouse testis during the postnatal development are illustrated in Fig. 2-13.

Discussion

Eph receptors and ephrin ligands serve as a cell-cell communication system that has diverse roles in biological processes extensively characterized in developing tissues (Kullander and Klein, 2002; Pasquale, 2005). Recently EphB receptors and ephrin-B ligands have been implicated in the maintenance of epithelial integrity, homeostasis and boundary

formation in variety of epithelia in the intestine, stomach, epidermis, and mammary glands (Ishii et al., 2011b; Miao and Wang, 2009; Ogawa et al., 2013; Ogawa et al., 2011b; Pasquale, 2008; Perez White and Getsios, 2014; Uchiyama et al., 2015). Thus the author examined EphB and ephrin-B expressions in epithelia of the intratesticular excurrent duct system in the adult mouse which composed of straight tubules, the rete testis and the efferent ductules, and found that the ephrin-B1- and EphB2/EphB4-predominant expression compartment appear alternately along the excurrent duct system in the testis and epididymis (see Chapter 1). As a series of studies, here the author examined ephrin-B1, EphB2 and EphB4 expression and localization in the mouse testis during the postnatal development to determine when those expression compartments are formed/completed in the epithelia during the postnatal development.

A study by Ashley *et al.* shows that relative ephrin-B1 expression levels were high at the prenatal (embryonic day 17) and early postnatal ages (day 1 and day 10) in the development of the rat ventral prostate (Ashley et al., 2010), whose development depends on testosterone like the testis. Semi-quantitative RT-PCR analyses revealed that the relative expression levels of ephrin-B1, EphB2 and EphB4 in the testis were high at 1 day compared to those at 8 weeks of age, decreased with age until 4 weeks, and thereafter the expression levels were almost similar until 8 weeks. The relative volume proportion of the stroma (connective tissues) to seminiferous tubules decreases in the testis with age during the postnatal development (Montoto et al., 2012). The author also found that the relative ratio of the stroma to seminiferous tubules rapidly decreased from 1 day towards 3-4 weeks of age during the postnatal development, and ephrin-B1, EphB2 and EphB4 were expressed in ER-TR7-positive mesenchymal cells/fibroblasts strongly only at 1 day and 1 week, when these cells densely occupied in the stroma. Therefore the relative expression levels of ephrin-B1, EphB2 and EphB4 transcripts in the testis which are higher in the earlier postnatal developmental ages likely correspond to a density and number of mesenchymal cells/fibroblasts in the stroma.

Spermatogenesis starts shortly after birth (postnatal days 3 to 6) and the first wave of spermatogenesis is completed at postnatal day 35 and spermiation occur around this time in mice (Abe et al., 1991; Griswold, 2016; Montoto et al., 2012). Therefore, all types of germ cells in differentiation process appear in seminiferous tubules at 5 weeks of age in mouse, i.e., seminiferous tubules are completed in the adult morphology at 5 weeks. The author found the predominant ephrin-B1 and EphB2/EphB4 complementary expression alternatively present in epithelia of the intratesticular excurrent duct system at 2 weeks of age and thereafter during

the postnatal development while ephrin-B1 and EphB2 were uniformly expressed in the epithelia at 1 day and 1 week and EphB4 expression compartments unclearly and incompletely appeared in the epithelia from the beginning of the postnatal development examined. Therefore the intratesticular excurrent duct system of mouse is completed far earlier than the time when spermiation starts in terms of ephrin-B1 and EphB2/EphB4 expression although expression levels of ephrin-B1, EphB2 and EphB4 examined by RT-PCR are close to those in the adult until 4 weeks of age.

Gonocytes differentiate into spermatogonial stem cells/spermatogonia during days 3–6 after birth in the mouse and spermatogenesis starts at the same time as their differentiation starts (postnatal days 3 to 6) (Abe et al., 1991; Montoto et al., 2012; Tiptanavattana et al., 2015). These indicate that spermatogonia being in differentiation are not present in seminiferous tubules at 1 day in the mouse testis. The author found that ephrin-B1 and EphB4 immunoreactivity were faint or almost negative in germ cells, cells excluding Sertoli cells in the seminiferous epithelium at 1 day while they were clearly positive at 1 week and thereafter. Therefore ephrin-B1 and EphB4 are unlikely expressed in gonocytes and likely in spermatogonia. It is well accepted that gonocytes and spermatogonia are localized in the luminal and basal side of seminiferous tubules, respectively (Bellve et al., 1977). Based on these the author suggests that EphB4/ephrin-B1 signaling may be involved in the process of proliferation and/or differentiation in spermatogonia, and moreover EphB4 and ephrin-B1 are likely markers useful to discriminate spermatogonia from gonocytes in seminiferous tubules during the early postnatal development.

The first wave of spermatogenesis, an entire differentiation process from spermatogonia (spermatogonial stem cells) into spermatozoa, completes within the postnatal day 35 in mice (Montoto et al., 2012): gonocytes differentiate into spermatogonial stem cells/spermatogonia during days 3–6 after birth (Abe et al., 1991; Montoto et al., 2012; Tiptanavattana et al., 2015) and spermatogonial stages last a few days in spermatogenesis, and primary spermatocytes appear in seminiferous tubules at the postnatal day 10 (Bellve et al., 1977) and; meiosis occurred in spermatocytes lasts 13 days; spermiogenesis, a metamorphosis from round spermatids into spermatozoa via elongated spermatids, lasts 13.5 days (Bellve et al., 1977; Gilbert, 2000). However, the duration of spermatogenesis in the first round is shortened by ~2.5 days in mice (Griswold, 2016). The author found that EphB2-positive spermatids abruptly appeared sparsely in some seminiferous tubules at 4 weeks and densely accumulated in many seminiferous tubules at 5 weeks and thereafter. Thus EphB2 immunoreactivity is likely a good indicator to determine the completion of the first wave of

spermatogenesis. Therefore the author suggests that the EphB2 immunoreactivity is a good tool to examine male reproductive toxicity using mice.

During testicular development, fetal Leydig cells differentiate in the fetal testes at E12.5 to E13.5 in rodents; after birth, adult Leydig cells are gradually replace with fetal ones during the postnatal development to produce testosterone to support spermatogenesis as fetal ones undergo degeneration in neonatal and pre-pubertal testes (Wen et al., 2016). During the postnatal development, adult Leydig cells differentiate from stem Leydig cells via progenitor Leydig cells and then immature Leydig cells; stem and progenitor Leydig cells show spindle-shaped while immature and adult Leydig cells are round-shaped cells with large and small lipid droplets, respectively; stem, progenitor, immature, and adult Leydig cells show no, low, intermediate and high testosterone synthesis property, respectively (Chen et al., 2009). In mice immature Leydig cells begin to transform into adult Leydig cells by the postnatal day 25 (Kilcoyne et al., 2014). The authors found that CYP17A1-positive Leydig cells expressed ephrin-B1 and EphB4 throughout the postnatal development examined. Moreover, ephrin-B1 immunoreactivity in Leydig cells was increased gradually until 4 weeks and remained strong thereafter, and CYP17A1-positive Leydig cells became large in size until 4 weeks and remained large thereafter. Thus these findings may indicate that (1) both fetal and adult Leydig cells likely express ephrin-B1 and EphB4, (2) ephrin-B1 is expressed highly in adult Leydig cells and weakly in fetal and immature Leydig cells. The author did not use markers specific for labeling stem and progenitor Leydig cells, and therefore further studies are necessary to determine whether these undifferentiated Leydig cell lineages express ephrin-B1 and EphB4 or not.

Summary

The present study represents the first expression analysis of ephrin-B1, EphB2 and EphB4 in the normal mouse testis during the postnatal development. The relative expression levels of ephrin-B1, EphB2 and EphB4 by RT-PCR were decreased with age during the early postnatal development and became close to those of the adult levels in the testis until 4 weeks of age. The relative ratio of stromata to seminiferous tubules was rapidly decreased from 1 day towards 3-4 weeks of age, and ER-TR7-positive stromal cells expressing ephrin-B1, EphB2 and EphB4 were dense in the stroma during the early postnatal development and less dense with age. These immunohistochemical expression patterns are almost identical to those

by RT-PCR. The author found that ephrin-B1 and EphB2/EphB4 complementary expression compartments in epithelia of the intratesticular excurrent duct system were formed until 2 weeks of age during the postnatal development. Therefore the intratesticular excurrent duct system in mouse is completed far earlier than the time when spermiation starts in terms of ephrin-B1 and EphB2/EphB4 expressions in the epithelia. The author also found (1) ephrin-B1 and EphB4 immunoreactivity in spermatogonia at 1 week and thereafter during the postnatal development, and (2) EphB2 immunoreactivity in spermatids from 4 weeks. These findings suggest that (1) EphB4 and ephrin-B1 are likely markers useful to discriminate spermatogonia from gonocytes in seminiferous tubules during the early postnatal development and (2) EphB2 is likely a good indicator to determine the completion of the first wave of spermatogenesis.

Table 2-1 Primers and cycle numbers for PCR amplification

Primer			Product size (bp)	Annealing temp. (°C)	Cycle number
ephrin-B1	Forward	5´-TGCTTGATCCCAATGTACTG-3´	520	55.0	29
	Reverse	5´-CGGAGCTTGAGTAGTAGGAC-3´			
EphB2	Forward	5´-CGACGAGAACATGAACACTA-3´	583	53.0	31
	Reverse	5´-CCCGTTACAGTAGAGTTTGA-3´			
EphB4	Forward	5´-AGCCCCAAATAGGAGACGAG-3´	540	57.9	29
	Reverse	5´-GGATAGCCCATGACAGGATC-3´			
β-actin	Forward	5´-TCATGAAGATCCTGACCGAG-3´	312	47.0	21
	Reverse	5´-GGTCTTTACGGATGTCAACG-3´			

Table 2-2 Fixation conditions of tissue samples for immunohistochemistry

Age of mice	Fixation time	Washing time	Soaking time in 30% sucrose solution	Amount of fixative/tissue
1d	2 hr	1 hr	3.5 hr	1 ml
1w	2 hr	1 hr	4.5 hr	1 ml
2w	3.5 hr	1 hr	7 hr	10 ml
3w, 4w, 5w, 6w, 8w	4 hr	1 hr	Overnight	10 ml

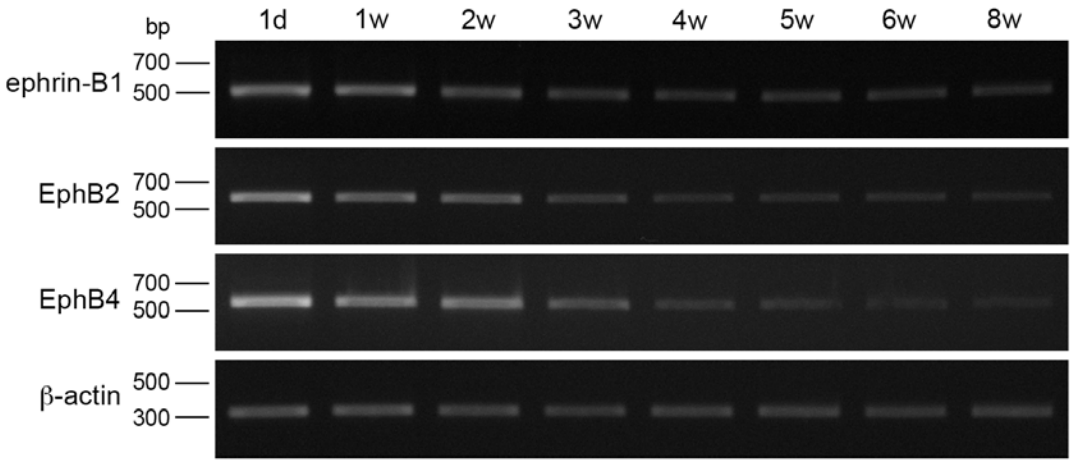
bp
1d
1w
2w
3w
4w
5w
6w
8w
ephrin-B1
700
500
EphB2
700
500
EphB4
700
500
β-actin
500
300

Fig. 2-1

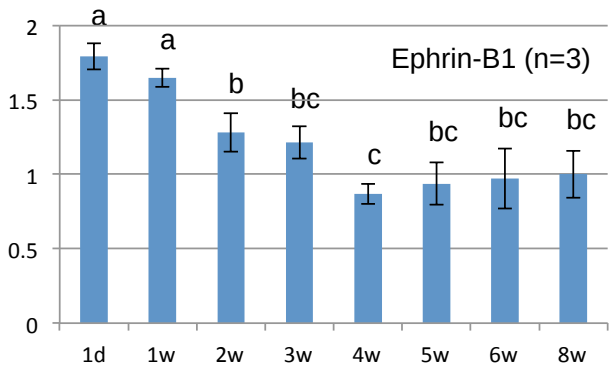

Values with different superscripts indicate significant differences (p<0.05)

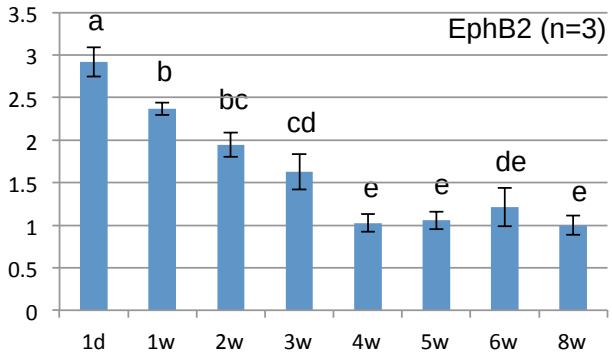

Values with different superscripts indicate significant differences (p<0.05)

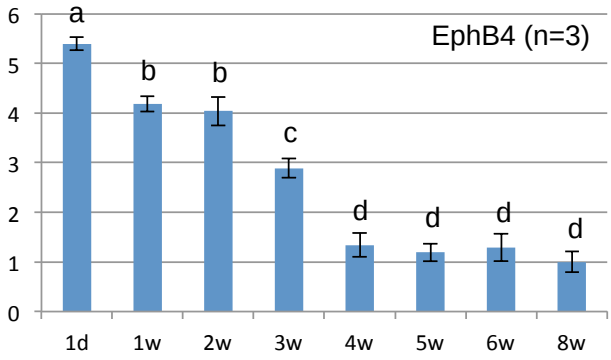

Values with different superscripts indicate significant differences (p<0.05)

Fig. 2-2

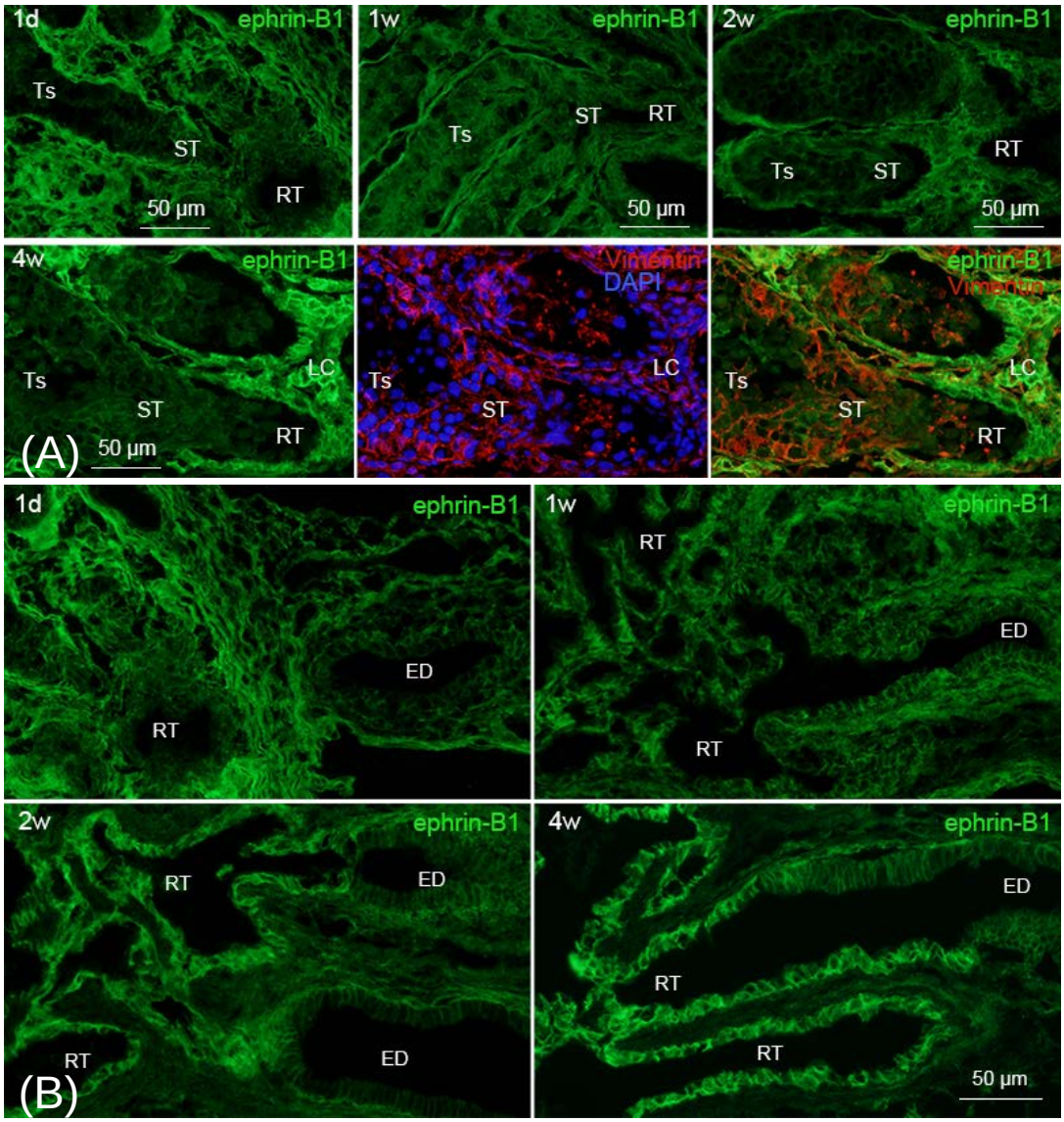
1d
ephrin-B1
Ts
ST
RT
50 μm
1w
ephrin-B1
Ts
ST
RT
50 μm
2w
ephrin-B1
Ts
ST
RT
50 μm
4w
ephrin-B1
Ts
ST
LC
RT
(A)
50 μm
Vimentin
DAPI
Ts
ST
LC
ephrin-B1
Vimentin
Ts
ST
LC
RT
1d
ephrin-B1
RT
ED
1w
ephrin-B1
RT
ED
RT
2w
ephrin-B1
RT
ED
RT
ED
(B)
4w
ephrin-B1
ED
RT
RT
50 μm

Fig. 2-3

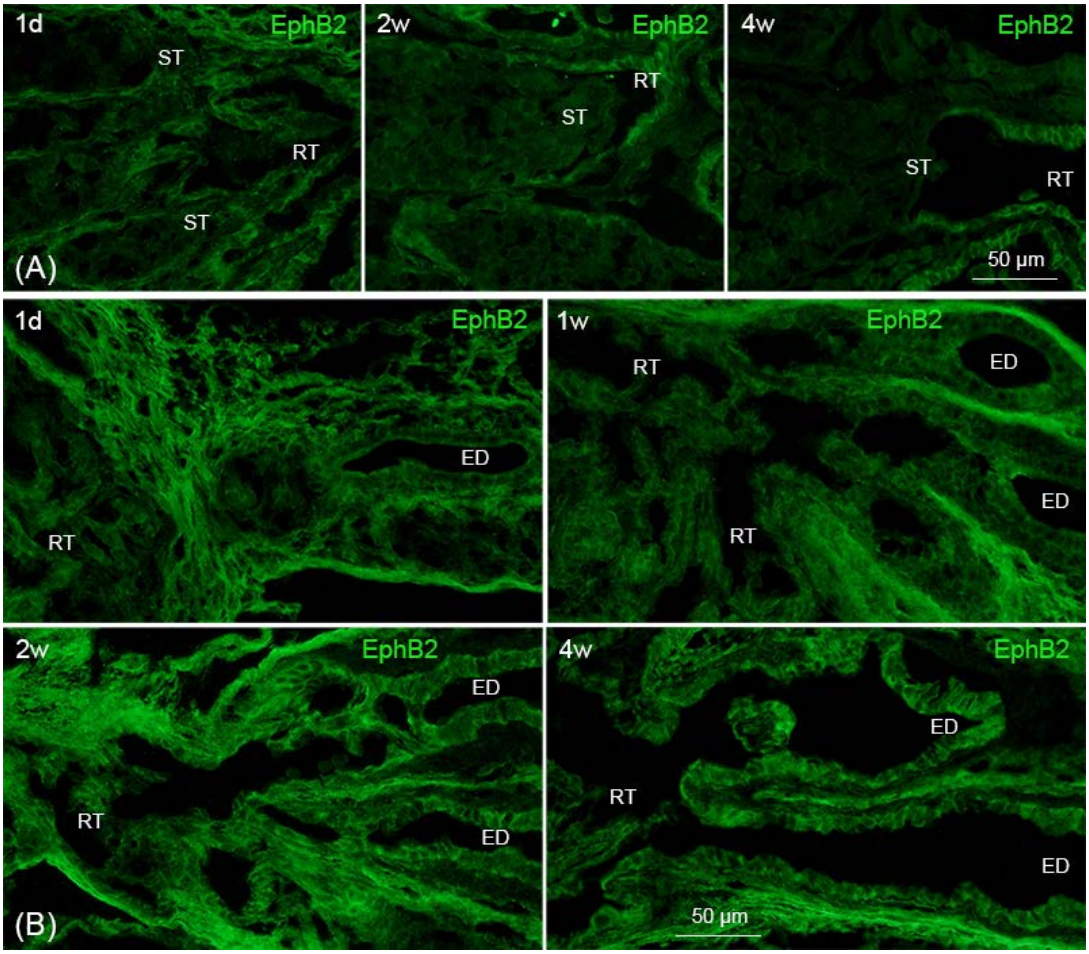
1d
EphB2
ST
RT
ST
(A)
2w
EphB2
RT
ST
4w
EphB2
ST
RT
50 μm
1d
EphB2
ED
RT
1w
EphB2
RT
ED
ED
RT
2w
EphB2
ED
RT
ED
(B)
4w
EphB2
ED
RT
ED
50 μm

Fig. 2-4

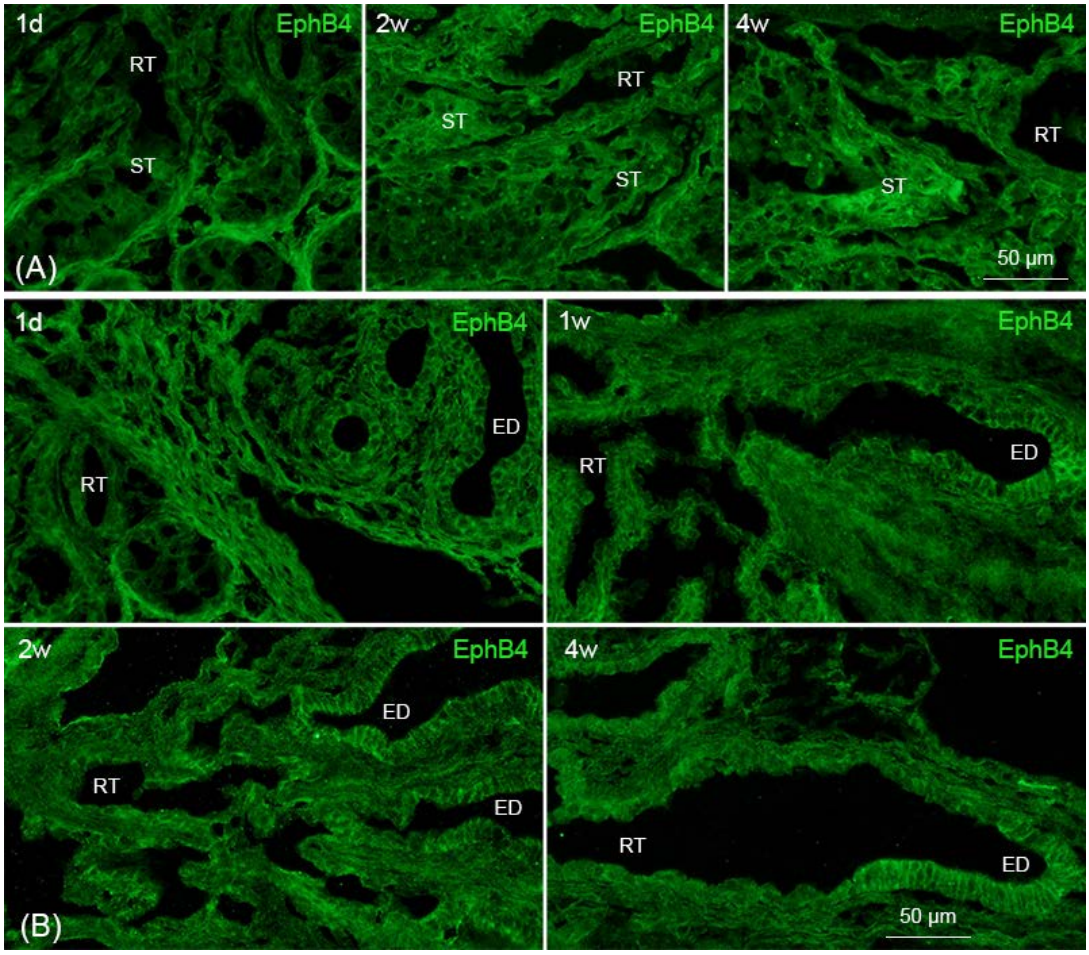
1d
EphB4
RT
ST
2w
EphB4
RT
ST
4w
EphB4
RT
ST
50 μm
(A)
1d
EphB4
ED
RT
1w
EphB4
RT
ED
2w
EphB4
ED
RT
ED
4w
EphB4
RT
ED
50 μm
(B)

Fig. 2-5

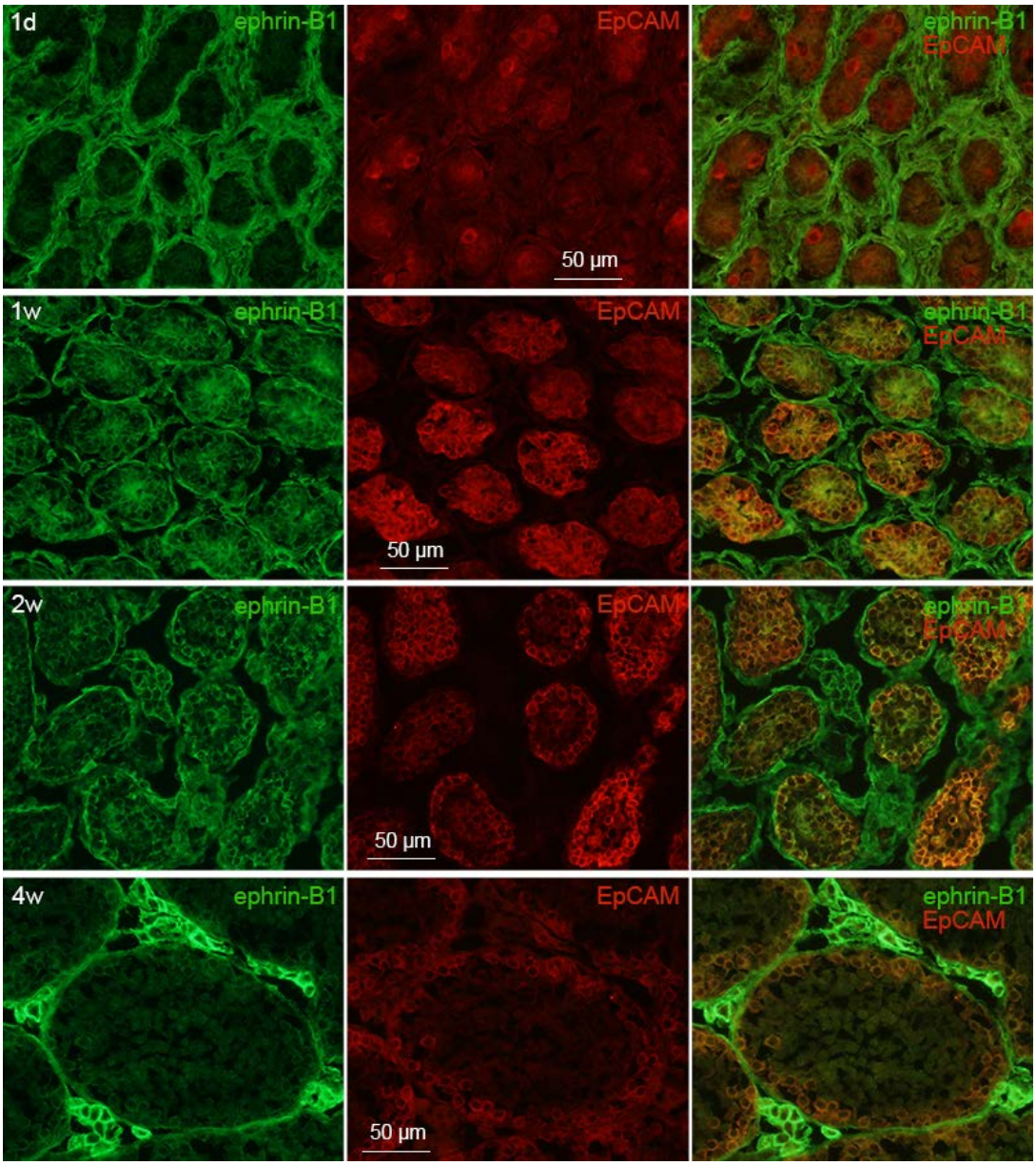
1d
ephrin-B1
EpCAM
ephrin-B1
EpCAM
50 μm
1w
ephrin-B1
EpCAM
ephrin-B1
EpCAM
50 μm
2w
ephrin-B1
EpCAM
ephrin-B1
EpCAM
50 μm
4w
ephrin-B1
EpCAM
ephrin-B1
EpCAM
50 μm

Fig. 2-6

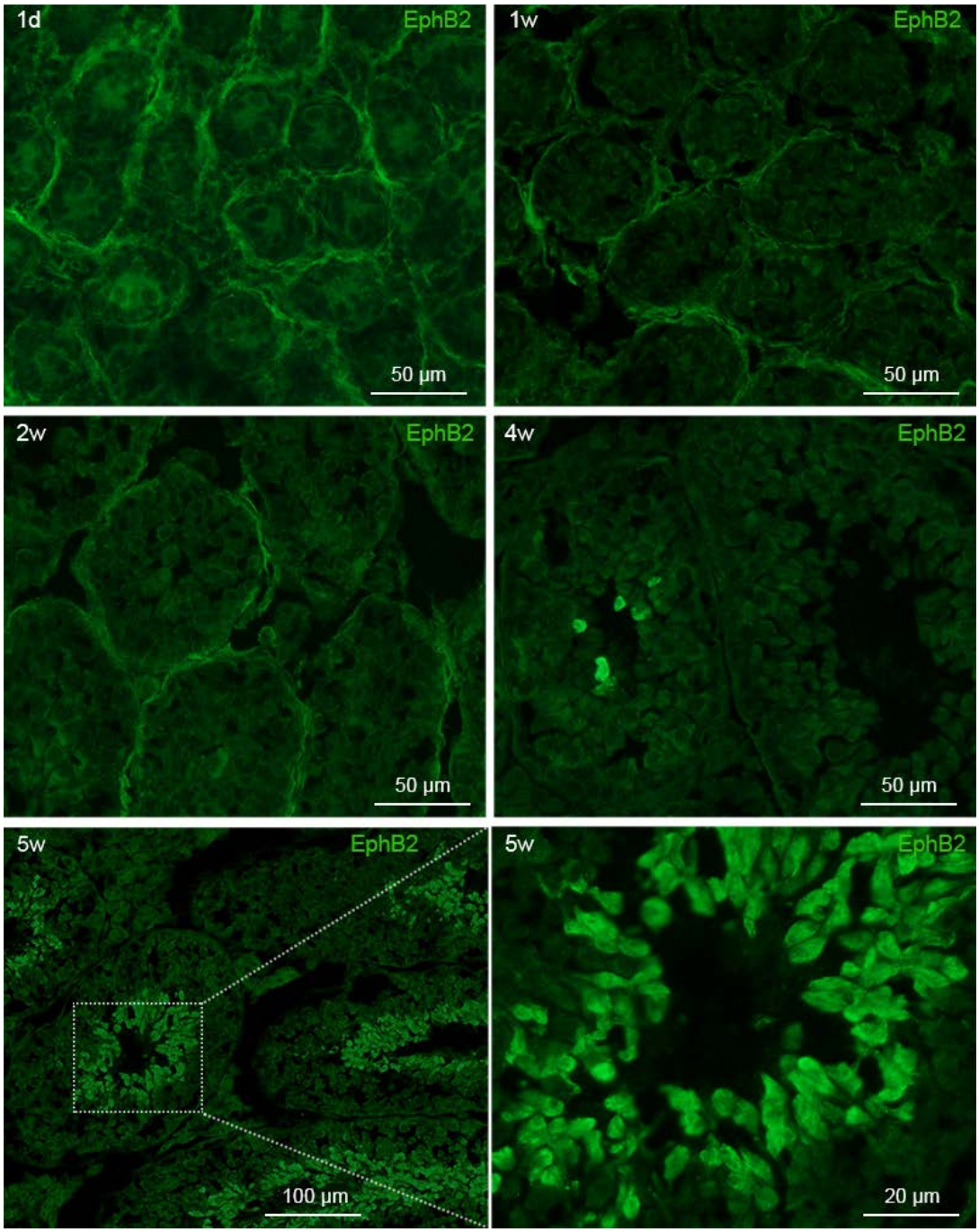
1d
EphB2
50 μm
1w
EphB2
50 μm
2w
EphB2
50 μm
4w
EphB2
50 μm
5w
EphB2
100 μm
5w
EphB2
20 μm

Fig. 2-7

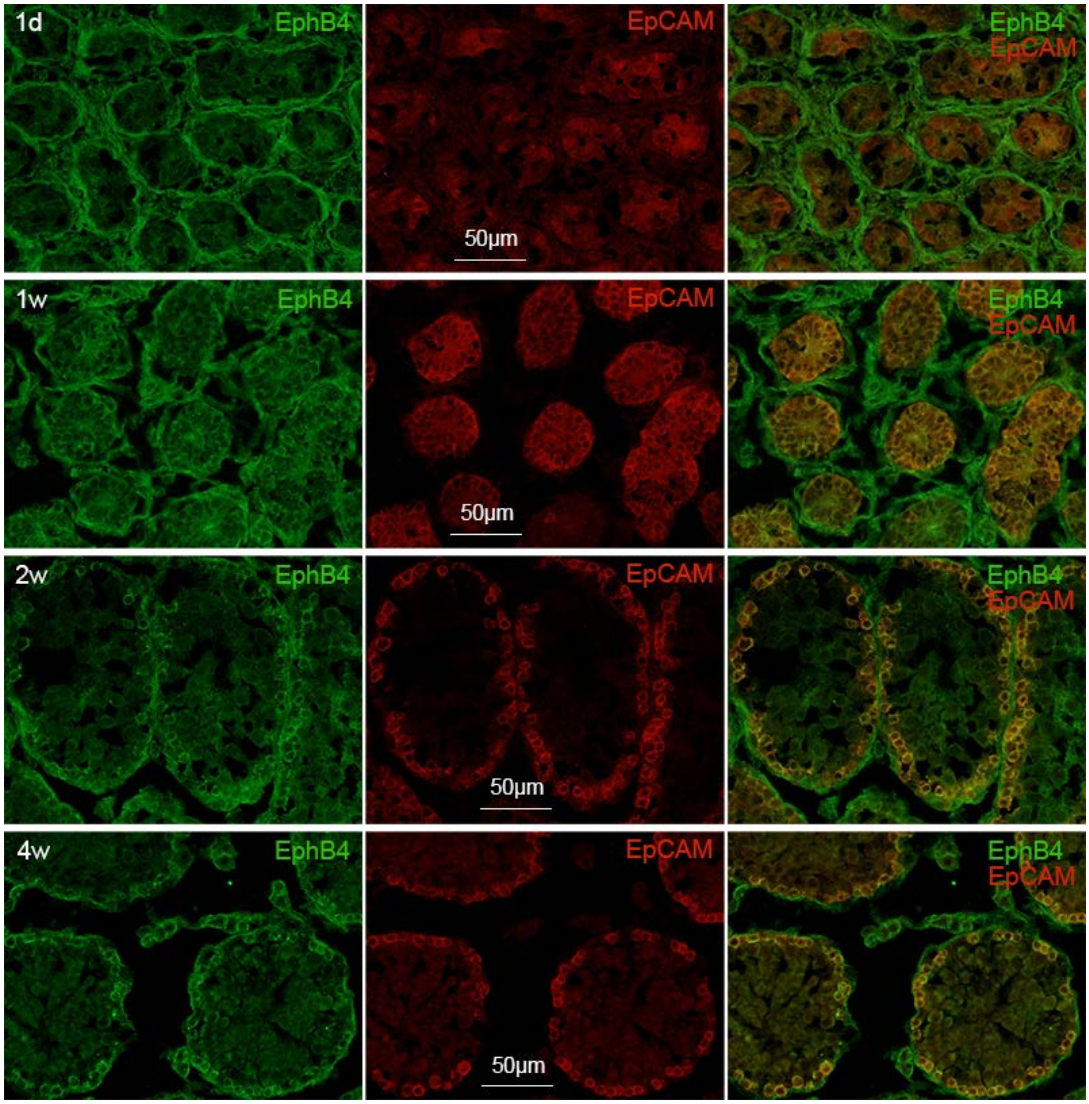
1d
EphB4
EpCAM
EphB4
EpCAM
50μm
1w
EphB4
EpCAM
EphB4
EpCAM
50μm
2w
EphB4
EpCAM
EphB4
EpCAM
50μm
4w
EphB4
EpCAM
EphB4
EpCAM
50μm

Fig. 2-8

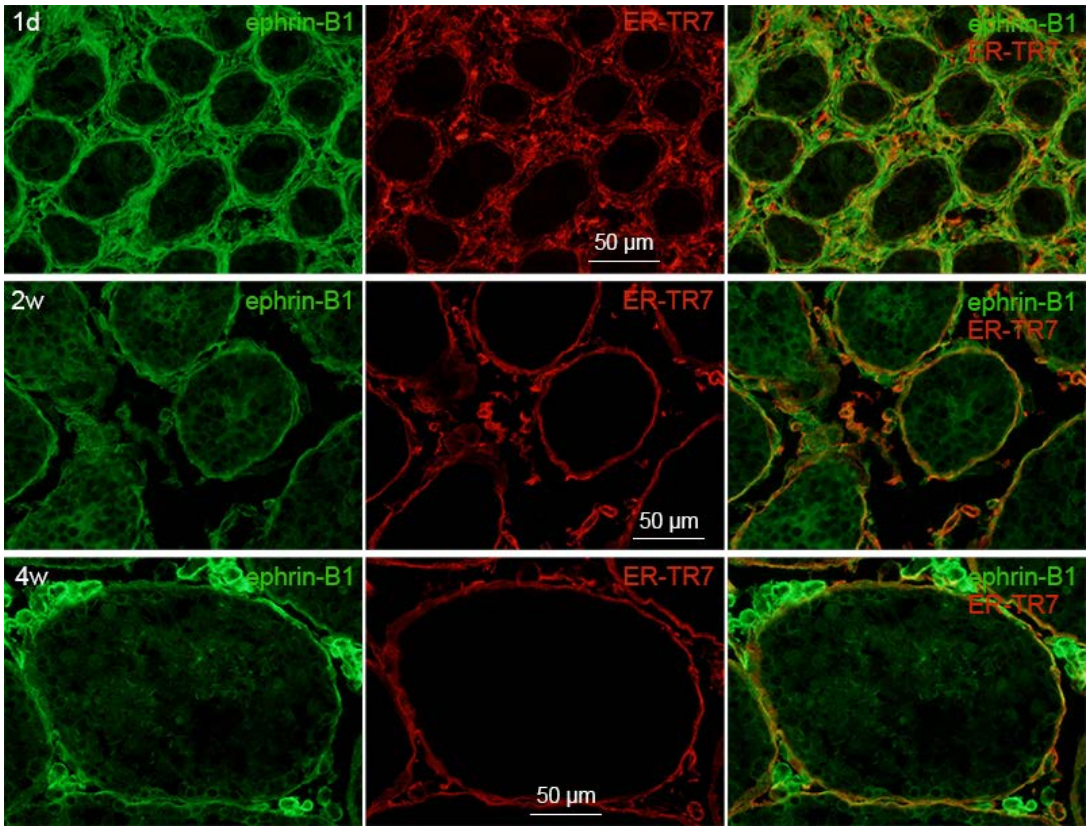
1d
ephrin-B1
ER-TR7
50 μm
2w
ephrin-B1
ER-TR7
50 μm
4w
ephrin-B1
ER-TR7
50 μm

Fig. 2-9

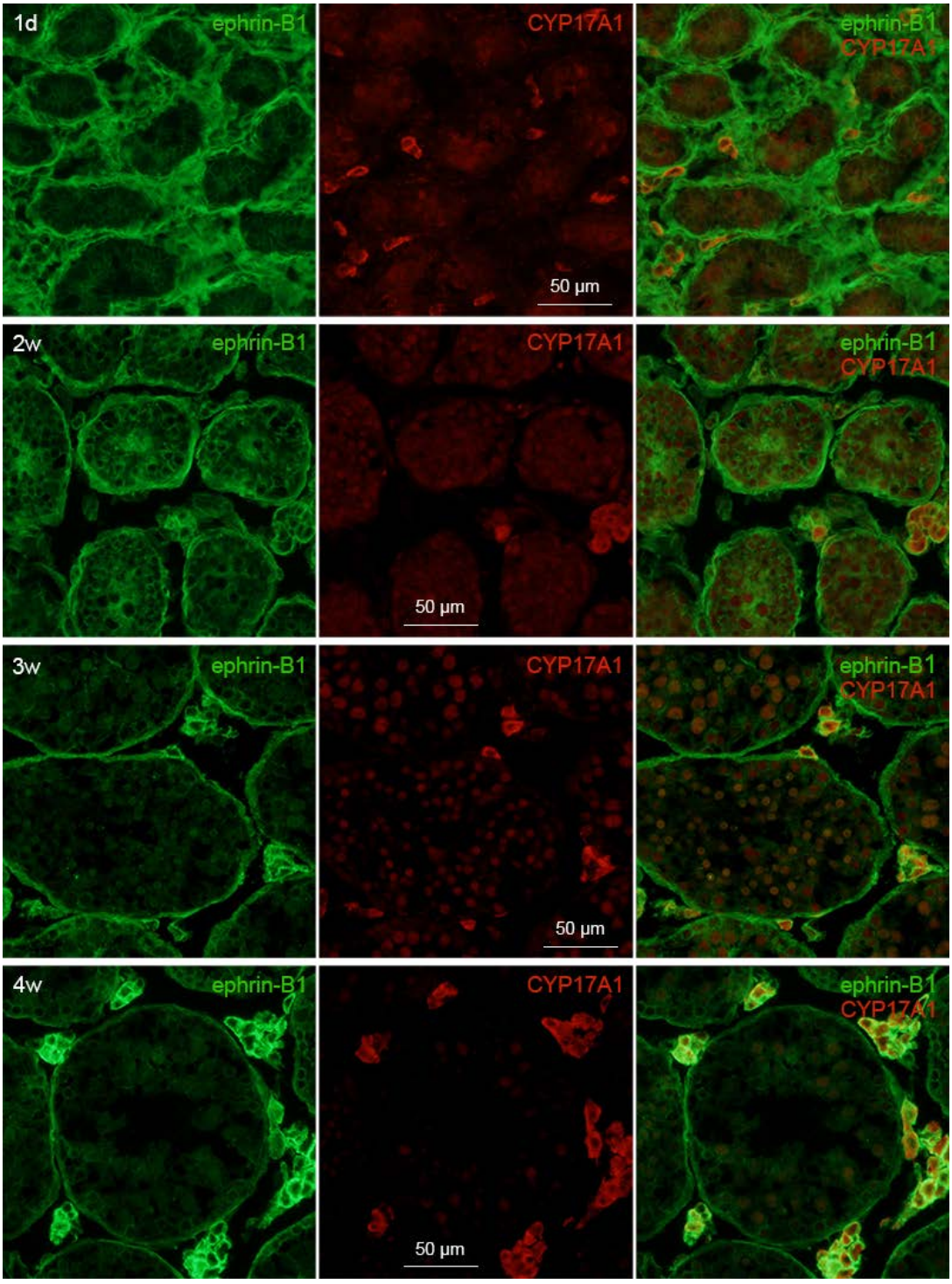
1d
ephrin-B1
CYP17A1
ephrin-B1
CYP17A1
50 μm
2w
ephrin-B1
CYP17A1
ephrin-B1
CYP17A1
50 μm
3w
ephrin-B1
CYP17A1
ephrin-B1
CYP17A1
50 μm
4w
ephrin-B1
CYP17A1
ephrin-B1
CYP17A1
50 μm

Fig. 2-10

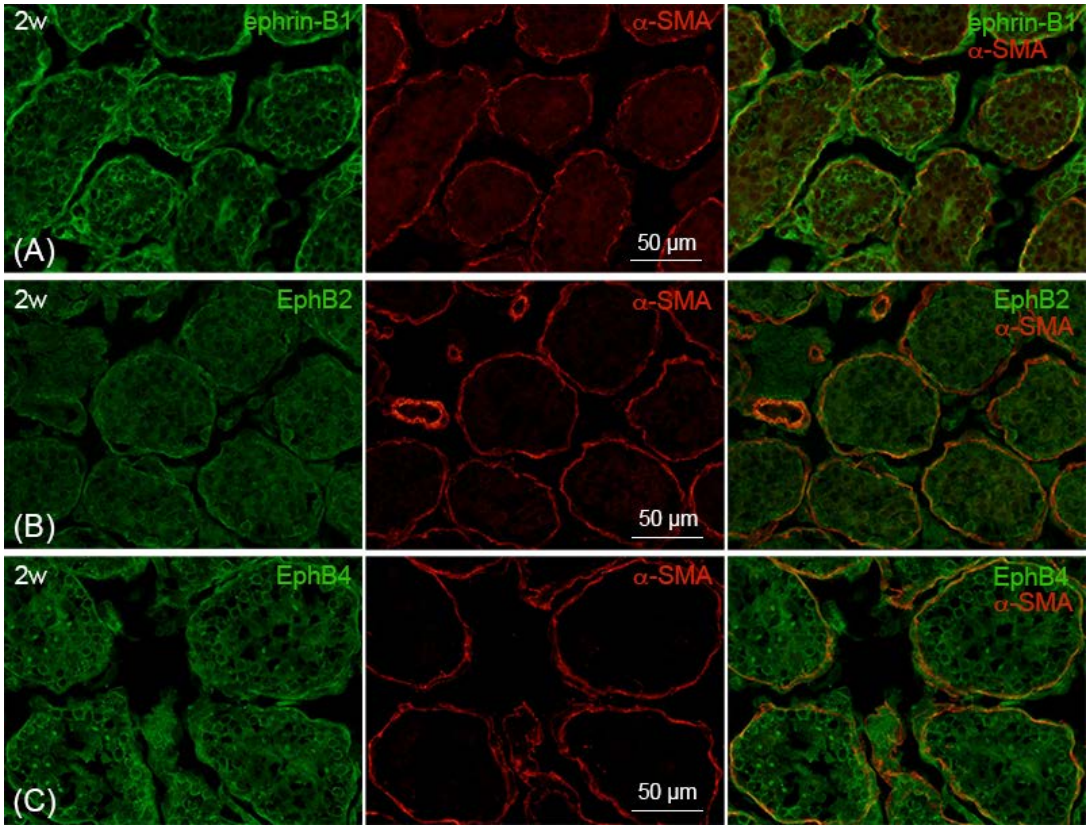
2w
ephrin-B1
α-SMA
ephrin-B1
α-SMA
(A)
50 μm
2w
EphB2
α-SMA
EphB2
α-SMA
(B)
50 μm
2w
EphB4
α-SMA
EphB4
α-SMA
(C)
50 μm

Fig. 2-11

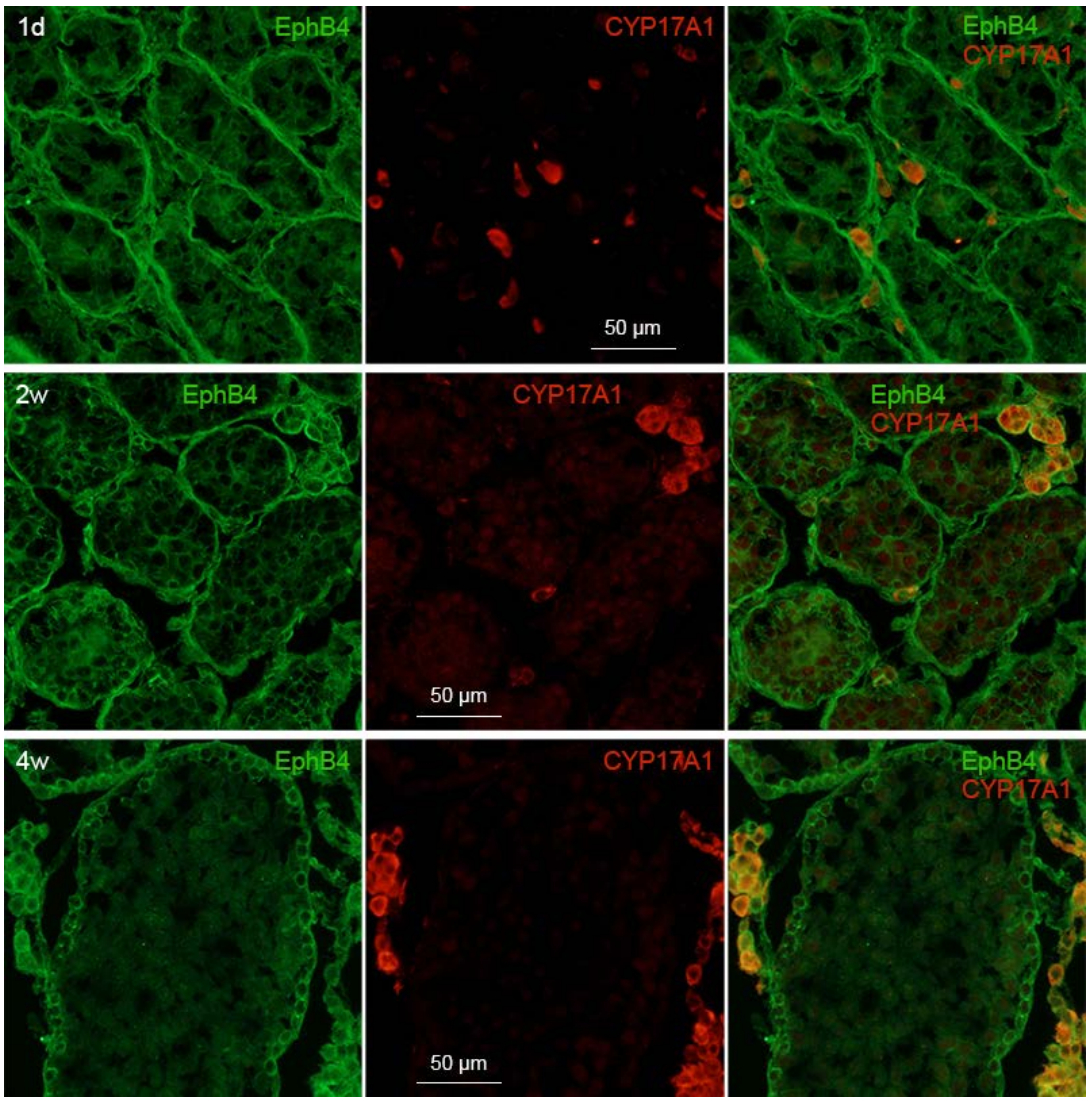
1d
EphB4
CYP17A1
EphB4
CYP17A1
50 μm
2w
EphB4
CYP17A1
EphB4
CYP17A1
50 μm
4w
EphB4
CYP17A1
EphB4
CYP17A1
50 μm

Fig. 2-12

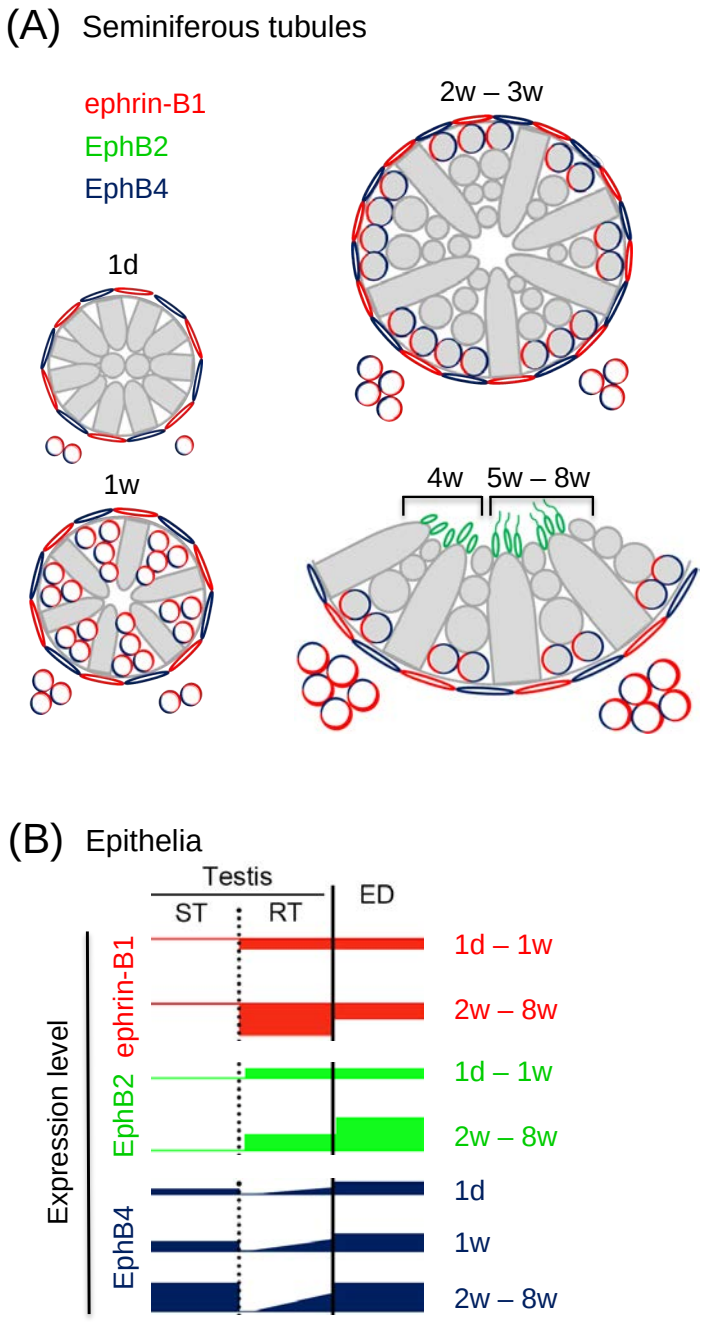
(A) Seminiferous tubules
ephrin-B1
EphB2
EphB4
1d
1w
2w – 3w
4w
5w – 8w
(B) Epithelia
Testis
ST
RT
ED
Expression level
ephrin-B1
EphB2
EphB4
1d – 1w
2w – 8w
1d – 1w
2w – 8w
1d
1w
2w – 8w

Fig. 2-13

Figure legends

Figure 2-1

Expression of ephrin-B1, EphB2 and EphB4 in the mouse testis during the postnatal development. Amplification of mRNA for ephrin-B1, EphB2 and EphB4 by RT-PCR. Total RNA was isolated from the ICR mice testis at 1 day (1d), 1 week (1w), 2 weeks (2w), 3 weeks (3w), 4 weeks (4w), 5 weeks (5w), 6 weeks (6w), and 8 weeks (8w) of age and transcribed into first-strand cDNA using M-MLV reverse transcriptase, RNase H^-, and oligo $(dT)_{18}$ primer. The reaction mixture was amplified by PCR with Taq DNA polymerase to detect endogenous ephrin-B1, EphB2 and EpB4. Transcripts of ephrin-B1, EphB2 and EphB4 are detected in testis at all postnatal ages examined.

Figure 2-2

Densitometric quantification of mRNA expression levels from three independent experiments, normalized to β-actin, is shown as means ± SD. One-way ANOVA was used to determine the statistical significance of the results. The relative expression levels of ephrin-B1, EphB2 and EphB4 are decreased with age until 4 weeks, and thereafter are almost unchanged until 8 weeks.

Figure 2-3

Immunofluorescence micrographs showing ephrin-B1 localization in epithelia of the intratesticular excurrent duct system during the postnatal development. Sections were stained with the indicated antibodies and/or DAPI. Vimentin immunostaining was used to identify Sertoli cells. (A) Ephrin-B1 expression in epithelia of seminiferous and straight tubules. Ephrin-B1 expression is faint or almost negative in Sertoli cells of straight tubule at 1 day (1d), 1 week (1w), 2 weeks (2w) and 4 weeks (4w) of age. (B) Ephrin-B1 expression in the rete testis and efferent ductules. Ephrin-B1 immunoreactivity in epithelia of the rete testis is stronger than those of the efferent ductules at 2w and 4w. Ts, seminiferous tubule; ST, straight tubule; RT, rete testis; LC, Leydig cell; ED, efferent ductule.

Figure 2-4

Immunofluorescence micrographs showing EphB2 localization in epithelia of the intratesticular excurrent duct system during the postnatal development. (A) EphB2 expression in epithelia of straight tubules and rete testis. EphB2 immunoreactivity is faint or almost

negative in epithelia of the straight tubule at 1 day (1d), 2 weeks (2w) and 4 weeks (4w) of age. (B) EphB2 expression in the rete testis and efferent ductules. EphB2 expression in epithelia of the efferent ductules is stronger than those of the rete testis at 2w and 4w. ST, straight tubule; RT, rete testis; ED, efferent ductule.

Figure 2-5

Immunofluorescence micrographs showing EphB4 localization in epithelia of the intratesticular excurrent duct system during the postnatal development. (A) EphB4 expression in epithelia of straight tubules and rete testis. EphB4 immunoreactivity is faint in epithelia of straight tubules at 1 day (1d) but substantial at 2 weeks (2w) and 4 weeks (4w) of age. (B) EphB4 immunoreactivity is faint in epithelia of the rete testis but substantial in those of the efferent ductules at 1d. The EphB4 expression boundary between the rete testis and efferent ductules are clear at 1 week (1w), 2w and 4w. ST, straight tubule; RT, rete testis; ED, efferent ductule.

Figure 2-6

Immunofluorescence micrographs showing ephrin-B1 expression in spermatogonia during the postnatal development. Sections were stained with the indicated antibodies. Ephrin-B1 expression in EpCAM-positive spermatogonia is negative at 1 day (1d), prominent at 1 week (1w) and 2 weeks (2w), and faint at 4 weeks (4w) of age.

Figure 2-7

Immunofluorescence micrographs showing EphB2 expression in germ cells during the postnatal development. EphB2 immunoreactivity faintly appears in spermatogonia at 1 day (1d) of age. EphB2-positive spermatids are present sparsely in a seminiferous tubule at 4 weeks (4w) and accumulate in the luminal margin of seminiferous tubules at 5 weeks (5w) of age.

Figure 2-8

Immunofluorescence micrographs showing EphB4 expression in spermatogonia during the postnatal development. Sections were stained with the indicated antibodies. EphB4 is expressed in EpCAM-positive spermatogonia at 1 week (1w), 2 weeks (2w) and 4 weeks (4w) of age but faintly or not in germ cells/gonocytes at 1 day (1d) of age.

Figure 2-9

Immunofluorescence micrographs showing ephrin-B1 expression in ER-TR7-positive stromal cells in the testis during the postnatal development. Sections were stained with the indicated antibodies. Ephrin-B1 immunoreactivity is almost unchanged in ER-TR7-positive cells, fibroblasts and preritubular myoid cells, among 1 day (1d), 2 weeks (2w) and 4 weeks (4w) of ages, while ephrin-B1-positive fibroblasts are prominent at 1d and became less prominent among testicular stromal cells at 2w and 4w due to decrease of fibroblasts with the advance of weeks of age.

Figure 2-10

Immunofluorescence micrographs showing ephrin-B1 expression in CYP17A1-positive Leydig cells in the testis during the postnatal development. Sections were stained with the indicated antibodies. Ephrin-B1 immunoreactivity in CYP17A1-positive Leydig cells at 1 day (1d) of age is weak similar to other stromal cells, becomes strong gradually from 1d towards 4 weeks (4w) of age. Cell sizes of CYP17A1-positive Leydig cells also become large from 1d towards 4w.

Figure 2-11

Immunofluorescence micrographs showing ephrin-B1, EphB2 and EphB4 expression in α-SMA-positive preritubular myoid cells in the mouse testis at 2 weeks (2w) of age. Sections were stained with the indicated antibodies.

Figure 2-12

Immunofluorescence micrographs showing EphB4 expression in CYP17A1-positive Leydig cells in the testis during the postnatal development. Sections were stained with the indicated antibodies. EphB4 is expressed in CYP17A1-positive Leydig cells at 1 day (1d), 2 weeks (2w) and 4 weeks (4w) of age. EphB4 immunoreactivity is largely unchanged in CYP17A1-positive Leydig cells during the postnatal development.

Figure 2-13

Schematic drawings of the postnatal developing testis illustrating expression patterns and levels of ephrin-B1, EphB2, and EphB4 during the postnatal development. (A) Schematic drawing of the seminiferous tubule illustrating the expression patterns of ephrin-B1, EphB2, and EphB4 during postnatal development. (B) Schematic drawing illustrating the relative

expression levels of ephrin-B1, EphB2, and EphB4 in epithelia in the intratesticular excurrent system. Ephrin-B1- and EphB2/EphB4-predominant expression compartments appear alternately in the epithelia along the intratesticular excurrent duct system until 2 weeks of age during the postnatal development. ST, straight tubule; RT, rete testis; ED, efferent ductule.

Chapter 3

Expression and localization of ephrin-B1, EphB2 and EphB4 in the mouse epididymis during the postnatal development

Introduction

The excurrent duct system in the epididymis consisting of the efferent ductules and the ductus epididymis originates from the mesonephric tubules and the mesonephric duct, respectively (Aughey and Frye, 2001; Lupien et al., 2006; Ross and Pawlina, 2015). They connect with each other around embryonic day 13.5 (E13.5) in the mouse (Murashima et al., 2015). This developmental boundary is assigned at the histological boundary between the efferent ductules and the ductus epididymis. The epididymis is composed of the stroma and parenchyma. The parenchyma consists of several short ductules (termed efferent ductules) located in the proximal part of the caput and connected to a single long duct termed the ductus epididymis, which is highly convoluted and divided into several segments separated by the connective tissue septa (Belleannee et al., 2012; Bjorkgren et al., 2012). At birth, the ductus epididymis is poorly developed and thus the epididymis is occupied by mesenchymal tissues/stromata. During the first few days after birth in the mouse, the epididymis undergoes extensive remodeling: the ductus epididymis becomes elongated and convoluted, and accordingly extends into the stroma (Mendive et al., 2006). In the first few weeks during the postnatal development, epithelial cells continue to undergo mitosis frequently in the ductus epididymis, which is occupied by many immature or undifferentiated columnar epithelial cells and a few mitotic cells. Thereafter epithelial cells begin to mature or differentiate, and principal cells and basal cells appear in the epididymal epithelium: accordingly the ductus epididymis turns to be functional (Bjorkgren et al., 2012; Jun et al., 2014; Robaire et al., 2006). The epididymis acquires histological and histochemical properties defined as the adult at 5 weeks of age in the mouse or during puberty when spermatozoa appeared in the lumen of the ductus epididymis (Abou-Haila and Fain-Maurel, 1985; Jun et al., 2014; Mendive et al., 2006). The mature epididymis is grossly divided into three parts: the caput, corpus, and cauda epididymis. It can be divided into more segments histologically and histochemically based on specific expression of glycoconjugates or sugar chains in the epithelium (Burkett et al., 1987). These segments are also morphologically divided by the connective tissue septa that

structurally support and precisely delimit the ductus epididymis characterized by the expression of specific genes (Luedtke et al., 2000; Turner et al., 2003). After spermiation occurs in the testis, spermatozoa travel through the excurrent duct system of the epididymis where they mature, i.e., acquire motility and fertilizing ability to oocytes (Bjorkgren et al., 2012; Cornwall, 2009).

Eph receptors and ephrin ligands serve as a cell-cell communication system and are involved in a variety of biological processes in developing tissues (Pasquale, 2005; Pasquale, 2010). Recently EphB receptors and ephrin-B ligands have been implicated in the physiology and homeostasis of normal adult tissues and organs such as essential roles on the maintenance of epithelial integrity, homeostasis and boundary formation in variety of epithelia in the intestine, stomach, epidermis, and mammary glands (Ishii et al., 2011b; Miao and Wang, 2009; Ogawa et al., 2013; Ogawa et al., 2011b; Pasquale, 2008; Perez White and Getsios, 2014; Uchiyama et al., 2015). However, to the best of the author's knowledge, the expression patterns of EphB and ephrin-B have not been reported in the epididymis in the adult as well as during the postnatal development. Therefore, the author investigated the expression and localization of EphB and ephrin-B in the adult epididymis, and found the ephrin-B1- and EphB2/B4-predominant expression compartments appear along the excurrent duct system in the adult mouse epididymis, which is lined with the ductule/duct-specific epithelia (see Chapter 1). This compartmentalization corresponds to the histological compartments in the intratesticular excurrent duct system as well as the developmental compartments composed of the testicular cords and mesonephric tubules. Therefore in this Chapter, the author investigated the expression and localization of ephrin-B1, EphB2 and EphB4 in the mouse epididymis during the postnatal development to determine when their expression compartments are formed/completed during the postnatal development. In Chapter 1, the author also found that smooth muscle cells surrounding the ductus epididymis express ephrin-B1 and EphB4, spermatozoa in the lumen of the ductus epididymis in the caput and corpus express EphB2, and fibroblasts in the septa express EphB2. Therefore the author also investigated these expressions during the postnatal development to determine the expression behaviors in those cells during the postnatal development.

Materials and methods

Animals

The epididymis of ICR mice of 1 day, 1, 2, 3, 4, 5, 6, and 8 week-old were used for the reverse transcription-polymerase chain reaction (RT-PCR) and immunohistochemical analyses. The animal experimentation protocol was approved by the Animal Research Committee of the Osaka Prefecture University.

Total RNA extraction and semi-quantitative RT-PCR analysis

Total RNA was isolated from the epididymis of 1 day, 1, 2, 3, 4, 5, 6, and 8 week-old mice using TRIzol reagent (Invitrogen, Carlsbad, CA, USA), and RT-PCR analysis was performed as described in the previous chapter (Chapter 2, page 41). The primer pairs (ephrin-B1, EphB2, EphB4, and β-actin) were the same as those used for the semi-quantitative analysis on the testis of the postnatal development (Table 2-1, page 50). PCR cycle numbers for the amplification of ephrin-B1, EphB2 and EphB4 were 29, 32 and 29, respectively. The RT reaction was omitted for the negative controls. Expression levels of amplified ephrin-B1, EphB2 and EphB4 mRNA were determined from three independent experiments, normalized to the levels of β-actin mRNA as an internal control (amplified over 21 cycles), and compared with those of the testis of 8 week-old mice.

Statistical analysis

Statistical analyses were performed with Microsoft Excel and the statistical software on the web (http://statpages.info/anova1sm.html). The bar graphs represent means ± SD. Differences in mean ephrin-B1/EphB2/EphB4 mRNA expression levels among postnatal developing ages were evaluated by one-way ANOVA, followed by Turkey HSD post-hoc analysis. *P* values less than 0.05 were considered significant.

Antibodies and lectins

Goat polyclonal antibodies against the mouse ephrin-B1 extracellular domain, the mouse EphB2 extracellular domain, and the mouse EphB4 extracellular domain were obtained from R&D Systems, Inc. (Minneapolis, MN, USA). The detailed information of these antibodies is described in the previous section (Chapter 1-2, pages 10). Anti-alpha smooth muscle actin (α-SMA) rabbit polyclonal antibody (ab5694) was purchased from Abcam (Cambridge, UK). Rat anti-mouse thymic stromal cell antigen (ER-TR7) monoclonal

antibody was obtained from Novus Biologicals (Littleton, CO, USA) and rat anti-mouse CD31 monoclonal antibody was obtained from BD Biosciences (Franklin Lakes, NJ, USA). Alexa Fluor 488-conjugated donkey anti-goat IgG, Alexa Fluor 568-conjugated donkey anti-rabbit IgG, and Alexa Fluor 594-conjugated donkey anti-rat IgG were obtained from Molecular Probes, Inc. (Eugene, OR, USA). Fluorescein isothiocyanate-conjugated peanut agglutinin lectin (FITC-PNA) and rhodamine-conjugated Ulex Europaeus Agglutinin I lectin (Rh-UEA-I) were obtained from Sigma-Aldrich (St. Louis, MO, USA) and Vector Laboratories (Burlingame, CA, USA), respectively.

Immunofluorescence and lectin fluorescence staining

The fixation of the mouse epididymis at the different postnatal ages and the subsequent processing for tissue sections was performed as the same protocol as described in Chapter 2 (page 42; Table 2-2, page 51). Single- or double-immunofluorescence staining as well as lectin fluorescence staining were performed as the same protocol described in Chapter 1-2 (pages 11-12).

Results

Ephrin-B1, EphB2 and EphB4 mRNA expression in the mouse epididymis during the postnatal development

To investigate relative expression levels of ephrin-B1, EphB2 and EphB4 in the mouse epididymis during the postnatal development, semi-quantitative RT-PCR was performed using epididymis of 1 day, 1, 2, 3, 4, 5, 6, and 8 week-old ICR mice. Transcripts of ephrin-B1, EphB2 and EphB4 were detected in the epididymis at all postnatal ages examined (Fig. 3-1). The transition pattern of relative expression levels in the epididymis during the postnatal development was similar between ephrin-B1 and EphB2 but that of EphB4 was somewhat different form the other molecules. The relative expression levels of ephrin-B1 and EphB2 decreased gradually with ages until 4 weeks, and thereafter remained almost unchanged until 8 weeks of age. In contrast the relative expression levels of EphB4 did not differ until 2 weeks, then decreased sharply towards 4 weeks, and were almost unchanged until 8 weeks of age. These findings indicate that expression levels of ephrin-B1, EphB2 and EphB4 are close to those in the adult until 4 weeks of age (Fig. 3-2).

PNA and UEA-I lectin staining patterns in the efferent ductule and epididymis during the postnatal development

In Chapter 1, the author clearly showed that staining patterns in epithelia by a combination of PNA and UEA-I lectin are identical for the histological segments of the adult mouse epididymis consisting of the efferent ductules and the segment I, II, and III of the ductus epididymis in the caput, and the segment IV and V in the corpus and cauda epididymis, respectively (Table 1-2 and Fig. 1-6). Thus the author determined when epididymal epithelia show the same segment-specific property as seen in the adult epithelia in terms of the lectin staining during the postnatal development. At two weeks of age, PNA lectin uniformly labeled smooth muscle cells surrounding the efferent ductules and ductus epididymis as well as luminal substances in the excurrent ductules/ducts but not in these epithelia. Epithelia of the epididymis were also negative by UEA-I lectin staining although it faintly labeled uniformly luminal substances in the excurrent ductules/ducts. By contrast at three weeks of age, epithelia of the epididymis turned to be abruptly labeled by both PNA and UEA-I: epithelia of the efferent ductules were weakly PNA-positive and UEA-I-negative; epithelia of the segment I were PNA-negative and faintly UEA-I-positive; epithelia of the segment II and III were faintly PNA-positive and weakly UEA-I-positive; epithelia of the segment IV were faintly PNA- and UEA-I-positive; epithelia of the segment V were weakly PNA-positive and faintly UEA-I-positive (Fig. 3-3). Moreover, PNA lectin labeled strongly both smooth muscle cells surrounding both efferent ductules and the ductus epididymis. At 5 weeks, the lectin staining patterns were almost the same as those at 8 weeks of age (the adult): epithelia of the efferent ductules were strongly PNA-positive but UEA-I-negative; epithelia of the segment I were PNA-negative and faintly UEA-I-positive; epithelia of the segment II were weakly PNA-positive and strongly UEA-I-positive; epithelia of the segment III were strongly PNA- and UEA-I-positive; epithelia of the segment IV were strongly PNA-positive and weakly UEA-I-positive; epithelia of the segment V were strongly PNA-positive and faintly UEA-I-positive. Moreover, smooth muscle cells surrounding efferent ductules were strongly PNA-positive and those surrounding the ductus epididymis were weakly/faintly PNA-positive (Fig. 3-3). These PNA and UEA-I lectin staining patterns at 3 and 5 weeks of age are summarized in Table 3-1. Therefore the lectin staining patterns were almost the same as those in the adult until 5 weeks of age.

Ephrin-B1, EphB2, and EphB4 localization in epithelia of the excurrent duct system of the epididymis during postnatal development

In Chapter 1 the author found differences in epithelial ephrin-B1 expression levels among the epididymal segments in the adult mouse and therefore tried to determine when these appear during the postnatal development. Ephrin-B1 immunoreactivity, which was detected in epithelia of the epididymis in all ages of the postnatal development examined, was faint and almost uniform among those of the efferent ductules and the ductus epididymis at 1 day (Fig. 3-4). Ephrin-B1 immunoreactivity became weak and began to be different among the epithelia from 1–2 weeks of age: ephrin-B1 expression in the ductus epididymis became slightly strong compared to that in the efferent ductules from 1–2 weeks of age; Ephrin-B1 immunoreactivity was slightly stronger in the segment IV and V than the other segments among epithelia of the ductus epididymis at 3 weeks and became strong in the segment I as well as IV and V at 4 weeks and thereafter while remained almost unchanged in the segment II and III (Fig. 3-4). Thus staining patterns of ephrin-B1 in the segmented epithelia in the epididymis became close to those in the adult (8 weeks) from 4 weeks of age. Moreover ephrin-B1 immunoreactivity was clearly localized in the basolateral membrane of epithelial cells of the efferent ductules and the ductus epididymis from 1 day of age (Fig. 3-5). In contrast, EphB2 immunoreactivity was detected in epithelia of efferent ductules from 1 day but almost not in those of the ductus epididymis in all ages of postnatal development examined. EphB2 immunoreactivity in epithelia of efferent ductules was faint until 2 weeks, and became weak at 3 weeks of age and thereafter (Fig. 3-6). By contrast, EphB4 was weakly expressed in epithelia of the ductus epididymis clearly until 2 weeks as well as those of the efferent ductules in all ages during the postnatal development. EphB4 immunoreactivity was weak in epithelia of the ductus epididymis until 2 weeks while it was abruptly disappeared in principal cells at 3 weeks but was still faint in basal cells at 3 weeks and thereafter until 8 weeks of age (Fig. 3-7). These findings indicate that ephrin-B1 and EphB2/EphB4 staining patterns in the excurrent ductules/ducts of the epididymis turn to be those in the adult until 3 weeks of age. Therefore, the excurrent duct system in the epididymis is likely completed until 3 weeks of age in terms of ephrin-B1 and EphB2/EphB4 expressions.

Ephrin-B1, EphB2 and EphB4 localization in stromal cells of the epididymis during postnatal development

In Chapter 1, the author found ephrin-B1 and EphB4 expression in periductal smooth muscle cells and fibroblasts, and EphB2 expression in fibroblasts in the epididymal stroma and therefore investigated their expression behaviors in the stromal cells during the postnatal development. ER-TR7 immunostaining was used to identify the fibroblasts; α-SMA

immunostaining was used to identify the periductal smooth muscle cells; CD31 immunostaining was used to identify the endothelial cells of blood vessels. ER-TR7 as a marker for fibroblasts labels also α-SMA-positive cells like periductal smooth muscle cells and vascular smooth muscle cells in the epididymis, and thus ER-TR7 immunostaining is likely useful to determine stromal areas and stromal margin against parenchyma in tissue sections: The relative ratio of the stroma covered by ER-TR7 immunoreactivity to parenchyma (the ductus epididymis) was sharply decreased from 1 day towards 3-4 weeks of age (Fig. 3-8, 3-9, 3-10). Ephrin-B1, EphB2 and EphB4 were expressed in ER-TR7-positive stroma cells at early stages until 1 week and their expressions converged to stromal cells definitely differentiated and localized in the stroma of the epididymis until 2 weeks of age.

Staining patterns and staining behaviors in the stroma of the epididymis during the postnatal development were almost the same between ephirn-B1 and EphB4. Ephrin-B1 and EphB4 was uniformly expressed in ER-TR7-positive fibroblasts, and ER-TR7- and α-SMA-positive periductal smooth muscle cells at 1 day, which were indistinguishable only by ER-TR7 immunostaining due to a similar immunoreactivity between the two cells. Both ephrin-B1 and EphB4 immunoreactivity remained almost unchanged in periductal smooth muscle cells during the postnatal development, while those in fibroblasts were weak at 1 day, became gradually faint until 4 weeks of age, and remained faint or almost negative thereafter until 8 weeks of age (Fig. 3-8, 3-10, 3-11). As an exception, ephin-B1 continued to be expressed substantially in ER-TR7-positive fibroblasts forming septa between segments of the ductus epididymis during the postnatal development. In contrast, EphB2 immunoreactivity was weak in ER-TR7-positive fibroblasts as well as ER-TR7- and α-SMA-positive periductal smooth muscle cells at 1 day and 1 week, and it became faint or almost negative in periductal smooth muscle cells at 2 weeks and thereafter while fibroblasts continued to express EphB2 substantially until 8 weeks of age (Fig. 3-9, 3-11). EphB2 expression was prominent in fibroblasts forming septa between segments of the epididymis due to their strong expression at 2 weeks of age and thereafter during the postnatal development (Fig. 3-9). Moreover until 4 weeks of age spermatozoa were not present in the lumen of the excurrent duct system in the epididymis (Fig. 3-9) while EphB2-positive spermatozoa abruptly appeared in the lumen of the ductus epididymis of the caput and corpus epididymis, and EphB2-negative spermatozoa in the cauda epididymis at 5 weeks of age and thereafter (Fig. 3-12). Furthermore, CD31-positive blood vessels, which expressed EphB4, distributed around the ductus epididymis equally among segments until 3 weeks but more densely in the segment I than the other segments at 4 weeks of age and thereafter during the postnatal development (Fig. 3-13). The

overall expression patterns of ephrin-B1, EphB2 and EphB4 in the mouse epididymis during the postnatal development are illustrated in Fig. 3-14.

Discussion

Eph receptors and ephrin ligands act as a cell-cell communication system with diverse roles in biological processes extensively characterized in developing tissues (Kullander and Klein, 2002; Pasquale, 2005). Recently EphB receptors and ephrin-B ligands have been implicated in the maintenance of epithelial integrity, homeostasis and boundary formation in variety of epithelia in the intestine, stomach, epidermis, and mammary glands (Ishii et al., 2011b; Miao and Wang, 2009; Ogawa et al., 2013; Ogawa et al., 2011b; Pasquale, 2008; Perez White and Getsios, 2014; Uchiyama et al., 2015). Moreover EphB and ephrin-B are involved in cell proliferation and the formation of the glands in the rodent prostate during postnatal development (Ashley et al., 2010). However, to the best of the author's knowledge, EphB and ephrin-B in the epididymis in the adult and the postnatal development has not yet been examined. Thus the author examined EphB and ephrin-B expressions in the adult mouse epididymis, especially focused on epithelia of efferent ductules in the caput and the ductus epididymis, which divides into five segments. Accordingly the author found EphB2/EphB4-predominant expression in efferent ductules and ephrin-B1-predominant expression in the ductus epididymis, where ephrin-B1 immunoreactivity was different among the segments (see Chapter 1). As a series of studies, here the author examined ephrin-B1, EphB2 and EphB4 expression and localization in the mouse epididymis during the postnatal development to determine when those expression compartments are formed/completed in the epithelia during the postnatal development.

A study by Ashley *et al.* shows that relative ephrin-B1 expression levels were high at the prenatal (embryonic day 17) and early postnatal ages (day 1 and day 10) in the development of the rat ventral prostate (Ashley et al., 2010), whose development depends on testosterone like the epididymis. Semi-quantitative RT-PCR analyses revealed that of ephrin-B1, EphB2 and EphB4 in the epididymis were high at 1 day compared to those at 8 weeks of age; the relative expression levels of ephrin-B1 and EphB2 gradually decreased with age until 4 weeks, and thereafter remained almost unchanged until 8 weeks; the relative EphB4 expression levels were largely unchanged from 1 day until 2 weeks, decreased sharply towards 4 weeks, and thereafter remained almost unchanged until 8 weeks. These findings

indicate that expression levels of ephrin-B1, EphB2 and EphB4 are close to those in the adult until 4 weeks of age, and this expression behavior is similar to those in the testis during the postnatal development (see Chapter 2). The author also found that the relative ratio of the stroma to the ductus epididymis rapidly decreased from 1 day towards 3-4 weeks of age during the postnatal development, and ephrin-B1, EphB2 and EphB4 were expressed in ER-TR7-positive mesenchymal cells/fibroblasts relatively strongly at 1 day and 1 week, when these cells densely occupied in the stroma. Thereafter their immunoreactivity in ER-TR7-positive cells turned to weak or faint in the stroma except for the EphB2 expression in the capsule and septa of the epididymis. Therefore the relatively expression levels of ephrin-B1, EphB2 and EphB4 transcripts in the epididymis higher in the earlier postnatal developmental ages likely correspond to a density and number of mesenchymal cells/fibroblasts in the stroma.

In Chapter 1, the author found that efferent ductules in the caput is the predominant EphB2/EphB4-expression compartment and the ductus epididymis is the predominant ephrin-B1-expression compartment in the adult mouse epididymis. Here the author also found that this ephrin-B1 and EphB2/EphB4-expression compartment is formed after 3 weeks of age in the postnatal development: ephrin-B1 immunoreactivity was uniform in epithelia both of the efferent ductules and the ductus epididymis at 1 day, and ephrin-B1 expression in the ductus epididymis became slightly strong compare to that in the efferent ductules from 1–2 weeks of age; EphB2 immunoreactivity in epithelia of efferent ductules was faint until 2 weeks, and became weak at 3 weeks of age and thereafter, but not of the ductus epididymis in all ages of the postnatal development; EphB4 immunoreactivity was uniform in epithelia both of the efferent ductules and the ductus epididymis in the earlier postnatal developmental ages, and became faint or disappeared only in the ductus epididymis at 3 weeks and thereafter. Therefore the excurrent duct system in the epididymis may complete the ephrin-B1 and EphB2/EphB4 expression property close to that in the adult far earlier than the time when the first wave of spermatogenesis is completed and/or spermatozoa enter into the epididymis, i.e., at 5 weeks in the mouse (Abou-Haila and Fain-Maurel, 1985; Montoto et al., 2012).

At birth, the ductus epididymis is poorly developed and thus the epididymis is occupied by mesenchymal tissues/stromata. During the first few days after birth in the mouse, the epididymis undergoes extensive remodeling: the ductus epididymis becomes elongated and convoluted, and accordingly extends into the stroma (Mendive et al., 2006). In the first few weeks during the postnatal development, epithelial cells continue to undergo mitosis frequently in the ductus epididymis, which is occupied by many immature or undifferentiated columnar epithelial cells and a few mitotic cells. Thereafter epithelial cells begin to mature or

differentiate, and principal cells and basal cells appear in the epididymal epithelium: accordingly the ductus epididymis turns to be functional (Bjorkgren et al., 2012; Jun et al., 2014; Robaire et al., 2006). The auther found that (1) EphB4 and ephrin-B1 were expressed uniformly in epithelial cells in the ductus epididymis in the earlier postnatal development, (2) the ephrin-B1 expression remained unchanged in the later postnatal development towards the adult, and (3) EphB4 expression abruptly decreased or disappeared in principal cells in the ductus epididymis at 3 weeks of age and thereafter while basal cells expressed EphB4. These indicate that (1) immature or undifferentiated epithelial cells like basal cells in the ductus epididymis express both EphB4 and ephrin-B1 and mature epithelial cells like principal cells express only ephrin-B1 because principal cells appear in epithelia of the ductus epididymis at a few weeks of age during the postnatal development as described above, and (2) EphB4/ephrin-B1 signaling likely occurs within immature epithelial cells in the ductus epididymis during the postnatal development. The Eph/ephrin signaling induced by overlapped expression of Eph receptor and ephrin ligands within the epithelium promotes differentiation of keratinocytes (Lin et al., 2010). Moreover, deregulated ephrin-B2 signaling in the mammary epithelium induces the delayed differentiation and aberrant tissue architecture (Haldimann et al., 2009). Further studies are necessary to determine the implication of EphB4/ephrin-B1 signaling in epithelial cell maturation and proliferation in the ducutus epididymis.

Summary

The present study represents the first expression analysis of ephrin-B1, EphB2 and EphB4 in the normal mouse epididymis during the postnatal development. The relative expression levels of ephrin-B1, EphB2 and EphB4 by RT-PCR were decreased with age during early postnatal development and became close to those of the adult levels in the epididymis until 4 weeks of age. The author also found that the predominant ephrin-B1- and EphB2/EphB4-expression compartment appeared in epithelia of the excurrent duct system in the epididymis until 3 weeks of age during the postnatal development. Therefore, the excurrent duct system in the epididymis is close to the adult property in terms of ephrin-B1 and EphB2/EphB4 expression, and thus may be completed until 3 weeks of age, far earlier than the time when spermatozoa enter into the excurrent duct.

Table 3-1 PNA and UEA-I lectin staining patterns at 3 and 5 weeks in the epithelium of the excurrent duct system of epididymis

Epithelium	PNA		UEA-I	
	3w	5w	3w	5w
Efferent ductule (ED)	+	++	−	−
Segment I, epididymis (Seg I)	−	−	±	±
Segment II, epididymis (Seg II)	±	+	+	++
Segment III, epididymis (Seg III)	±	++	+	++
Segment IV, epididymis (Seg IV)	±	++	±	+
Segment V, epididymis (Seg V)	+	++	±	±

-, negative; ±, faint stain; +, weak stain; ++, strong stain

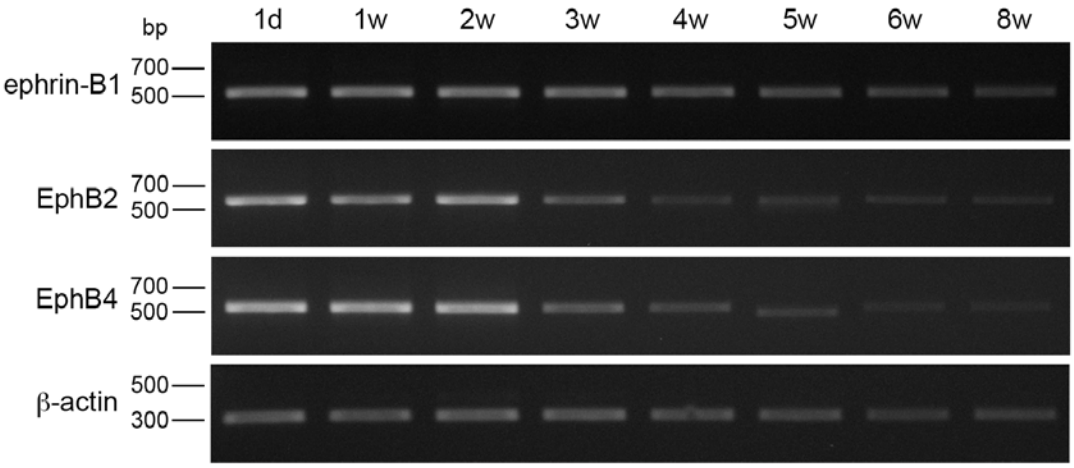
bp
1d
1w
2w
3w
4w
5w
6w
8w
ephrin-B1
700
500
EphB2
700
500
EphB4
700
500
β-actin
500
300

Fig. 3-1

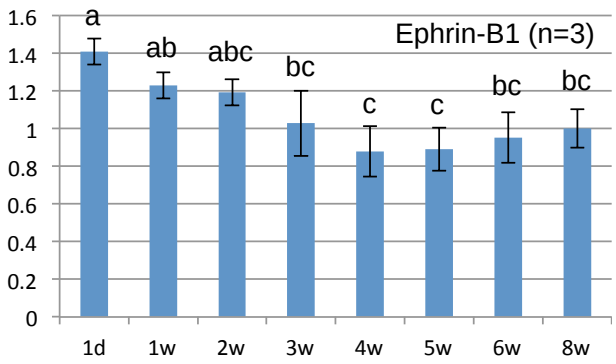

Values with different superscripts indicate significant differences (p<0.05)

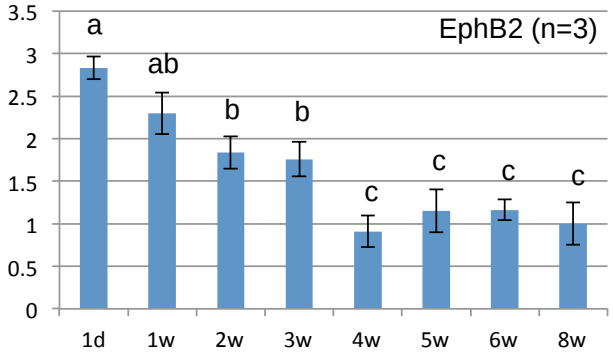

Values with different superscripts indicate significant differences (p<0.05)

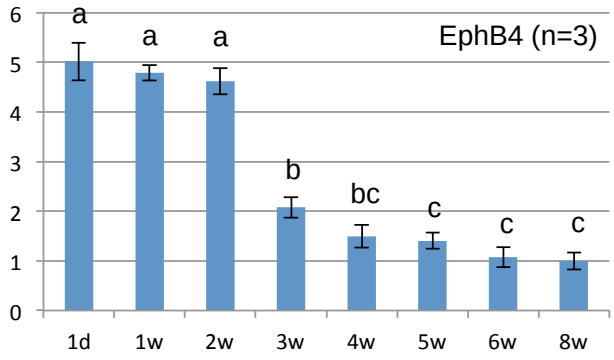

Values with different superscripts indicate significant differences (p<0.05)

Fig. 3-2

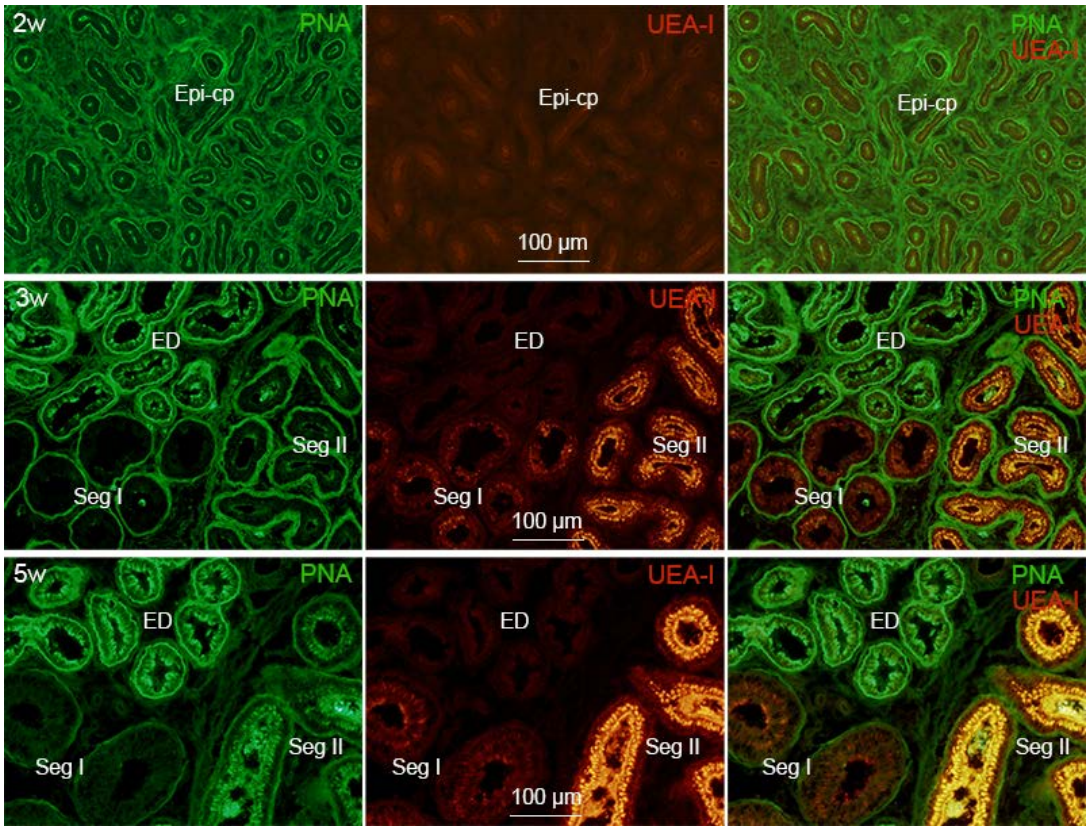
2w
PNA
Epi-cp
UEA-I
Epi-cp
100 μm
PNA
UEA-I
Epi-cp
3w
PNA
ED
Seg II
Seg I
UEA-I
ED
Seg II
Seg I
100 μm
PNA
UEA-I
ED
Seg II
Seg I
5w
PNA
ED
Seg II
Seg I
UEA-I
ED
Seg II
Seg I
100 μm
PNA
UEA-I
ED
Seg II
Seg I

Fig. 3-3

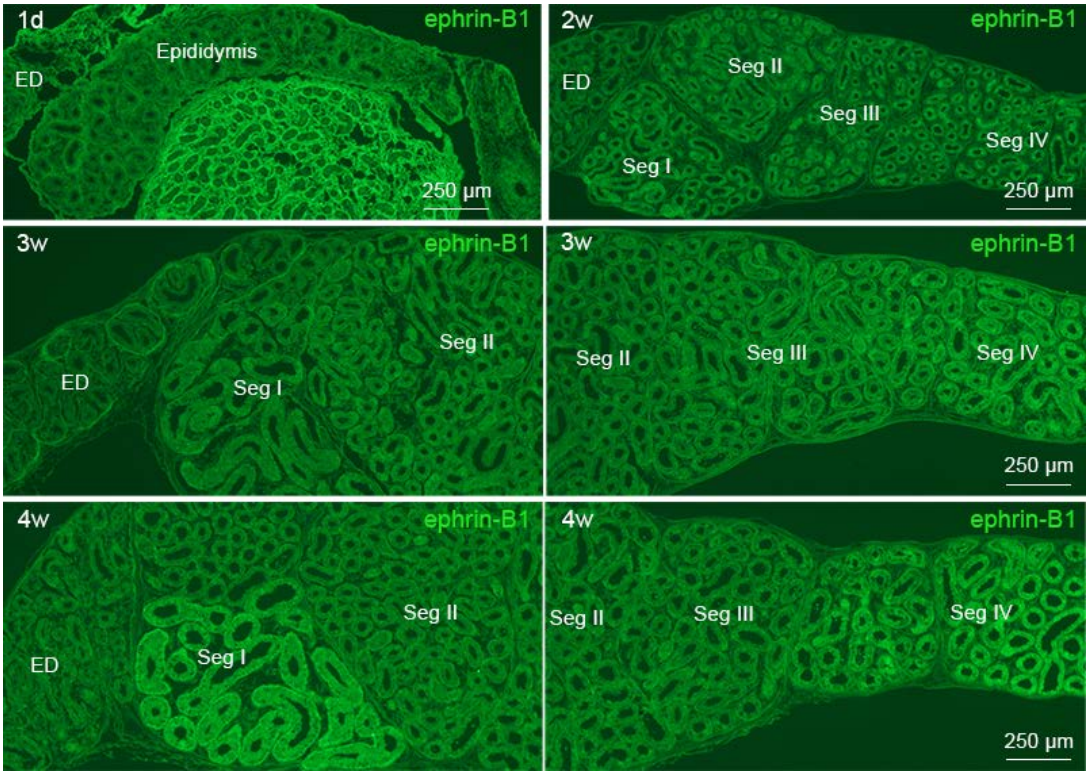
1d
ephrin-B1
Epididymis
ED
250 μm
2w
ephrin-B1
Seg II
ED
Seg III
Seg IV
Seg I
250 μm
3w
ephrin-B1
Seg II
ED
Seg I
3w
ephrin-B1
Seg II
Seg III
Seg IV
250 μm
4w
ephrin-B1
Seg II
Seg I
ED
4w
ephrin-B1
Seg II
Seg III
Seg IV
250 μm

Fig. 3-4

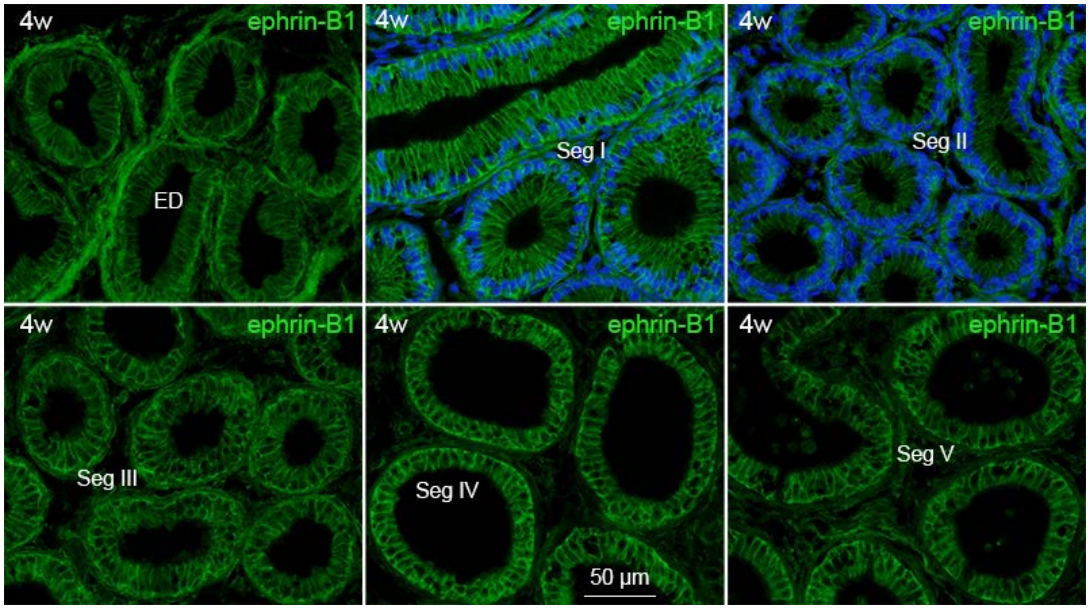
4w
ephrin-B1
ED
4w
ephrin-B1
Seg I
4w
ephrin-B1
Seg II
4w
ephrin-B1
Seg III
4w
ephrin-B1
Seg IV
50 μm
4w
ephrin-B1
Seg V

Fig. 3-5

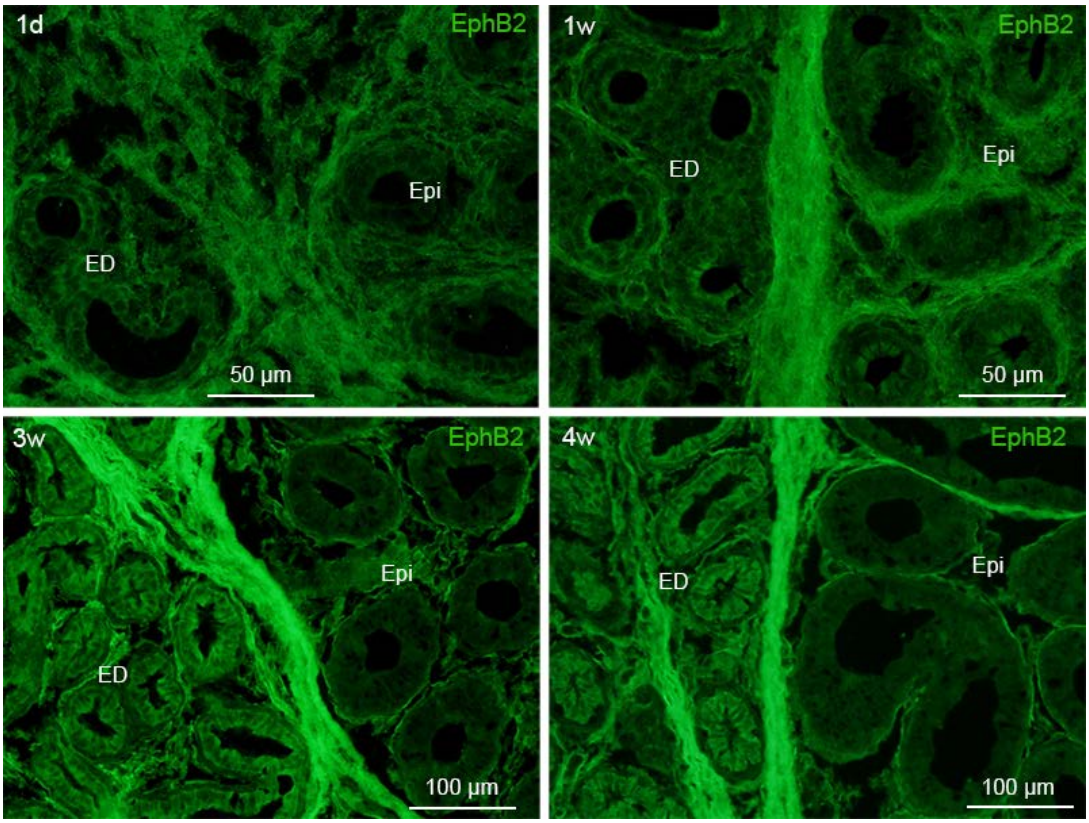
1d
EphB2
Epi
ED
50 μm
1w
EphB2
ED
Epi
50 μm
3w
EphB2
Epi
ED
100 μm
4w
EphB2
ED
Epi
100 μm

Fig. 3-6

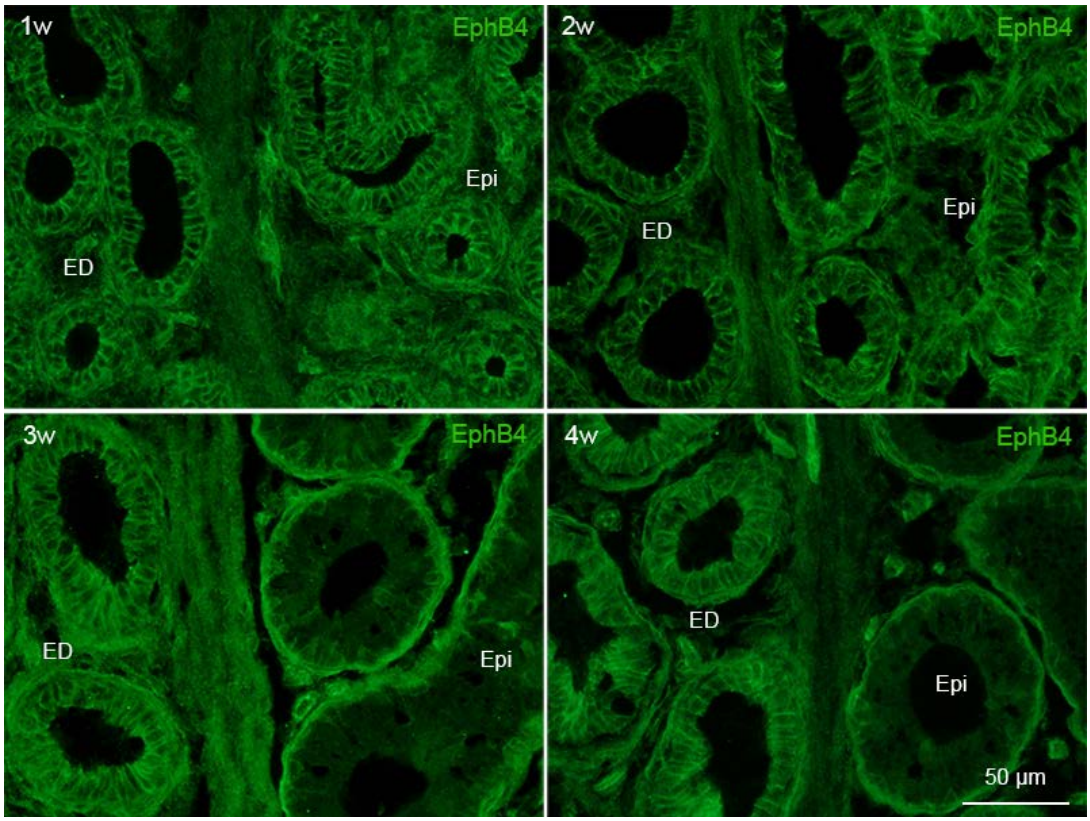
1w
EphB4
Epi
ED
2w
EphB4
ED
Epi
3w
EphB4
ED
Epi
4w
EphB4
ED
Epi
50 μm

Fig. 3-7

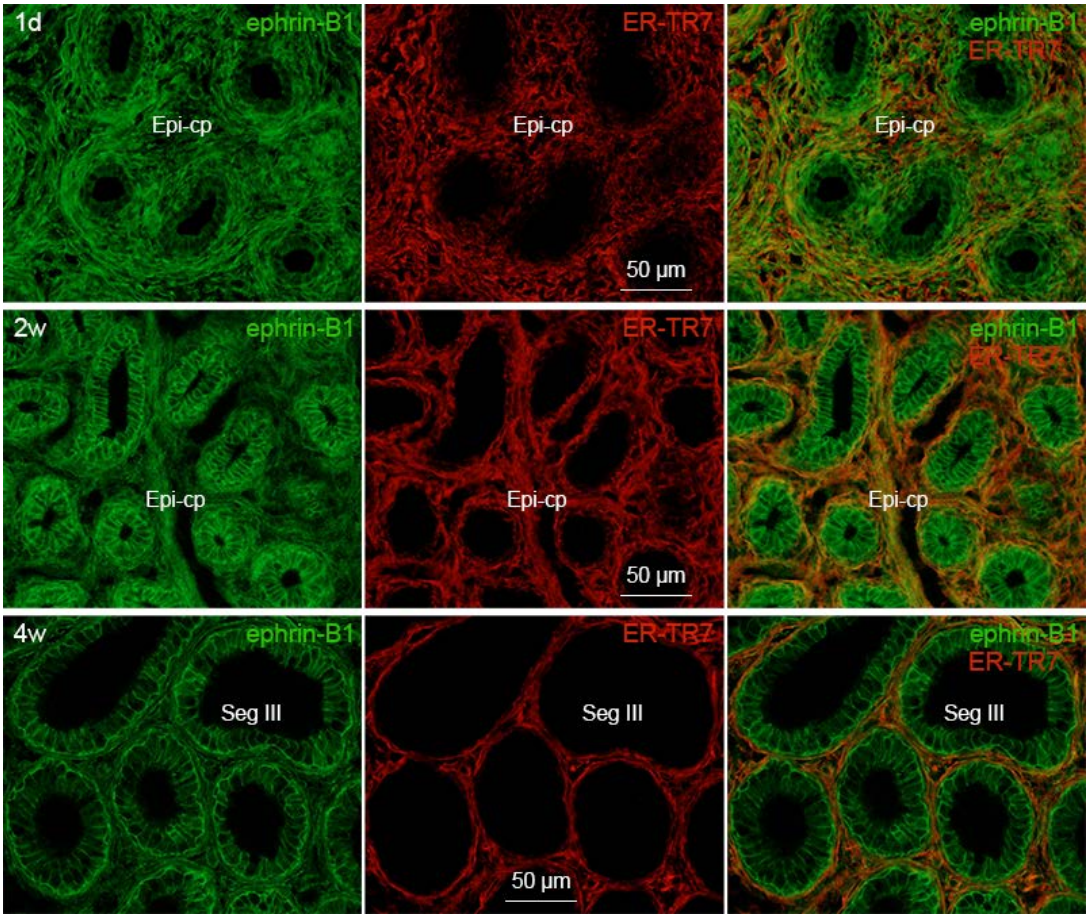
1d
ephrin-B1
Epi-cp
ER-TR7
Epi-cp
50 μm
ephrin-B1
ER-TR7
Epi-cp
2w
ephrin-B1
Epi-cp
ER-TR7
Epi-cp
50 μm
ephrin-B1
ER-TR7
Epi-cp
4w
ephrin-B1
Seg III
ER-TR7
Seg III
50 μm
ephrin-B1
ER-TR7
Seg III

Fig. 3-8

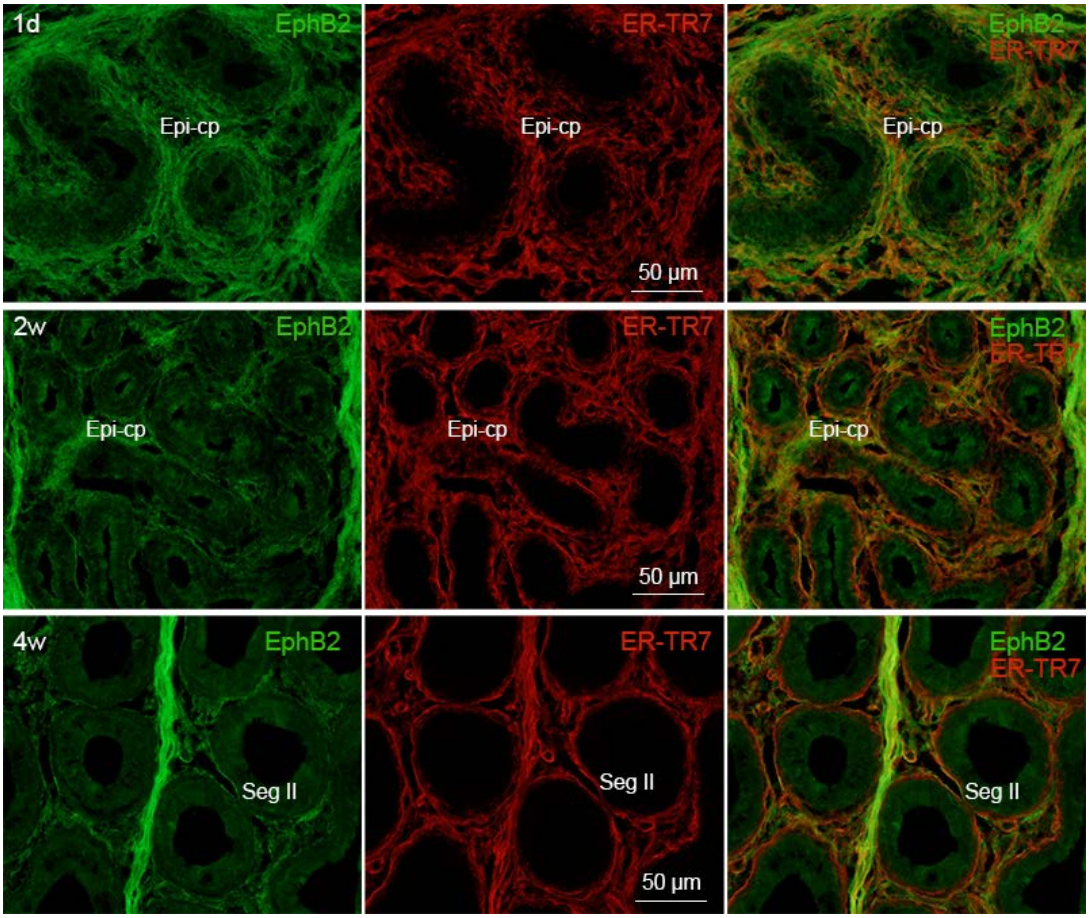
1d
EphB2
Epi-cp
ER-TR7
Epi-cp
EphB2
ER-TR7
Epi-cp
50 μm
2w
EphB2
Epi-cp
ER-TR7
Epi-cp
EphB2
ER-TR7
Epi-cp
50 μm
4w
EphB2
Seg II
ER-TR7
Seg II
EphB2
ER-TR7
Seg II
50 μm

Fig. 3-9

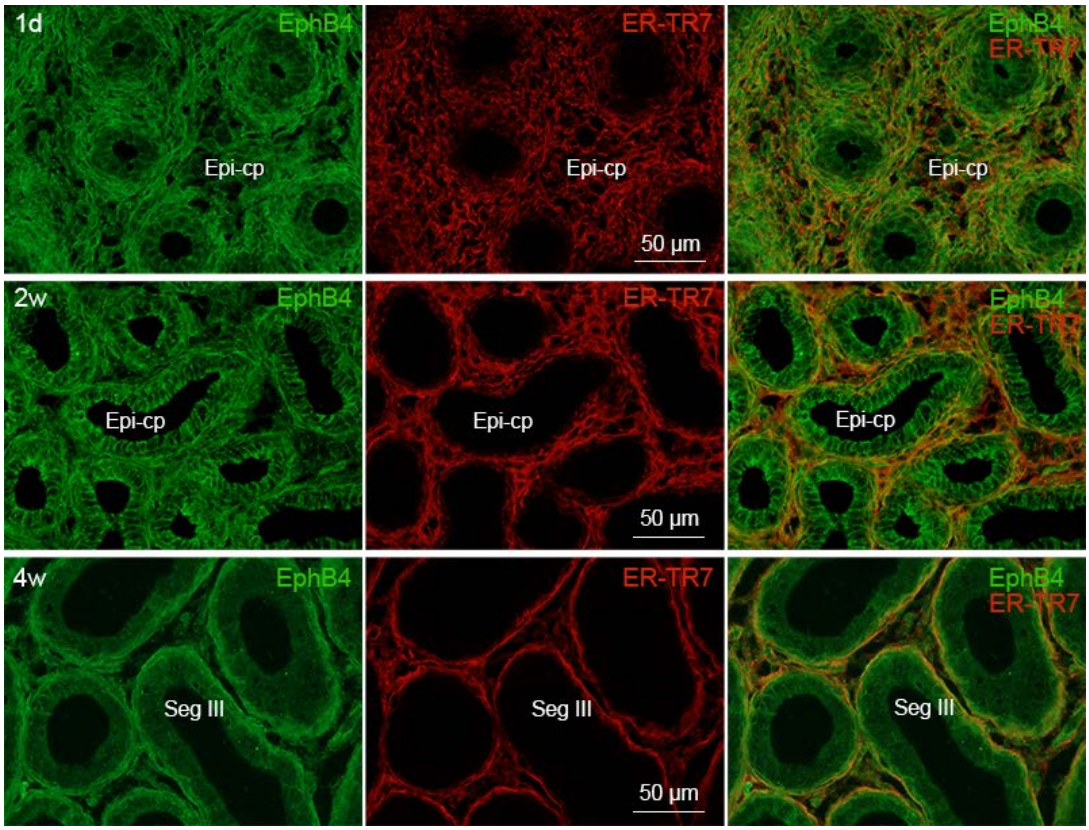
1d
EphB4
Epi-cp
ER-TR7
Epi-cp
50 μm
EphB4
ER-TR7
Epi-cp
2w
EphB4
Epi-cp
ER-TR7
Epi-cp
50 μm
EphB4
ER-TR7
Epi-cp
4w
EphB4
Seg III
ER-TR7
Seg III
50 μm
EphB4
ER-TR7
Seg III

Fig. 3-10

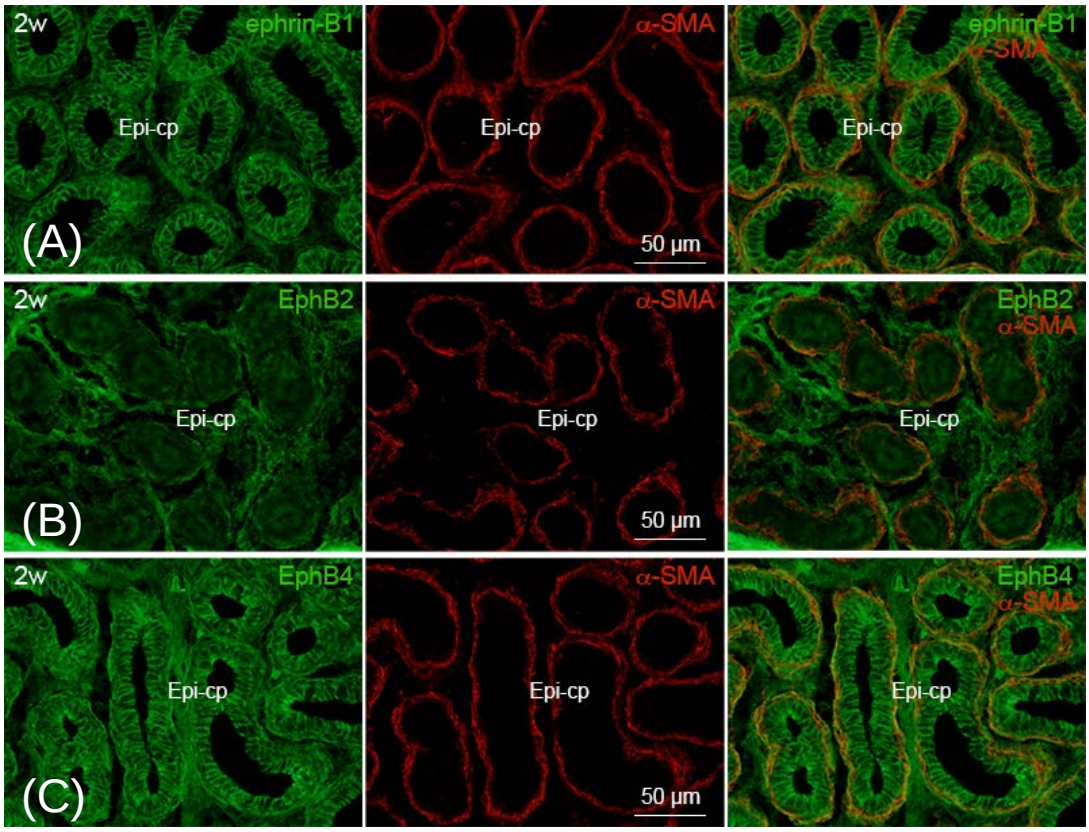
2w
ephrin-B1
Epi-cp
α-SMA
Epi-cp
50 μm
ephrin-B1
α-SMA
Epi-cp
(A)
2w
EphB2
Epi-cp
α-SMA
Epi-cp
50 μm
EphB2
α-SMA
Epi-cp
(B)
2w
EphB4
Epi-cp
α-SMA
Epi-cp
50 μm
EphB4
α-SMA
Epi-cp
(C)

Fig. 3-11

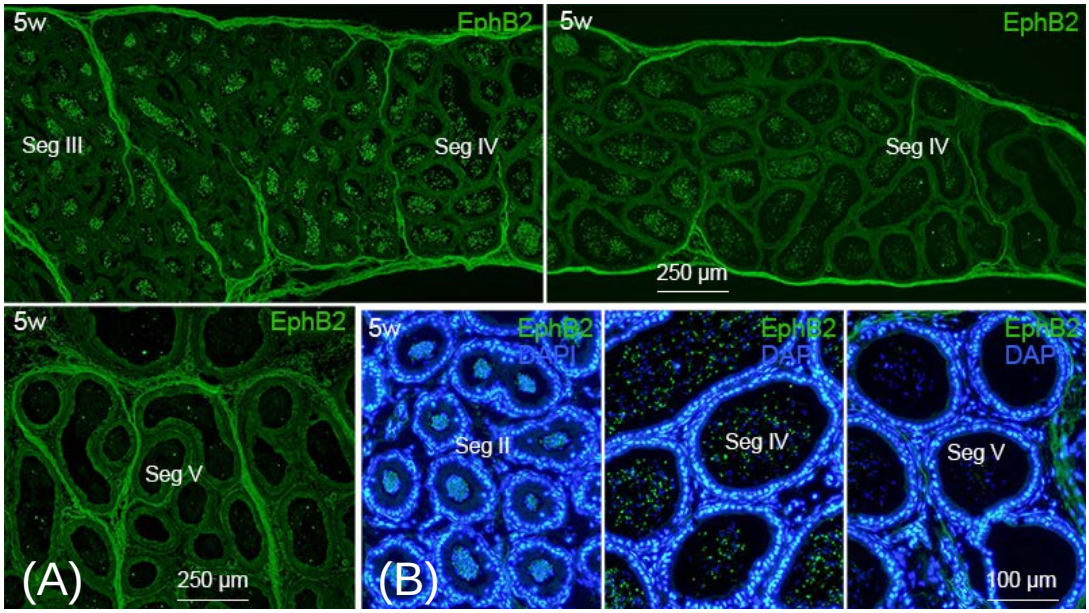
5w
EphB2
Seg III
Seg IV
5w
EphB2
Seg IV
250 μm
5w
EphB2
Seg V
(A)
250 μm
5w
EphB2
DAPI
Seg II
(B)
EphB2
DAPI
Seg IV
EphB2
DAPI
Seg V
100 μm

Fig. 3-12

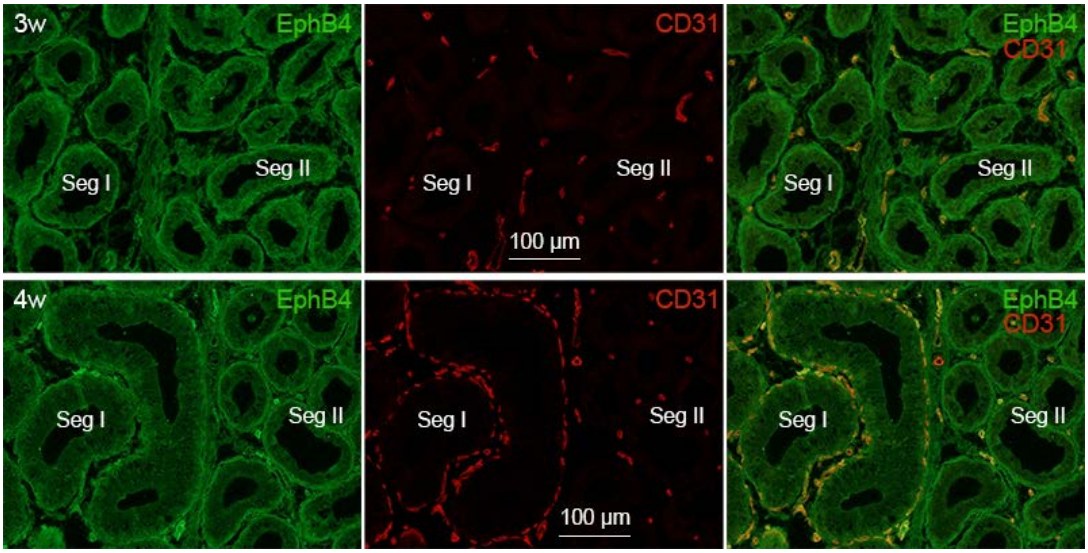
3w
EphB4
Seg I
Seg II
CD31
Seg I
Seg II
100 μm
EphB4
CD31
Seg I
Seg II
4w
EphB4
Seg I
Seg II
CD31
Seg I
Seg II
100 μm
EphB4
CD31
Seg I
Seg II

Fig. 3-13

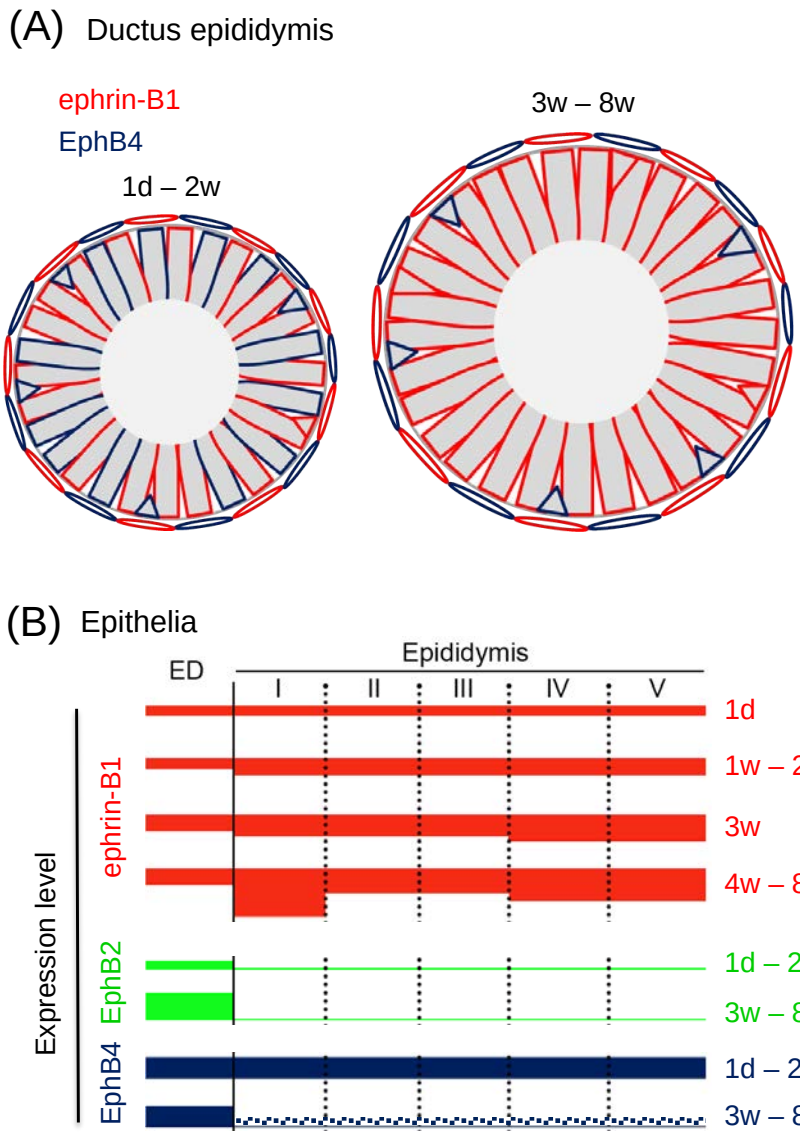
(A) Ductus epididymis
ephrin-B1
EphB4
1d – 2w
3w – 8w
(B) Epithelia
ED
Epididymis
I
II
III
IV
V
Expression level
ephrin-B1
EphB2
EphB4
1d
1w – 2w
3w
4w – 8w
1d – 2w
3w – 8w
1d – 2w
3w – 8w

Fig. 3-14

Figure legends

Figure 3-1

Expression of ephrin-B1, EphB2 and EphB4 in the mouse epididymis during the postnatal development. Amplification of mRNA for ephrin-B1, EphB2 and EphB4 by RT-PCR. Total RNA was isolated from the ICR mice epididymis at 1 day (1d), 1 weeks (1w), 2 weeks (2w), 3 weeks (3w), 4 weeks (4w), 5 weeks (5w), 6 weeks (6w), and 8 weeks (8w) of age and transcribed into first-strand cDNA using M-MLV reverse transcriptase, RNase H^-, and oligo $(dT)_{18}$ primer. The reaction mixture was amplified by PCR with Taq DNA polymerase to detect endogenous ephrin-B1, EphB2 and EpB4. Transcripts of ephrin-B1, EphB2 and EphB4 are detected in the epididymis at all postnatal ages examined.

Figure 3-2

Densitometric quantification of mRNA expression levels from three independent experiments, normalized to β-actin, is shown as means ± SD. One-way ANOVA was used to determine the statistical significance of the results. The relative expression levels of ephrin-B1and EphB2 are decreased gradually with age until 4 weeks, and thereafter almost unchanged until 8 weeks whereas the relative EphB4 expression levels remain almost unchanged until 2 weeks, then decrease sharply towards 4 weeks, and are almost similar until 8 weeks of age.

Figure 3-3

Immunofluorescence micrographs showing PNA and UEA-I lectin stainings in the efferent ductule and ductus epididymis during the postnatal development. Epithelia of the efferent ductules and ductus epididymis are not labeled by PNA and UEA-I lectins at 2 weeks (2w) but those are labeled at 3 (3w) and 5 weeks (5w) of age: PNA lectin uniformly labels luminal substances in the efferent ductules and ductus epididymis as well as smooth muscle cells surrounding the ductules/ducts but not these epithelia at 2w. At 3w, epithelia of the efferent ductules (ED) are weakly PNA-positive and UEA-I-negative; epithelia of the segment I (Seg I) are PNA-negative and faintly UEA-I-positive; epithelia of the segment II (Seg II) are faintly PNA-positive and weakly UEA-I-positive. At 5w, the lectin staining patterns are almost the same as those in the adult (see Fig. 1-6 in Chapter 1): epithelia of the efferent ductules are strongly PNA-positive but UEA-I-negative; epithelia of the segment I are PNA-negative and faintly UEA-I-positive; epithelia of the segment II are weakly PNA-positive and strongly UEA-I-positive. ED, efferent ductule; Epi-cp, caput epididymis; Seg, segment.

Figure 3-4

Immunofluorescence micrographs showing an overview of ephrin-B1 expression in epithelia of the excurrent duct system of the mouse epididymis during the postnatal development. Ephrin-B1 immunoreactivity is faint and almost uniform among epithelia of the efferent ductules and the ductus epididymis at 1 day (1d), and slightly strong in the ductus epididymis of the segment I, II, III and IV compare to that in the efferent ductules at 2 weeks (2w) of age. Ephrin-B1 immunoreactivity is slightly stronger in the segment IV than the other segments among epithelia of the ductus epididymis at 3 weeks (3w), and strong in the segment I and IV at 4 weeks (4w) of age. ED, efferent ductule; Seg, segment.

Figure 3-5

Immunofluorescence micrographs showing ephrin-B1 localization in epithelial cells of the ductus epididymis at 4 weeks (4w) of age. Sections were stained with the ephrin-B1 antibody and/or DAPI. Ephrin-B1 immunoreactivity is localized in the basolateral membrane of epithelial cells, i.e., principal cells and basal cells in the efferent ductules and the ductus epididymis. ED, efferent ductule; Seg, segment.

Figure 3-6

Immunofluorescence micrographs showing EphB2 expression in the excurrent duct system of the mouse epididymis during the postnatal development. EphB2 expression is faint in epithelia of the efferent ductules at 1 day (1d) and 1 week (1w), and weak at 3 weeks (3w) and 4 weeks (4W) of age whereas EphB2 expression in those of the ductus epididymis is faint or almost negative at these postnatal ages. EphB2 is faintly positive at 1d, weakly at 1w, and strongly at 2w and 3w in stromal cells between the efferent ductules and the ductus epididymis, where septa is clearly formed. ED, efferent ductule; Epi, epididymis.

Figure 3-7

Immunofluorescence micrographs showing EphB4 localization in the excurrent duct system of the mouse epididymis during the postnatal development. EphB4 immunoreactivity is clearly detected in the basolateral membrane of epithelia in the efferent ductules at 1 week (1w), 2 weeks (2w), 3 weeks (3w) and 4 weeks (4w) of age. EphB4 immunoreactivity is also detected in epithelia of the ductus epididymis at 1w and 2w while it is almost negative in principal cells but still faint in basal cells at 3w and 4w. EphB4 is expressed in stromal cells

surrounding the efferent ductules and the ductus epididymis. ED, efferent ductule; Epi, epididymis.

Figure 3-8

Immunofluorescence micrographs showing ephrin-B1 expression in ER-TR7-positive stromal cells in the epididymis during the postnatal development. Sections were stained with the indicated antibodies. ER-TR7-positive stromal cells are prominent at 1 day (1d) and became less prominent at 2 weeks (2w) and 4 weeks (4w) of age. Ephrin-B1 immunoreactivity in ER-TR7-positive fibroblasts is substantial at 1d, and faint at 2w and 4w. Epi-cp, caput epididymis; Seg, segment.

Figure 3-9

Immunofluorescence micrographs showing EphB2 expression in ER-TR7-positive stromal cells in the epididymis during the postnatal development. Sections were stained with the indicated antibodies. ER-TR7-positive stromal cells are prominent at 1 day (1d) and became less prominent at 2 weeks (2w) and 4 weeks (4w) of age. EphB2 is weakly expressed in ER-TR7-positive fibroblasts at 1d, 2w and 4w, and is prominently in the fibroblasts forming septa between the segments of epididymis at 2w and 4w. Epi-cp, caput epididymis; Seg, segment.

Figure 3-10

Immunofluorescence micrographs showing EphB4 expression in ER-TR7-positive stromal cells in the epididymis during the postnatal development. Sections were stained with the indicated antibodies. ER-TR7-positive stromal cells are prominent at 1 day (1d) and became less prominent at 2 weeks (2w) and 4 weeks (4w) of age. EphB4 immunoreactivity is weak in ER-TR7-positive fibroblasts at 1d, and faint at 2w and 4w while it is still weak in ER-TR7-positive stromal cells surrounding the ductus epididymis, i.e., smooth muscle cells. Epi-cp, caput epididymis; Seg, segment.

Figure 3-11

Immunofluorescence micrographs showing ephrin-B1 and EphB2 and EphB4 expression in α-SMA-positive periductal smooth muscle cells in the mouse epididymis at 2 weeks (2w) of age. Sections were stained with the indicated antibodies. Ephrin-B1 (A) and EphB4 (C) expression is weak, and EphB2 (B) expression is faint or almost not in α-SMA-positive periductal smooth muscle cells. Epi-cp, caput epididymis.

Figure 3-12

Immunofluorescence micrographs showing EphB2 expression in spermatozoa in lumen of the ductus epididymis at 5 weeks (5w) of age. Sections were stained with the EphB2 antibody and/or DAPI. (A, B) EphB2 immunoreactivity in spermatozoa in the lumen of the ductus epididymis is gradually decreased from segment III to segment V, in which most spermatozoa are EphB2-negative. Seg, segment.

Figure 3-13

Immunofluorescence micrographs showing EphB4 expression in CD31-positive blood vessels in the mouse epididymis during the postnatal development. Sections were stained with the indicated antibodies. EphB4 is expressed in CD31-positive blood vessels, which are distributed around the ductus epididymis equally in the segment I (Seg I) and II (Seg II) at 3 weeks (3w) but more densely in the segment I than the segment II at 4 weeks (4w) of age. Seg, segment.

Figure 3-14

Schematic drawings of the postnatal developing epididymis illustrating expression patterns and levels of ephrin-B1, EphB2, and EphB4 during the postnatal development. (A) Schematic drawing of the ductus epididymis illustrating the expression patterns of ephrin-B1, EphB2, and EphB4 during the postnatal development. (B) Schematic drawing illustrating the relative expression levels of ephrin-B1, EphB2, and EphB4 in epithelia in the excurrent system of the epididymis. Ephrin-B1- and EphB2/EphB4-predominant expression compartments appear in the epithelia along the excurrent system of the epididymis until 3 weeks of age during the postnatal development. ED, efferent ductule; I–V, segments I–V.

General discussion

EphB receptor tyrosine kinases and their interacting ephrin-B ligands are transmembrane proteins, and together, they function as cell–cell communication molecules to play crucial roles in the establishment of spatial organization of cells in various tissues and organs by repulsive or adhesive signals arising from contact between EphB- and ephrin-B-bearing cells. The role of EphB and ephrin-B has been extensively characterized in developing tissues (Klein, 2012; Kullander and Klein, 2002; Pasquale, 2005). Recently EphB receptors and ephrin-B ligands have been implicated in the maintenance of epithelial integrity, homeostasis and boundary formation in variety of epithelia in the intestine, stomach, epidermis, and mammary glands (Ishii et al., 2011b; Miao and Wang, 2009; Ogawa et al., 2013; Ogawa et al., 2011b; Pasquale, 2008; Perez White and Getsios, 2014; Uchiyama et al., 2015) and their diverse functions in the epithelial tissues are mainly related to complementary expression pattern of the receptors and ligands in adjacent epithelial compartments (Miao and Wang, 2009). Thus the author examined EphB and ephrin-B expressions in epithelia of the excurrent duct system in the mouse testis and epididymis in the adult and during the postnatal development. The author found that the ephrin-B1- and EphB2/EphB4-predominant expression compartments appear alternately along the excurrent system of the adult mouse, which is lined with the tubule/ductule/duct-specific epithelia. Thus, the compartmentalization based on the ephrin-B and EphB expression patterns corresponds to the histological as well as the developmental compartments in the excurrent tubule/ductule/duct system. Moreover, the author found that such ephrin-B1- and EphB2/EphB4-predominant expression compartments were formed in the epithelium of intratesticular excurrent duct system until 2 weeks of age and in the excurrent duct system of the epididymis until 3 weeks of age during postnatal development. Therefore in terms of ephrin-B1 and EphB2/EphB4 expressions, the male genital excurrent duct system is completed far earlier than the time when the first wave of spermatogenesis is completed and spermatozoa enter into the ductus epididymis. Those ephrin-B1 and EphB2/EphB4 expression patterns suggest that strong EphB/ephrin-B signaling likely arises at every epithelial junction along the excurrent tubule/ductule/duct system of the testis and epididymis. It is well accepted that the EphB/ephrin-B cell–cell communication system is involved in tissue-border formation by initiating cell–cell repulsive signals between ephrin-B-bearing and EphB-bearing cells (Batlle and Wilkinson, 2012; Kullander and Klein, 2002; Pasquale, 2005). Therefore, the author proposes that the interplay

between EphB and ephrin-B may regulate/maintain epithelial boundaries along the excurrent tubule/ductule/duct system of the testis and epididymis in the adult as well as during the postnatal development from 2-3 weeks of age.

In the testis, ephrin-B1 and EphB4 expressions were faint or almost negative in germ cells in seminiferous tubules at 1 day but positive in EpCAM-positive-spermatogonia from 1 week of age. This indicates that ephrin-B1 and EphB4 are unlikely expressed in gonocytes because gonocytes differentiate into spermatogonial stem cells/spermatogonia during days 3–6 after birth (Abe et al., 1991; Montoto et al., 2012; Tiptanavattana et al., 2015). It is well accepted that gonocytes and spermatogonia are localized in the luminal and basal side of seminiferous tubules, respectively (Bellve et al., 1977). Based on these the author suggests that EphB4/ephrin-B1 signaling may involve in the process of proliferation and/or differentiation in spermatogonia, and moreover EphB4 and ephrin-B1 are likely markers useful to discriminate spermatogonia from gonocytes in seminiferous tubules during the early postnatal development. Moreover EphB2-positive spermatids abruptly appeared sparsely in some seminiferous tubules at 4 weeks and densely accumulated in many seminiferous tubules at 5 weeks and thereafter. The first wave of spermatogenesis, an entire differentiation process from spermatogonia (spermatogonial stem cells) into spermatozoa, completes within the postnatal day 35 in mice (Montoto et al., 2012). Thus EphB2 immunoreactivity is likely a good indicator to determine the completion of the first wave of spermatogenesis. Therefore the author suggests that the EphB2 immunoreactivity is a good tool to examine male reproductive toxicity using mice. The author also found that peritubular myoid cells and Leydig cells expressed ephrin-B1 and EphB4 throughout the postnatal development and in the adult. Collectively form those and these findings, spermatogonia, peritubular myoid cells and Leydig cells in testis express ephrin-B1 and EphB4. It is reported that in the bone marrow, EphB/ephrin-B is implicated in modulating the niche for hematopoietic stem cells (Nguyen et al., 2016). Thus it is intriguing whether EphB4/ephrin-B1 signaling mediated by cell–cell contacts among spermatogonia, myoid cells, and Leydig cells is involved in spermatogonial niche formation, similar to that observed in the niche for hematopoietic stem cells.

In the epididymis, the author found that immature or undifferentiated epithelial cells like basal cells in the ductus epididymis expressed both EphB4 and ephrin-B1 throughout the postnatal development and in the adult, and mature epithelial cells like principal cells expressed only ephrin-B1. This suggests that EphB4/ephrin-B1 signaling likely occurs within immature epithelial cells in the ductus epididymis in the earlier postnatal development and between principal and basal cells in the mature epithelium of the ductus epididymis. It is

reported that the Eph/ephrin signaling induced by overlapped expression of Eph receptor and ephrin ligands within the epithelium promotes differentiation of keratinocytes (Lin et al., 2010). Thus further studies are necessary to determine the implication of EphB4/ephrin-B1 signaling in epithelial cell maturation and proliferation in the ducutus epididymis. Moreover, ephrin-B1 in principle cells may modulate tight junction integration between epithelial cells in the ductus epididymis. It is reported that ephrin-B1 directly interacts with claudins, and this interaction affects tight junction integration in normal epithelial cells (Tanaka et al., 2005). The author also found that EphB2 was expressed in immature spermatozoa which were located in the lumen of the excurrent tubule/ductule system in the testis and the ductus epididymis in the caput and corpus, but not in mature spermatozoa located in the cauda epididymis. This indicates that EphB2 is unlikely required by mature spermatozoa and that EphB2 expression can be a new negative indicator for the maturation of spermatozoa.

Conclusions

The author investigated the expression and localization of EphB receptors and ephrin-B ligands in the mouse testis and epididymis in the adult and during the postnatal development, especially to determine whether their expression compartments exist in epithelia of tubules/ductules/ducts in a series of the excurrent duct system in the adult and when their expression boundaries are formed/completed during the postnatal development. The results obtained as follows:

1. EphB2 in the testis and EphB4 in the testis and epididymis in adult mouse are tyrosine-phosphorylated, suggesting that EphB2-bearing cells in the testis and EphB4-bearing cells in the testis and epididymis are in contact with ephrin-B-bearing cells and that these receptors are activated in the adult testis and/or epididymis *in vivo*.
2. The ephrin-B1- and EphB2/EphB4-predominant expression compartments appear alternately along the excurrent duct system of adult mouse, which is lined with the tubule/ductule/duct-specific epithelia. This compartmentalization corresponds to the histological as well as the developmental compartments.
3. EphB2 is expressed in immature spermatozoa but not in mature spermatozoa located in the lumen of the ductus epididymis in the cauda epididymis. Therefore EphB2 expression can be a new negative indicator for the maturation of spermatozoa.
4. The ephrin-B1- and EphB2/EphB4-predominant expression compartments are formed in the intratesticular excurrent duct system until 2 weeks and in the excurrent ducts in the epididymis until 3 weeks of age during the postnatal development.
5. Ephrin-B1 and EphB4 express in spermatogonia but not in gonocytes among germ cells in seminiferous tubules in the testis in the adult and during the postnatal development.
6. Leydig cells express ephrin-B1 and EphB4 throughout the postnatal development, and their expression levels increase with the ages in ephrin-B1 but not in EphB4.
7. Ephrin-B1 is expressed in immature and mature epithelial cells of the ductus epididymis in all ages during the postnatal development while EphB4 is expressed in the ductus epididymis consisting of immature epithelial cells during only the early postnatal ages until 2 weeks and thereafter in basal cells in the mature epithelium.

Acknowledgements

It is a great pleasure and honor of the author to acknowledge a group of extremely well people who made his doctoral thesis to appear. The author feels proud to express his deepest sense of gratitude, sincere appreciation, profound regards and immense indebtedness to his reverend supervisor Professor Dr. Kazushige Ogawa for his research planning, scholastic guidance, sympathetic supervision, utmost desire, valuable suggestions, wise criticism, constructive and constant inspiration throughout the entire period of the study, research work and in preparation of this manuscript. The author really wants to thank him from the bottom of his heart for being such a friendly and cooperative supervisor. The author would like to express the highest gratefulness and deepest sense of gratitude to Associate Professor Dr. Takayuki Nakajima for his kind co-operation, generous help and valuable comments throughout the entire period of the study.

The author would like to give sincere thanks to Professor Dr. Hiromichi Tamada and Professor Dr. Yoichi Nakamura for their critical and insightful comments and encouragement in reviewing this thesis.

The author is thankful to The Ministry of Education, Culture, Sports, Science, and Technology (MEXT) of Japan government for providing scholarship for his doctoral study and will remain grateful to Osaka Prefecture University for providing all nice academic facilities and quality staffs.

The author is really grateful to his tutors, Noritaka Saeki and Yukari Kohara for their sincere support in his research work and many other important issues during the early period in Japan. The author is also thankful to all lab members who were always friendly and helpful.

Thanks are extended to all of well-wishers for their direct and indirect inspiration and help in completing this research work.

Last but no way to the least, the author wishes to express ever grateful and immensely indebted to his respected parents, his wife, his only beloved son, affectionate sisters and relatives for their heartiest blessings, affectionate feelings, encouragement and all sorts of sacrifices for the author's higher education and successful completion of this humble research work.

The Author

March, 2019

References

Abe, K., L.S. Shen, and H. Takano. 1991. The cycle of the seminiferous epithelium and stages in spermatogenesis in dd-mice. *Hokkaido Igaku Zasshi.* 66:286-299.

Abou-Haila, A., and M.A. Fain-Maurel. 1985. Postnatal differentiation of the enzymatic activity of the mouse epididymis. *Int J Androl.* 8:441-458.

Ashley, G.R., O.C. Grace, G. Vanpoucke, and A.A. Thomson. 2010. Identification of EphrinB1 expression in prostatic mesenchyme and a role for EphB-EphrinB signalling in prostate development. *Differentiation.* 80:89-98. doi: 10.1016/j.diff.2010.1006.1003. Epub 2010 Jul 1015.

Aughey, E., and F.L. Frye. 2001. Male Reproductive System. *In:* Comparative Veterinary Histology With Clinical Correlates. Manson Publishing Ltd. , London, UK.

Batlle, E., and D.G. Wilkinson. 2012. Molecular mechanisms of cell segregation and boundary formation in development and tumorigenesis. *Cold Spring Harb Perspect Biol.* 4:a008227. doi: 008210.001101/cshperspect.a008227.

Belleannee, C., V. Thimon, and R. Sullivan. 2012. Region-specific gene expression in the epididymis. *Cell Tissue Res.* 349:717-731. doi: 710.1007/s00441-00012-01381-00440. Epub 02012 Mar 00418.

Bellve, A.R., J.C. Cavicchia, C.F. Millette, D.A. O'Brien, Y.M. Bhatnagar, and M. Dym. 1977. Spermatogenic cells of the prepuberal mouse. Isolation and morphological characterization. *J Cell Biol.* 74:68-85.

Bjorkgren, I., L. Saastamoinen, A. Krutskikh, I. Huhtaniemi, M. Poutanen, and P. Sipila. 2012. Dicer1 ablation in the mouse epididymis causes dedifferentiation of the epithelium and imbalance in sex steroid signaling. *PLoS One*. 7:e38457. doi: 38410.31371/journal.pone.0038457. Epub 0032012 Jun 0038456.

Buchanan, P.C., K.L.M. Boylan, B. Walcheck, R. Heinze, M.A. Geller, P.A. Argenta, and A.P.N. Skubitz. 2017. Ectodomain shedding of the cell adhesion molecule Nectin-4 in ovarian cancer is mediated by ADAM10 and ADAM17. *J Biol Chem.* 292:6339-6351. doi: 6310.1074/jbc.M6116.746859. Epub 742017 Feb 746823.

Burkett, B.N., B.A. Schulte, and S.S. Spicer. 1987. Histochemical evaluation of glycoconjugates in the male reproductive tract with lectin-horseradish peroxidase conjugates: I. Staining of principal cells and spermatozoa in the mouse. *Am J Anat.* 178:11-22. doi: 10.1002/aja.1001780103.

Chen, H., R.S. Ge, and B.R. Zirkin. 2009. Leydig cells: From stem cells to aging. *Mol Cell Endocrinol.* 306:9-16. doi: 10.1016/j.mce.2009.1001.1023. Epub 2009 Feb 1017.

Cornwall, G.A. 2009. New insights into epididymal biology and function. *Hum Reprod Update.* 15:213-227. doi: 210.1093/humupd/dmn1055. Epub 2009 Jan 1098.

Cortina, C., S. Palomo-Ponce, M. Iglesias, J.L. Fernandez-Masip, A. Vivancos, G. Whissell, M. Huma, N. Peiro, L. Gallego, S. Jonkheer, A. Davy, J. Lloreta, E. Sancho, and E. Batlle. 2007. EphB-ephrin-B interactions suppress colorectal cancer progression by compartmentalizing tumor cells. *Nat Genet.* 39:1376-1383. doi: 1310.1038/ng.2007.1311. Epub 2007 Sep 1330.

Cyr, D.G., M. Gregory, E. Dube, J. Dufresne, P.T. Chan, and L. Hermo. 2007. Orchestration of occludins, claudins, catenins and cadherins as players involved in maintenance of the blood-epididymal barrier in animals and humans. *Asian J Androl.* 9:463-475. doi: 410.1111/j.1745-7262.2007.00308.x.

Dacheux, J.L., and F. Dacheux. 2014. New insights into epididymal function in relation to sperm maturation. *Reproduction.* 147:R27-42. doi: 10.1530/REP-1513-0420. Print 2014 Feb.

Foley, G.L. 2001. Overview of male reproductive pathology. *Toxicol Pathol.* 29:49-63. doi: 10.1080/019262301301418856.

Gilbert, S.F. 2000. Developmental Biology. Sinauer Associates, Inc., USA.

Griswold, M.D. 2016. Spermatogenesis: The Commitment to Meiosis. *Physiol Rev.* 96:1-17. doi: 10.1152/physrev.00013.02015.

Hager, M., K. Gawlik, A. Nystrom, T. Sasaki, and M. Durbeej. 2005. Laminin {alpha}1 chain corrects male infertility caused by absence of laminin {alpha}2 chain. *Am J Pathol.* 167:823-833.

Haldimann, M., D. Custer, N. Munarini, C. Stirnimann, G. Zurcher, V. Rohrbach, V. Djonov, A. Ziemiecki, and A.C. Andres. 2009. Deregulated ephrin-B2 expression in the mammary gland interferes with the development of both the glandular epithelium and vasculature and promotes metastasis formation. *Int J Oncol.* 35:525-536.

Hess, R.A. 2015. Small tubules, surprising discoveries: from efferent ductules in the turkey to the discovery that estrogen receptor alpha is essential for fertility in the male. *Anim Reprod.* 12:7-23.

Ishii, M., I. Mueller, T. Nakajima, E.B. Pasquale, and K. Ogawa. 2011a. EphB signaling inhibits gap junctional intercellular communication and synchronized contraction in

cultured cardiomyocytes. *Basic Res Cardiol.* 106:1057-1068. doi: 1010.1007/s00395-00011-00219-00393. Epub 02011 Sep 00393.

Ishii, M., T. Nakajima, and K. Ogawa. 2011b. Complementary expression of EphB receptors and ephrin-B ligand in the pyloric and duodenal epithelium of adult mice. *Histochem Cell Biol.* 136:345-356. doi: 310.1007/s00418-00011-00849-00414. Epub 02011 Aug 00415.

Johnston, D.S., S.A. Jelinsky, H.J. Bang, P. DiCandeloro, E. Wilson, G.S. Kopf, and T.T. Turner. 2005. The mouse epididymal transcriptome: transcriptional profiling of segmental gene expression in the epididymis. *Biol Reprod.* 73:404-413. doi: 410.1095/biolreprod.1105.039719. Epub 032005 May 039714.

Jun, H.J., J. Roy, T.B. Smith, L.B. Wood, K. Lane, S. Woolfenden, D. Punko, R.T. Bronson, K.M. Haigis, S. Breton, and A. Charest. 2014. ROS1 signaling regulates epithelial differentiation in the epididymis. *Endocrinology.* 155:3661-3673. doi: 3610.1210/en.2014-1341. Epub 2014 Jun 3627.

Kania, A., and R. Klein. 2016. Mechanisms of ephrin-Eph signalling in development, physiology and disease. *Nat Rev Mol Cell Biol.* 17:240-256. doi: 210.1038/nrm.2015.1016. Epub 2016 Jan 1021.

Kilcoyne, K.R., L.B. Smith, N. Atanassova, S. Macpherson, C. McKinnell, S. van den Driesche, M.S. Jobling, T.J. Chambers, K. De Gendt, G. Verhoeven, L. O'Hara, S. Platts, L. Renato de Franca, N.L. Lara, R.A. Anderson, and R.M. Sharpe. 2014. Fetal programming of adult Leydig cell function by androgenic effects on stem/progenitor cells. *Proc Natl Acad Sci U S A.* 111:E1924-1932. doi: 1910.1073/pnas.1320735111. Epub 1320732014 Apr 1320735121.

Klein, R. 2012. Eph/ephrin signalling during development. *Development.* 139:4105-4109. doi: 4110.1242/dev.074997.

Koenen, R.R., J. Pruessmeyer, O. Soehnlein, L. Fraemohs, A. Zernecke, N. Schwarz, K. Reiss, A. Sarabi, L. Lindbom, T.M. Hackeng, C. Weber, and A. Ludwig. 2009. Regulated release and functional modulation of junctional adhesion molecule A by disintegrin metalloproteinases. *Blood.* 113:4799-4809. doi: 4710.1182/blood-2008-4704-152330. Epub 152009 Mar 152333.

Kormano, M., and O. Hovatta. 1972. Contractility and histochemistry of the myoid cell layer of the rat seminiferous tubules during postnatal development. *Z Anat Entwicklungsgesch.* 137:239-248.

Kullander, K., and R. Klein. 2002. Mechanisms and functions of Eph and ephrin signalling. *Nat Rev Mol Cell Biol.* 3:475-486. doi: 410.1038/nrm1856.

Li, D., P. Sekhon, K.J. Barr, L. Marquez-Rosado, P.D. Lampe, and G.M. Kidder. 2013. Connexins and steroidogenesis in mouse Leydig cells. *Can J Physiol Pharmacol.* 91:157-164. doi: 110.1139/cjpp-2012-0385. Epub 2013 Feb 1125.

Lin, S., K. Gordon, N. Kaplan, and S. Getsios. 2010. Ligand targeting of EphA2 enhances keratinocyte adhesion and differentiation via desmoglein 1. *Mol Biol Cell.* 21:3902-3914. doi: 3910.1091/mbc.E3910-3903-0242. Epub 2010 Sep 3922.

Luedtke, C.C., S. Andonian, S. Igdoura, and L. Hermo. 2000. Cathepsin A is expressed in a cell- and region-specific manner in the testis and epididymis and is not regulated by testicular or pituitary factors. *J Histochem Cytochem.* 48:1131-1146. doi: 1110.1177/002215540004800810.

Lupien, M., A. Dievart, C.R. Morales, L. Hermo, E. Calvo, D.G. Kay, C. Hu, and P. Jolicoeur. 2006. Expression of constitutively active Notch1 in male genital tracts results in ectopic growth and blockage of efferent ducts, epididymal hyperplasia and sterility. *Dev Biol.* 300:497-511. doi: 410.1016/j.ydbio.2006.1009.1010. Epub 2006 Sep 1014.

Malolina, E.A.K., and A.Y. Kulibin. 2017. Rete testis and the adjacent seminiferous tubules during postembryonic development in mice. *Russ J Dev Biol*. 48:385-392.

Mendive, F., P. Laurent, G. Van Schoore, W. Skarnes, R. Pochet, and G. Vassart. 2006. Defective postnatal development of the male reproductive tract in LGR4 knockout mice. *Dev Biol.* 290:421-434. doi: 410.1016/j.ydbio.2005.1011.1043. Epub 2006 Jan 1019.

Miao, H., and B. Wang. 2009. Eph/ephrin signaling in epithelial development and homeostasis. *Int J Biochem Cell Biol.* 41:762-770. doi: 710.1016/j.biocel.2008.1007.1019. Epub 2008 Aug 1019.

Montoto, L.G., L. Arregui, N.M. Sanchez, M. Gomendio, and E.R. Roldan. 2012. Postnatal testicular development in mouse species with different levels of sperm competition. *Reproduction.* 143:333-346. doi: 310.1530/REP-1511-0245. Epub 2011 Dec 1520.

Murashima, A., B. Xu, and B.T. Hinton. 2015. Understanding normal and abnormal development of the Wolffian/epididymal duct by using transgenic mice. *Asian J Androl.* 17:749-755. doi: 710.4103/1008-4682X.155540.

Nakagawa, T., M. Sharma, Y. Nabeshima, R.E. Braun, and S. Yoshida. 2010. Functional hierarchy and reversibility within the murine spermatogenic stem cell compartment. *Science.* 328:62-67. doi: 10.1126/science.1182868. Epub 1182010 Mar 1182818.

Nguyen, T.M., A. Arthur, and S. Gronthos. 2016. The role of Eph/ephrin molecules in stromal-hematopoietic interactions. *Int J Hematol.* 103:145-154. doi: 110.1007/s12185-12015-11886-x.

Nguyen, T.M., A. Arthur, R. Panagopoulos, S. Paton, J.D. Hayball, A.C. Zannettino, L.E. Purton, K. Matsuo, and S. Gronthos. 2015. EphB4 Expressing Stromal Cells Exhibit an Enhanced Capacity for Hematopoietic Stem Cell Maintenance. *Stem Cells.* 33:2838-2849. doi: 2810.1002/stem.2069. Epub 2015 Jun 2823.

Nikolova, Z., V. Djonov, G. Zuercher, A.C. Andres, and A. Ziemiecki. 1998. Cell-type specific and estrogen dependent expression of the receptor tyrosine kinase EphB4 and its ligand ephrin-B2 during mammary gland morphogenesis. *J Cell Sci.* 111:2741-2751.

Noren, N.K., and E.B. Pasquale. 2004. Eph receptor-ephrin bidirectional signals that target Ras and Rho proteins. *Cell Signal.* 16:655-666. doi: 610.1016/j.cellsig.2003.1010.1006.

Ogawa, K., N. Saeki, Y. Igura, and Y. Hayashi. 2013. Complementary expression and repulsive signaling suggest that EphB2 and ephrin-B1 are possibly involved in epithelial boundary formation at the squamocolumnar junction in the rodent stomach. *Histochem Cell Biol.* 140:659-675. doi: 610.1007/s00418-00013-01129-00412. Epub 02013 Jul 00424.

Ogawa, K., N. Takemoto, M. Ishii, E.B. Pasquale, and T. Nakajima. 2011a. Complementary expression and repulsive signaling suggest that EphB receptors and ephrin-B ligands control cell positioning in the gastric epithelium. *Histochemistry and cell biology.* 136:617-636.

Ogawa, K., N. Takemoto, M. Ishii, E.B. Pasquale, and T. Nakajima. 2011b. Complementary expression and repulsive signaling suggest that EphB receptors and ephrin-B ligands control cell positioning in the gastric epithelium. *Histochem Cell Biol.* 136:617-636. doi: 610.1007/s00418-00011-00867-00412. Epub 02011 Sep 00430.

Ogawa, K., H. Wada, N. Okada, I. Harada, T. Nakajima, E.B. Pasquale, and S. Tsuyama. 2006. EphB2 and ephrin-B1 expressed in the adult kidney regulate the cytoarchitecture of medullary tubule cells through Rho family GTPases. *J Cell Sci.* 119:559-570. doi: 510.1242/jcs.02777.

Okubo, T., N. Yanai, and M. Obinata. 2006. Stromal cells modulate ephrinB2 expression and transmigration of hematopoietic cells. *Exp Hematol.* 34:330-338. doi: 310.1016/j.exphem.2005.1012.1003.

Palmer, A., and R. Klein. 2003. Multiple roles of ephrins in morphogenesis, neuronal networking, and brain function. *Genes Dev.* 17:1429-1450. doi: 1410.1101/gad.1093703.

Pasquale, E.B. 2005. Eph receptor signalling casts a wide net on cell behaviour. *Nat Rev Mol Cell Biol.* 6:462-475. doi: 410.1038/nrm1662.

Pasquale, E.B. 2008. Eph-ephrin bidirectional signaling in physiology and disease. *Cell.* 133:38-52. doi: 10.1016/j.cell.2008.1003.1011.

Pasquale, E.B. 2010. Eph receptors and ephrins in cancer: bidirectional signalling and beyond. *Nat Rev Cancer.* 10:165-180. doi: 110.1038/nrc2806.

Perez White, B.E., and S. Getsios. 2014. Eph receptor and ephrin function in breast, gut, and skin epithelia. *Cell Adh Migr.* 8:327-338. doi: 310.4161/19336918.19332014.19970012.

Poliakov, A., M. Cotrina, and D.G. Wilkinson. 2004. Diverse roles of eph receptors and ephrins in the regulation of cell migration and tissue assembly. *Dev Cell.* 7:465-480. doi: 410.1016/j.devcel.2004.1009.1006.

Potter, S.J., and T. DeFalco. 2017. Role of the testis interstitial compartment in spermatogonial stem cell function. *Reproduction.* 153:R151-R162. doi: 110.1530/REP-1516-0588. Epub 2017 Jan 1523.

Qian, X., D.D. Mruk, Y.H. Cheng, E.I. Tang, D. Han, W.M. Lee, E.W. Wong, and C.Y. Cheng. 2014. Actin binding proteins, spermatid transport and spermiation. *Semin Cell Dev Biol.* 30:75-85.:10.1016/j.semcdb.2014.1004.1018. Epub 2014 Apr 1013.

Robaire, B., and M. Hamzeh. 2011. Androgen action in the epididymis. *J Androl.* 32:592-599. doi: 510.2164/jandrol.2111.014266. Epub 012011 Jul 014215.

Robaire, B., B.T. Hinton, and M.C. Orgebin-Crist. 2006. The Epididymis. *In*: Neill JD, Knobil and Neill's Physiology of Reproduction, 3rd edn, Elsevier.

Ross, M.H., and W. Pawlina. 2015. Male Reproductive System. *In*: Histology: A Text and Atlas: With Correlated Cell and Molecular Biology. Wolters Kluwer, Philadelphia, PA, USA.

Saftig, P., and S.F. Lichtenthaler. 2015. The alpha secretase ADAM10: A metalloprotease with multiple functions in the brain. *Prog Neurobiol.* 135:1-20.:10.1016/j.pneurobio.2015.1010.1003. Epub 2015 Oct 1029.

Shima, Y., K. Miyabayashi, S. Haraguchi, T. Arakawa, H. Otake, T. Baba, S. Matsuzaki, Y. Shishido, H. Akiyama, T. Tachibana, K. Tsutsui, and K. Morohashi. 2013.

Contribution of Leydig and Sertoli cells to testosterone production in mouse fetal testes. *Mol Endocrinol.* 27:63-73. doi: 10.1210/me.2012-1256. Epub 2012 Nov 1212.

Silvan, U., and J. Arechaga. 2012. Anatomical basis for cell transplantation into mouse seminiferous tubules. *Reproduction.* 144:385-392. doi: 310.1530/REP-1512-0043. Epub 2012 Jun 1529.

Sipila, P., and I. Bjorkgren. 2016. Segment-specific regulation of epididymal gene expression. *Reproduction.* 152:R91-99. doi: 10.1530/REP-1515-0533. Epub 2016 May 1524.

Solanas, G., C. Cortina, M. Sevillano, and E. Batlle. 2011. Cleavage of E-cadherin by ADAM10 mediates epithelial cell sorting downstream of EphB signalling. *Nat Cell Biol.* 13:1100-1107. doi: 1110.1038/ncb2298.

Sullivan, R., and R. Mieusset. 2016. The human epididymis: its function in sperm maturation. *Hum Reprod Update.* 22:574-587. doi: 510.1093/humupd/dmw1015. Epub 2016 Jun 1015.

Tanaka, M., R. Kamata, and R. Sakai. 2005. Phosphorylation of ephrin-B1 via the interaction with claudin following cell-cell contact formation. *EMBO J.* 24:3700-3711. doi: 3710.1038/sj.emboj.7600831. Epub 7602005 Oct 7600836.

Tiptanavattana, N., A. Radtanakatikanon, P. Hyttel, H. Holm, S. Buranapraditkun, P. Setthawong, M. Techakumphu, and T. Tharasanit. 2015. Determination phase at transition of gonocytes to spermatogonial stem cells improves establishment efficiency of spermatogonial stem cells in domestic cats. *J Reprod Dev*. 61:581-588. doi: 510.1262/jrd.2015-1094. Epub 2015 Sep 1227.

Turner, T.T., D. Bomgardner, J.P. Jacobs, and Q.A. Nguyen. 2003. Association of segmentation of the epididymal interstitium with segmented tubule function in rats and mice. *Reproduction.* 125:871-878.

Uchiyama, S., N. Saeki, and K. Ogawa. 2015. Aberrant EphB/ephrin-B expression in experimental gastric lesions and tumor cells. *World J Gastroenterol.* 21:453-464. doi: 410.3748/wjg.v3721.i3742.3453.

Urriola-Munoz, P., C. Lizama, R. Lagos-Cabre, J.G. Reyes, and R.D. Moreno. 2014. Differential expression and localization of ADAM10 and ADAM17 during rat spermatogenesis suggest a role in germ cell differentiation. *Biol Res.* 47:31.:10.1186/0717-6287-1147-1131.

Vergouwen, R.P., R. Huiskamp, R.J. Bas, H.L. Roepers-Gajadien, J.A. Davids, and D.G. de Rooij. 1993. Postnatal development of testicular cell populations in mice. *J Reprod Fertil.* 99:479-485.

Wen, Q., C.Y. Cheng, and Y.X. Liu. 2016. Development, function and fate of fetal Leydig cells. *Semin Cell Dev Biol.* 59:89-98.:10.1016/j.semcdb.2016.1003.1003. Epub 2016 Mar 1018.

Xia, G., S.R. Kumar, R. Masood, S. Zhu, R. Reddy, V. Krasnoperov, D.I. Quinn, S.M. Henshall, R.L. Sutherland, J.K. Pinski, S. Daneshmand, M. Buscarini, J.P. Stein, C. Zhong, D. Broek, P. Roy-Burman, and P.S. Gill. 2005. EphB4 expression and biological significance in prostate cancer. *Cancer Res.* 65:4623-4632. doi: 4610.1158/0008-5472.CAN-4604-2667.